University of Kentucky
UKnowledge

University of Kentucky Doctoral Dissertations | Graduate School

2010

SYNTHESIS AND CHARACTERIZATION OF MAGNETIC HYDROGEL NANOCOMPOSITES FOR CANCER THERAPY APPLICATIONS

Samantha Ann Meenach
University of Kentucky, sameen0@uky.edu

Right click to open a feedback form in a new tab to let us know how this document benefits you.

Recommended Citation

Meenach, Samantha Ann, "SYNTHESIS AND CHARACTERIZATION OF MAGNETIC HYDROGEL NANOCOMPOSITES FOR CANCER THERAPY APPLICATIONS" (2010). *University of Kentucky Doctoral Dissertations*. 108.
https://uknowledge.uky.edu/gradschool_diss/108

This Dissertation is brought to you for free and open access by the Graduate School at UKnowledge. It has been accepted for inclusion in University of Kentucky Doctoral Dissertations by an authorized administrator of UKnowledge. For more information, please contact UKnowledge@lsv.uky.edu.

ABSTRACT OF DISSERTATION

Samantha Ann Meenach

The Graduate School

University of Kentucky

2010

SYNTHESIS AND CHARACTERIZATION OF MAGNETIC HYDROGEL NANOCOMPOSITES FOR CANCER THERAPY APPLICATIONS

ABSTRACT OF DISSERTATION

A dissertation submitted in partial fulfillment of the
requirements for the degree of Doctor of Philosophy in the
College of Engineering at the University of Kentucky

By

Samantha Ann Meenach

Lexington, Kentucky

Co-Directors: Dr. Kimberly Ward Anderson, Professor of Chemical Engineering
Dr. James Zachary Hilt, Assistant Professor of Chemical Engineering

Lexington, Kentucky

2010

Copyright © Samantha Ann Meenach 2010

ABSTRACT OF DISSERTATION

SYNTHESIS AND CHARACTERIZATION OF MAGNETIC HYDROGEL NANOCOMPOSITES FOR CANCER THERAPY APPLICATIONS

Currently, cancer is the second leading cause of death in the United States. Conventional cancer treatment includes chemotherapy, radiation, and surgical resection, but unfortunately, all of these methods have significant drawbacks. Hyperthermia, the heating of cancerous tissues to between 41 and 45°C, has been shown to improve the efficacy of cancer therapy when used in conjunction with irradiation and/or chemotherapy. In this work, a novel method for remotely administering heat is presented. This method involves heating of tumor tissue using hydrogel nanocomposites containing magnetic nanoparticles which can be remotely heated upon exposure to an external alternating magnetic field (AMF). The iron oxide nanoparticles contained in the hydrogel nanocomposites are able to heat via an AMF due to Brownian and Neel relaxation processes. The administration of hyperthermia via hydrogel nanocomposites allows for local delivery of heat to tumor tissue while also providing a drug depot to deliver chemotherapeutic agents. Both in vivo and in vitro studies have demonstrated that numerous chemotherapeutic agents, when used in conjunction with hyperthermia, show improved efficacy in treating cancer

Various magnetic hydrogel nanocomposites were synthesized and characterized for this work including poly(ethylene glycol) (PEG)-based hydrogels, which were studied due to their inherent biocompatibility and "stealth" properties, as well as, poly(β-amino ester) (PBAE)-based hydrogels which have tailorable degradation properties. The PEG hydrogels were investigated for their temperature-responsiveness swelling, mechanical strength, heating capabilities, biocompatibility, ability to kill M059K glioblastoma cells via thermoablation, and the ability to deliver paclitaxel, a chemotherapeutic agent. PBAE hydrogels were also characterized for their degradation and swelling properties, ability to heat upon exposure to an AMF, biocompatibility, mechanical strength, and ability to deliver paclitaxel in a controlled fashion. Additionally, multiple cancer cell lines were exposed to a combination of paclitaxel and heat (at 42.5 °C) *in vitro* and it was shown that A539 lung carcinoma cells exhibit higher cytotoxicity when exposed to both heat and paclitaxel than either treatment alone. Overall, magnetic hydrogel nanocomposites are promising materials that can be utilized for the multi-modality treatment of cancer through the synergistic delivery of both heat and chemotherapeutic agents.

KEYWORDS: Hydrogel, Nanocomposite, Iron Oxide, poly(ethylene glycol), poly(β-amino ester)

Samantha Ann Meenach

April 19, 2010

SYNTHESIS AND CHARACTERIZATION OF MAGNETIC HYDROGEL NANOCOMPOSITES FOR CANCER THERAPY APPLICATIONS

By

Samantha Ann Meenach

Dr. Kimberly W. Anderson
Co-Director of Dissertation

Dr. J. Zach Hilt
Co-Director of Dissertation

Dr. Barbara Knutson
Director of Graduate Studies

April 19, 2020

RULES FOR THE USE OF DISSERTATIONS

Unpublished dissertations submitted for the Doctor's degree and deposited in the University of Kentucky Library are as a rule open for inspection, but are to be used only with due regard to the rights of the authors. Bibliographical references may be noted, but quotations or summaries of parts may be published only with the permission of the author, and with the usual scholarly acknowledgments.

Extensive copying or publication of the dissertation in whole or in part also requires the consent of the Dean of the Graduate School of the University of Kentucky.

A library that borrows this thesis for use by its patrons is expected to secure the signature of each user.

Name Date

_____

_____

_____

_____

_____

_____

_____

_____

_____

_____

DISSERTATION

Samantha Ann Meenach

The Graduate School

University of Kentucky

2010

SYNTHESIS AND CHARACTERIZATION OF MAGNETIC HYDROGEL NANOCOMPOSITES FOR CANCER THERAPY APPLICATIONS

DISSERTATION

A dissertation submitted in partial fulfillment of the
requirements for the degree of Doctor of Philosophy in the
College of Engineering at the University of Kentucky

By

Samantha Ann Meenach

Lexington, Kentucky

Co-Directors: Dr. Kimberly Ward Anderson, Professor of Chemical Engineering
Dr. James Zachary Hilt, Assistant Professor of Chemical Engineering

Lexington, Kentucky

2010

Copyright © Samantha Ann Meenach 2010

Dedicated to my mother and sister: cancer sucks!

ACKNOWLEDGEMENTS

The completion of this dissertation would not have been possible without the input, guidance, and sacrifice of many people. I would like to start my acknowledgements to where it all began, with my 8th grade science teacher, Tim Schneider. It was in his class where I first caught the science bug and truly realized my passion for exploring the unknowns of the world around me. His enthusiasm was infectious, and I will never forget my time in that classroom. There were two high school teachers that deserve my gratitude: Don Manker, who provided me with a solid education in mathematics, and Joyce Wainscott, whose freshman Introduction to Chemistry and Physics class was incredibly challenging and allowed me to learn more about basic science than I could have imagined at that age. Their dedication to teaching was always evident, and I remember more about what I learned in those classes than any others throughout my high school career.

I would also like to thank my doctoral committee for their support and assistance throughout my dissertation process, especially Dr. Leonidas Bachas for "filling in" at such short notice for my dissertation defense. Dr. Thomas Dziubla has been a great resource for my troubleshooting and was always more than willing to help me when I needed it. It goes without saying that without my co-advisor Dr. Zach Hilt, this dissertation would not have been possible. I could not begin to count the many times I was able to stop by his office for a chat (in addition to often meeting multiple times a week!) to ask questions about my research or just talk about science in general. I am grateful for his patience and support and the fact that I always knew he cared about my well-being beyond my performance in the lab.

I had the pleasure of meeting my co-advisor, Dr. Kim Anderson, when I was an undergraduate researcher in her lab nearly 8 years ago. Without her guidance and support I probably would not be a chemical engineer, yet alone completing a PhD in my field. As an undergraduate, she motivated me to complete my degree and helped give me the confidence that I had the ability to pursue my doctoral degree, and now pursue a position in academia.

When I returned to the University of Kentucky for my graduate work, she welcomed me with open arms and with Dr. Hilt provided me the opportunity to work with many undergraduate and high school students. Dr. Anderson's concern always extended beyond my work in the lab, and her support throughout the many concerns regarding my family means more than I can express. I feel fortunate that I have had not only a wonderful advisor, but a great mentor and friend throughout this process.

Without the help of the many undergraduate students who have worked with me on my research, I would not have been able to complete as much as I have in the time that I have. I need to extend a special thanks to Ashley Anderson Garrison for her dedication in helping me complete my first manuscript for my work at UK and for her continuing friendship. Both Jenna Shapiro and Chinedu Otu were extremely patient and supportive throughout last summer with the craziness surrounding my supervising 4 students in the lab as well as dealing with my mother's illness. Their flexibility and hard work allowed me to leave the lab in capable hands without my having to worry about the outcome. In addition, I would like to thank Jenna for her humor and willingness to listen to my many woes these past several months as I have been wrapping everything up!

To my sister and wonderful friend, Brooke: thank you for always supporting me, for providing a shoulder when I needed one, and for always allowing me to share both my frustrations and excitement with you. I am so proud of you for how you have handled your own battle with cancer! I owe my interest in chemical engineering to my father, Eddie Meenach, who introduced me to the field in high school while he was working as a chemical operator. He always believed in me, pushed me to do better, and instilled a sense of hard work and dedication and studies in me. Dad, thank you for your love and support and for never giving up on me. This dissertation is dedicated to my mother, Patty Charles, who has shown incredible strength and grace throughout her yearlong battle with cancer. Who knows how many hours we spent on the phone over the course of my graduate school career -- her

humor helped me overcome many down days of endless experiments and family woes. She is one of my closest confidants and I am lucky to have such a wonderful mother and friend.

Last but certainly not least, I would like to thank my husband, Kyle, for his unwavering support, ability to put up with my difficultness, and flexibility. He truly completes my life and I cannot imagine continuing on life's journey without him. Kyle, thank you for being my best friend and for bringing out the best in me -- I love you.

TABLE OF CONTENTS

LIST OF TABLES

LIST OF FIGURES

CHAPTER 1

1.1 Introduction

The development of cancer therapeutics is an important component of biomedical research today because even though much has been done to overcome and treat the disease, there are still many types of cancer, such as glioblastoma and pancreatic cancer (Sneed 1998), that have extremely poor treatment success rates. Therefore, multiple-modality treatment has become the preferred treatment approach. Hyperthermia, the heating of cancer tissues to between 41 and 45°C, has been proven to have the potential to provide a straightforward and effective way of treating cancer in combination with well-developed therapeutics such as irradiation and chemotherapy (Falk and Issels 2001). Thermoablation, the thermal destruction of cells at temperatures above 50°C, is another potential cancer therapy method involving heat therapy (Jordan 1999). A novel class of biomaterials based on nanocomposite hydrogels, specifically systems composed of poly(ethylene oxide) (PEG) or poly(β-amino ester) (PBAE) and iron oxide, have the potential to be used in such hyperthermia applications. The exposure of the gels to a high-frequency magnetic field leads to remote heating due to the magnetic particles in the nanocomposite.

Hydrogels are three-dimensional, hydrophilic, polymeric networks that can absorb up to thousands of times their dry weight in water or biological fluids (Corkhill 1989; Peppas 2000; Peppas 2006). They consist of polymeric chains with either physical or chemical crosslinks preventing their dissolution while allowing swelling upon interaction with aqueous solutions. They have been utilized in a wide variety of biomedical applications such as drug delivery, contact lenses, and tissue engineering (Peppas 1987; Peppas 2006; Frimpong and Hilt 2007). In particular, poly(ethylene glycol) (PEG)-based hydrogels have been widely investigated and are considered “stealth” systems due to their high water content and the presence of PEG chains which exhibit high biocompatibility. The biocompatibility of PEG

stems from its ability to repel protein absorption, due to the hydrophilic nature of the polymer (Nagaoka 1984; Jeon 1991). PBAE polymers are of interest due to the simplicity in synthesizing the macromers that make up the hydrogels, and the ability to tailor the properties of the systems (such as degradation and mechanical strength) based on the chemistry of the macromers used.

Despite the many advantages of using conventional hydrogels, their applications are often limited due to their poor mechanical strength and somewhat limited response and actuation properties (Xiang 2006). In recent years, hydrogel nanocomposites have received increased attention as a result of their unique properties and expanded applications (Brazel 2009; Hawkins 2009; Satarkar 2009). Hydrogel nanocomposites involve the incorporation of various nanoparticulate materials within a hydrogel matrix which provides an easy, straightforward methods for enhancing the properties of hydrogels. The incorporation of magnetic nanoparticles such as iron oxide nanoparticles into hydrogels can create tunable nanocomposites that can be remotely controlled by a magnetic field (Frimpong and Hilt 2008; Satarkar and Hilt 2008). In recent work by Satarkar and coworkers, remote-controlled heating and drug release using hydrogel nanocomposites based on N-isopropylacrylamide (NIPAAm) and Fe_3O_4 nanoparticles have been successfully demonstrated (Satarkar and Hilt 2008; Satarkar and Hilt 2008). This controlled release was due to the thermally-responsive nature of the NIPAAm, and the remote-controlled heating by applying an alternating magnetic field (AMF) which heated the magnetic nanoparticles present in the hydrogel matrix causing them to collapse and expel the drug.

In regards to the biocompatibility of hydrogel nanocomposites, a limited amount of cytocompatibility or hemocompatibility studies have been reported. However, a wide variety of literature is available regarding the biocompatibility of the hydrogels and nanoparticulate components alone that make up a hydrogel nanocomposite (Meenach 2009). One of the advantages of hydrogel nanocomposites is that hydrogels can provide increased

biocompatibility over exposed, uncoated nanoparticulates because they encapsulate the particulate matter in the composite matrix providing a barrier between the sensitive tissues and the more harmful nanoparticulates.

The magnetic hydrogel nanocomposites used in this work were synthesized using various PEG and PBAE macromer types and crosslinking amounts. This allowed for the tailoring of various properties such as swelling, mechanical strength, heating via an AMF, biocompatibility, and paclitaxel release profiles. Overall, these systems are promising for applications in cancer therapy due to their ability to deliver both heat and chemotherapeutic agents.

1.2 Objectives

The overall objective of this dissertation was to develop biocompatible magnetic hydrogel nanocomposites with tailorable properties for the controlled delivery of heat and therapeutic agents (e.g., paclitaxel) for synergistic cancer therapy applications. This involved four projects and the specific objectives of these are outlined as follows:

1. "Poly(ethylene glycol)-Based Magnetic Hydrogel Nanocomposites for Hyperthermia Cancer Therapy":
    a. Fabricate magnetic hydrogel nanocomposites based on PEG and iron oxide with various crosslinking densities.
    b. Analyze the swelling properties of the hydrogels.
    c. Analyze the heating properties of the nanocomposites at a fixed AMF strength and frequency.
    d. Control the heating of the hydrogels by changing the AMF strength and frequency.
    e. Characterize the toxicity potential of the hydrogels through the exposure of NIH 3T3 fibroblasts to the gels.

f. Demonstrate the ability of the hydrogels to kill M059K glioblastoma *in vitro* upon exposure to hydrogel nanocomposites heated in an AMF.

2. "Synthesis and Characterization of Thermoresponsive Poly(ethylene glycol)-Based Hydrogels and Their Magnetic Nanocomposites":
    a. Fabricate magnetic hydrogel nanocomposites based on temperature-responsive PEG methacrylates and iron oxide.
    b. Analyze the swelling characteristics of the hydrogels at various temperatures.
    c. Characterize the heating characteristics of hydrogel nanocomposites exposed to a constant AMF.
    d. Demonstrate the ability of the hydrogel nanocomposites to deswell rapidly upon exposure to an AMF due to the heating of the gels.

3. "Combined Hyperthermia and Chemotherapeutic Delivery Via PEG-Based Hydrogel Nanocomposites":
    a. Fabricate magnetic hydrogel nanocomposites based on PEG and iron oxide with various crosslinking densities.
    b. Analyze the swelling characteristics of the hydrogels at various temperatures.
    c. Characterize the heating properties of the hydrogel nanocomposites upon exposure to an AMF.
    d. Determine the compressive moduli of the hydrogel nanocomposites.
    e. Analyze and model paclitaxel release from the hydrogel nanocomposites.
    f. Analyze the cytotoxicity of various cancer cell lines exposed to both paclitaxel and heat versus either treatment alone.

4. “Controlled Synergistic Delivery of Paclitaxel and Heat from Poly(β-amino ester)/Iron Oxide-Based Hydrogel Nanocomposites”:
    a. Synthesize and characterize poly(β-amino ester) (PBAE) macromers based on poly(ethylene glycol) diacrylates and isobutylamine.
    b. Fabricate magnetic hydrogel nanocomposites based on various PBAE macromers and iron oxide.
    c. Characterize degradation and swelling response of hydrogel nanocomposites.
    d. Determine the compressive moduli of the hydrogel nanocomposites.
    e. Characterize iron oxide loss via thermogravimetric analysis.
    f. Characterize the heating properties of the hydrogel nanocomposites upon exposure to an AMF throughout the degradation process.
    g. Analyze and model paclitaxel release from the hydrogel nanocomposites.
    h. Analyze the cytotoxicity of PBAE hydrogel nanocomposite degradation products.

This dissertation starts with Chapter 2 with background information on hydrogels in cancer therapy applications including an introduction to hydrogels, a discussion of the conventional cancer therapies and their limitations, and a review of previous work focusing on hydrogel systems used in cancer therapy applications. Chapter 3 includes the project, “Poly(ethylene glycol)-Based Magnetic Hydrogel Nanocomposites for Hyperthermia Cancer Therapy,” which looks at PEG-based hydrogels capable of both hyperthermia and thermoablation. Chapter 4 focuses on the project, “Synthesis and Characterization of Thermoresponsive Poly(ethylene glycol)-Based Hydrogels and Their Magnetic Nanocomposites,” which demonstrates the temperature-responsiveness of PEG hydrogel nanocomposites for the first time. The project “Combined Hyperthermia and Chemotherapeutic Delivery Via PEG-Based Hydrogel Nanocomposites” is presented in Chapter 5 which examines PEG hydrogels for paclitaxel and heat delivery. Chapter 6 includes

the final project, "Controlled Synergistic Delivery of Paclitaxel and Heat from Poly(β-amino ester)/Iron Oxide-Based Hydrogel Nanocomposites," which focuses on synthesizing and characterizing degradable hydrogels capable of delivering paclitaxel and heat in a controlled manner. The conclusions of this work are summarized in Chapter 7.

References

All references are located at the end of the dissertation.

CHAPTER 2

Hydrogels for Cancer Applications

Hydrogels have been widely investigated for biomedical applications throughout the past several decades. They offer many optimal characteristics for drug delivery including the ability to tailor the release of drugs and their ability to be biocompatible due to their high water content. One area of research that has received increased interest more recently is the use of hydrogels to treat cancer. These materials have shown the ability to effectively deliver chemotherapeutics, radionucleotides, and immunotherapeutics in both *in vitro* and *in vivo* applications. This delivery has been achievable via hydrogel systems that are non-biodegradable, stimuli-responsive, natural, and/or biodegradable materials. Particulate hydrogels (nano- or micro-sized) have also been investigated for the delivery of cancer therapeutics, and these materials have been able to be delivered specifically to cancer cells via active ligand targeting and passive targeting via the enhanced permeation and retention effect. In addition to cancer therapy, hydrogels have been investigated for other cancer-related applications such as tumor embolization, three-dimensional cell culture to mimic the tumor microenvironment, tumor imaging, and biosensors. Overall, studies have shown that hydrogels offer many advantages in cancer treatment and applications and should be developed into more commercial and clinical applications. This review will cover conventional cancer therapies and their limitations, hydrogel systems that deliver chemotherapeutics, radiation, and/or immunotherapeutic agents, and an overview of other ways hydrogels are being used in cancer-related applications.

2.1 Introduction

2.1.1 Types of Common Cancer Therapies and Their Limitations

Currently, cancer is the second leading cause of death in the United States. In 2009 alone, there were an estimated 1.5 million new cases diagnosed (ACS 2009). Cancer is a disease that is characterized by aggressive growth of cells which divide without normal limitations, invade and destroy adjacent tissues, and spread to distant sites throughout the body through metastasis, which is a major cause of death (Ta 2008). Cancer may result from a wide variety of external factors including exposure of healthy cells to physical carcinogens such as ultraviolet and ionizing radiation, chemical carcinogens such as asbestos and tobacco smoke, and biological carcinogens such as infections by viruses and contamination of food by mycotoxins (Ta 2008). The most common types of cancer therapy include chemotherapy, radiation, and/or resection. This often involves treating solid tumors via surgical removal followed by irradiation and/or systemic chemotherapy to kill malignant cells which may have survived the surgery and to treat any metastasis that may have occurred. Hormonal therapy and immunotherapy are also being used, but their applications are currently limited to certain types of cancer.

Unfortunately, intravenously delivered chemotherapy for certain types of tumors often has limited effectiveness. Since only a small amount of systemic blood flow is directed to the tumor, only a small fraction of the total dose reaches the tumor site and the remainder of the dose is distributed to healthy organs and tissues (Weinburg 2008). Additionally, most chemotherapeutics are highly toxic and lack specificity in that they do not differentiate between normal and cancer cells, leading to such severe side effects throughout the body (Ta 2008). Initially, chemotherapy treatment is usually effective; however, this therapeutic response is often only seen in the short term. Between treatments, there is often re-growth of vascular endothelial cells that support the tumor which results in more aggressive cancers that

are resistant to the cytotoxic drug being used for treatment. While continuous drug delivery allowing for low levels of an anticancer agent over an extended period of time is ideal, patient compliance and inconvenience limits this type of therapy. Also, drugs often have limited bioavailability (the fraction of an administered dose of a drug that reaches the systemic circulation). For example, 90 % of the chemotherapeutic agent cisplatin is bound to plasma proteins in the blood causing decreased bioavailability. (Casolaro 2009). Therefore, drug delivery systems are needed to achieve higher concentration of the drug locally in tumor tissues and to control the release profile of these drugs. An alternative to conventional treatment is an implantable device that can release the drug at a controlled rate for longer periods of time. Implanting a biodegradable device loaded with a chemotherapeutic agent in the cavity created by tumor removal can provide a high local concentration of the drug, killing the surviving malignant cells while preventing systemic side effects. Additionally, clinicians can use this type of system to pre-treat solid tumors prior to surgery in order to expose the tumor to large concentrations of the drug (Shikanov 2008). The advantages of such implantable drug delivery devices may include more precise dose control, high release efficiency, and lower systemic toxicity (Casolaro 2009).

Radiation is a type of cancer therapy that uses ionizing radiation to destroy cancer cells at a specific site. Multiple types of cancer such as lung, breast, prostate, head and neck are treated with radiation and nearly 60% of patients diagnosed with cancer undergo this type of treatment (Azhdarinia 2005). Conventional external radiation can be limiting for certain types of unresectable tumors as there is a certain tissue tolerance that must be taken into account. Brachytherapy is a commonly used treatment option for prostate cancer as radioactive seeds are directly deposited intratumorally which spares the surrounding healthy tissue from damage. Unfortunately, these seeds are non-degradable and will remain at the tumor site after injection (Azhdarinia 2005) and this treatment often requires relatively complicated placement

and removal procedures (Azab 2007). Fortunately, there are several radionucleotides currently used for the treatment of cancer.

Beta-emitters are the most widely used in radiotherapy. β-Electrons from radionucleotides interact with atoms, mainly in water molecules, and lose their energy, which leads to the generation of excited and ionized atoms and free radicals. These are then responsible for DNA damage in cells by inducing single strand breaks in DNA, preventing cell division (Hamoudeh 2008). The ideal radiopharmaceutical should result in radioactive energy that reaches the tumor tissue with no radiation reaching beyond to normal tissue. Incorporating radiopharmaceuticals in nanoparticulate or microparticulate carriers can provide a useful means for controlling the tissue and cellular distribution profiles of such agents (Hamoudeh 2008). It is also possible to deliver radionucleotides more effectively and locally through incorporation of such agents in hydrogel systems.

Although not yet a conventional method for treating cancer, hyperthermia is becoming more prevalent as another tool for the multi-modality treatment of the disease. Hyperthermia is the heating of tumor tissue to temperatures between 41 and 45°C (Jordan 1999). It is used for up to a few hours in combination with other assisting toxic agents (mostly irradiation or chemotherapy) for reliable damage of tumor cells (Hergt 2006). Cellular stress from heat potentiates the effect of chemotherapy and ionizing radiation through increased intracellular drug uptake and intratumoral drug concentrations, enhanced DNA damage, and improved tissue oxygenation resulting from an increase in blood flow (van der Zee 2002; Janjetovic 2007). One of the advantages of this therapy is that the tissue damage for normal tissue is reversible while the tumor cells are irreversibly damaged (Neuberger 2005). When used with radiation, hyperthermia has been shown to improve local tumor control and overall survival in patients with advanced pelvic tumors, primary and recurrent breast cancer, head and neck tumors, and glioblastoma (Roca 2003). Regarding chemotherapy applications, many reports have discussed which anticancer drugs demonstrate a synergistic effect with hyperthermia and

have described the mechanism of hyperthermic enhancements. Some anti-cancer drugs known to have a synergistic effect with hyperthermia include bleomycin, mitomycin C, adriamycin, 5-fluorouracil, carboplatin, and cisplatin (Takahashi 2002).

Clinical hyperthermia can be divided into three separate categories: whole body hyperthermia, regional hyperthermia, and local hyperthermia (including superficial local and interstitial local hyperthermia). The clinical application of heat can be induced by an electromagnetic field technique, ultrasound, or perfusion methods (Falk and Issels 2001). One of the challenges in using hyperthermia for cancer treatment is the restriction of heating locally to the tumor site (Babincova 2001). Other limitations include the non-homogeneous distribution of temperature over the cancer site, low specificity, patient discomfort, and thermotolerance development (Guedes 2005). Additionally, many of the methods are moderately to severely invasive with negative side effects. Overall, hydrogels may potentially be used for the local, synergistic delivery of therapeutic agents for the treatment of cancer.

2.1.2 Hydrogels: Definitions and Applications

Hydrogels are an important class of polymeric materials that have been utilized in a wide variety of biomedical and pharmaceutical applications such as drug delivery, contact lenses, and tissue engineering. Hydrogels are three-dimensional, hydrophilic, polymeric networks that can absorb up to thousands of times their dry weight in water or biological fluids (Peppas 2000; Hoffman 2002). These systems consist of polymer chains with either physical or chemical crosslinks preventing the dissolution of the systems while resulting in swelling of the material upon interaction with aqueous solutions. Hydrogels are advantageous for many biomedical applications due to their resemblance of natural living tissue and inherent biocompatibility which can be partially attributed to their soft, flexible nature and high water content (Hoffman 2002). Hydrogel systems such as poly(hydroxyethyl methacrylate) (PHEMA), poly(N-isopropylacrylamide) (PNIPAAm), poly(vinyl alcohol) (PVA), and

poly(ethylene glycol) (PEG) have been widely investigated for a wide variety of biomedical and pharmaceutical applications.

Despite the many advantages of using conventional crosslinked hydrogels, their applications are often limited due to their poor mechanical and limited response properties (Xiang 2006). The random nature of the crosslinking reactions involved in hydrogel fabrication and the resulting morphological nonhomogeneity can induce these limitations (Haraguchi 2003). Recently, work has been done to improve hydrogel properties (e.g., mechanical strength) and to add unique properties (e.g., response to novel stimuli) through the fabrication of hydrogel nanocomposites (Frimpong 2006; Frimpong and Hilt 2008; Satarkar and Hilt 2008; Satarkar and Hilt 2008; Hawkins 2009; Meenach 2009; Meenach 2009; Satarkar 2009). Hydrogel nanocomposites involve the incorporation of various nanoparticulate materials within a hydrogel matrix which can provide easy, straightforward methods for enhancing the properties of hydrogels. Although a number of fabrication techniques have been used to create such systems, *in situ* polymerization of particles within a monomer solution is a common way to create hydrogel nanocomposites.

There are a handful of hydrogel-based systems that are currently commercially available. One of the more widely studied systems is a once-yearly administered histrelin acetate hydrogel implant that is used in the treatment of prostate cancer. The prolonged release of histrelin suppresses testosterone production in the body reducing and often arresting the growth of prostate tumors. This device has been used under the trade name Vantas (Indevus Pharmaceuticals Inc.) in the U.S. for more than four years for patients with advanced prostate cancer (Schlegel 2009). One study of this system shows the pharmacokinetics and pharmacodynamics of the hydrogel implant for patients for 1 year indicating its effectiveness for prolonged histrelin delivery for testosterone suppression (Dineen 2005).

ProGEL™ Pleural Air Leak Sealant, a hydrogel polymer sealant that forms when mixing human serum albumin and a PEG-based crosslinker, has been developed by Neomend

Inc. The resulting seal may be utilized to seal pleural air leaks during lung surgery (Neomend 2010). Amar Sawhney has turned several hydrogel-based inventions into FDA-approved products (McBride 2008). These include using hydrogels as surgical sealants, spacers between tissues undergoing radiation to protect healthy surrounding tissue, and a product to help treat adult incontinence. Other products include extended wear contact lenses (CooperVision 2008), NanoDOX™ Hydrogel, a topical doxycycline hydrogel for chronic wounds (NanoDox 2008), and Avogel Scar Reduction Hydrogel Sheeting to reduce scars (Avogel 2010).

Hydrogels are often used to delivery therapeutics for various applications, and have recently been more widely investigated for the treatment of cancer. A partial list of hydrogel systems currently being investigated and the cancer therapeutics they release can be seen in Table 2.1. The National Cancer Institute has a goal of localizing cancer therapy by using nanoparticles for localized chemotherapy, radiation, immunotherapy, hyperthermia delivery, or a combination of these therapies (Brazel 2009), and it is the belief of many that hydrogel systems may help achieve this goal. Hydrogels are often advantageous for drug delivery because, depending on their formulation, hydrogels can exhibit a variety of drug release profiles determined by their network structure. Thermosensitive and pH-sensitive hydrogels are extensively studied gels because of their responsive-release characteristics. Hydrogels have great swelling capacity and can therefore entrap high molecular weight drugs and often release them in a controlled fashion (DiRamio 2005). Drug release can easily be tailored in hydrogel systems by the type of polymer and crosslinking used, the density of crosslinking, the amount of drug loaded, the method of drug loading, the pH of the release medium, and external stimuli (Singh 2008). Additionally, many hydrogels are biodegradable and can be easily cleared from the body once they lose their functionality. Such degradation is determined by chemical reactions in the hydrogel matrix including polymeric chain breakage due to hydrolytic or enzymatic degradation within the hydrogel system. The degradation

Table 2.1. Partial lists of types of polymers used in hydrogel systems for cancer therapy applications and the types of therapeutics released from such systems.

Types of Polymers Used in Hydrogels

Synthetic Polymers	*Natural Polymers*
N-(2-hydroxypropyl)methacrylamide (HPMA)	Agarose
Poly(N-isopropylacrylamide (PNIPAAm)	Alginate
Poly(acrylamide) (PAAm)	Gelatin
Poly(β-amino ester) (PBAE)	Chitosan
Poly(ethylene glycol) (PEG)	Collagen
Poly(ethyleneimine) (PEI)	Dextran
Poly(lactic-co-glycolic acid) (PLGA)	Histrelin
Polaxamer	Human serum albumin (HSA)
Poly(organophosphazene)	Hyaluronan
Polyacrylamide (PA)	Psyllium
Polyether (PE)	Pullulan
Poly(vinyl alcohol) (PVA)	Silk
Poly(vinylpyrrolidone) (PVP)	

Types of Therapeutics Released from Hydrogel Systems

Chemotherapeutics	*Radionucleotides*	*Other Therapeutics*
Cisplatin (CDDP)	Rhenium-188 (^{188}Re)	Plasmid DNA
Adriamycin (ADM)	Holmium-166 (^{166}Ho)	supercoiled DNA
Paclitaxel (PTX)	^{131}I-norcholesterol (^{131}I)	interleukin-12 (IL-12)
Doxorubicin (DOX)		histrelin
5-fluorouracil (5-FU)		GMCSF
Camptothecin (CPT)		vaccinia virus vaccine
Topotecan (TPT)		
Daunomycin		
Bleomycin A5 (BLM)		
Methotrexate		
Mitomycin C		
Mitoxanthrone		

mechanisms possible for controlling release from biodegradable hydrogels can be surface or bulk erosion (Hamidi 2008). Ultimately, hydrogel implants may provide multi-modality therapies to more effectively treat cancer, especially those that currently have poor survival rates.

2.2 Implementation of Hydrogels for Cancer Therapy

Hydrogels can be implemented in a number of ways for the treatment of cancer. These include solid hydrogels implanted near or within a tumor, solid hydrogels placed at a tumor site post-resection, hydrogels that form *in situ* after being injected intratumorally, or hydrogel nanoparticles that are delivered systemically or intratumorally. A schematic of these methods may be seen in Figure 2.1. In most cases, hydrogels utilized in drug delivery are usually formed outside of the body and imbibed with drugs before placement in the body. Many crosslinking methods, such as UV, redox, or thermal polymerization, are available to form the hydrogels (Hoare and Kohane 2008). Intratumoral implantation of these hydrogels provides an optimal drug release profile that is characterized by the ability to deliver drug in a large volume and to rapidly reach the therapeutic concentration for an extended time. Previous studies have shown that limited drug penetration distance is one of the major restrictions on the efficacy of intratumoral treatments (Weinburg 2008).

Hydrogel nanoparticles are advantageous in that they are able to load and carry drugs yet they are small enough to travel systemically if desired (Hamidi, Azadi et al. 2008). Also, such nanoparticles can be functionalized so that they travel to and deliver drugs to cancer cells specifically. Targeted drug delivery systems increase the effective dose of the drug and decrease systemic drug toxicity (Hidaka 2006). This molecular targeting therapy is becoming more widely used as a therapeutic method for cancer treatment (Ferro-Flores and de Murphy 2008). Active targeting of cancerous tissue involves the conjugation of particles with a targeting ligand that binds with receptors in the tumor cells. Also, passive targeting takes

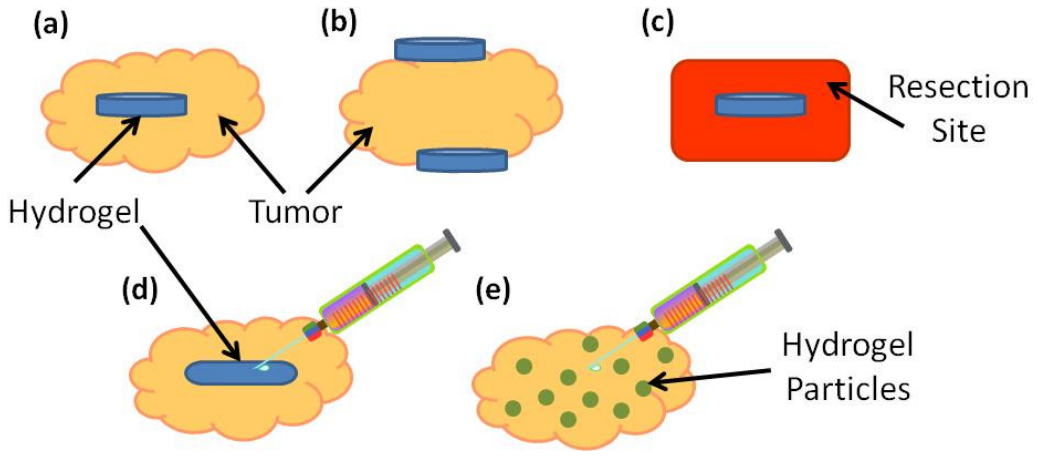

Figure 2.1. Schematic of the methods of implementation of hydrogels for cancer therapy applications. These include: (a) a hydrogel implanted intratumorally, (b) a hydrogel implanted near the tumor tissue, (c) a hydrogel implanted at a site where a tumor was surgically resected, (d) a hydrogel that formed *in situ* when administered via injection, and (e) hydrogel nanoparticles injected intratumorally.

advantage of the enhanced vascular leakage and diminished lymphatic clearance at the tumor site, which leads to the accumulation of the particles in tumor tissue (the so-called enhanced permeability and retention effect). It has been demonstrated that the optimal particle size for high cellular and tumor uptake is in the 100 to 200 nm range (Nair 2008). These methods of implementation can be utilized for the various types of delivery systems such as those delivering chemotherapeutics, radiotherapeutics, or immunotherapy agents.

2.3 Chemotherapeutic Delivery via Hydrogels

Using hydrogels for delivery of cancer therapeutics has been studied extensively. There are many types of bulk hydrogel systems that have been investigated for chemotherapeutic agent delivery comprised of a wide variety of materials which provide the systems with tailorable properties. These include, but are not limited to, stimuli-responsive materials, natural polymers, biodegradable materials, and sol-gel systems. Furthermore, hydrogel particles that have been investigated include both microgels and nanogels (hydrogel nanoparticles). Microgels are hydrogels formed as microscale particles whereas nanogels are particles formed at the nanoscale level. These systems are able to combine the advantages of both nanoparticles and polymeric hydrogels. Stimuli-responsive hydrogels are particularly advantageous as the swelling of the systems can be controlled by external stimuli. Temperature-responsive hydrogels are one of the most commonly studied classes of stimuli-responsive polymer systems in drug delivery research. A common characteristic of these polymers is the presence of hydrophobic groups, such as methyl, ethyl or propyl groups (Qiu and Park 2001). Hydrogel swelling may also be changed through modification in environmental pH or ionic strength, or by exposing the systems to electromagnetic radiation (Peppas 2000; Peppas 2006). In addition, biologically-responsive systems have been developed which include glucose, enzyme, antigen, or redox/thiol-responsive polymers. Field-responsive systems include electro-responsive, magneto-responsive, and ultrasound-

responsive polymers (Roy 2009). Natural polymers are also of great interest for hydrogel cancer therapy. The most common natural polymer, chitosan, has been used in biomedical applications as it is known to be metabolized by certain human enzymes and can be considered biodegradable and biocompatible (Seo 2009). There are also numerous types of biodegradable polymers which may be degraded via enzymatic of hydrolytic mechanisms.

Hydrogel particles are advantageous as they can retain the properties outlined above while being delivered systemically. The particles are often able to retain a large amount of drug and can be delivered to specific locations via ligand-mediated targeting or passive targeting. These systems are also able to be tailored for specific release rates and can be designed to degrade so there is little concern with their removal from the body. There are numerous types of polymers used in these systems including poly(butyl acrylate), poly(ethylene oxide-poly(ethyleneimine), poly(vinylpyrrolidone), and poly(N-isopropylacrylamide). Examples of all of these types of systems will be covered in the next section.

2.3.1 Hydrogel Systems

Hydrogels have been widely utilized in cancer therapy applications for the delivery of an assortment of chemotherapeutic agents. One of the first examples using hydrogels for delivery of chemotherapeutics was by Jeyanthi and coworkers (Jeyanthi and Rao 1990) who used collagen-poly(hydroxyethyl methacrylate) (HEMA) hydrogels for this application. The chemotherapeutics, 5-fluorouracil (5-FU), bleomycin A2 (BLM), and mitomycin C (MMC) were entrapped in the hydrogel matrix and their *in vitro* release rates were found to follow zero-order kinetics indicating controlled release. 98% of 5-FU was released in 10 days, 52% of MMC was released in 12 days, and 74% of BLM was released over 11 days (Jeyanthi and Rao 1990). Another group of investigators showed that N-(2-hydroxypropyl methacrylamide) (HPMA) hydrogels successfully delivered doxorubicin (DOX) for the treatment of BLC1

leukemia in mice. After the DOX-loaded hydrogels were implanted in the mice, the drug was detectable in the bloodstream at therapeutic concentrations for more than 4 days. In addition, animals treated with free DOX survived for 35 days versus 60 days for those treated with the DOX-loaded hydrogel implant showing better efficacy with this type of therapy (St'astny 2002). Hydrogels containing L-phenylalanine and L-histidine complexed with cisplatin were developed by Casolaro and coworkers (Casolaro 2009). The cisplatin release profile showed an initial burst effect followed by a near zero-order release profile over the course of 7 days. The poly(N-acryloyl-L-phenylalanine)-based hydrogel loaded with a water/DMSO mixture released cisplatin three times greater than a gel loaded with water alone. However, the cisplatin released from the hydrogels loaded with only water retained its cytotoxic activity toward Me665/2/21 human melanoma cells, whereas there was no cytotoxic effect from the drug released from the water/DMSO loaded hydrogels indicating more optimization may be necessary for this system.

A more sophisticated system developed by Tauro and coworkers included hydrogel matrices complexed with matrix metalloproteases (MMP) for the controlled delivery of active cisplatin to tumor tissues (Tauro and Gemeinhart 2005; Tauro and Gemeinhart 2005). Because MMPs are expressed and overactive in cancers such as malignant gliomas, such a hydrogel system will allow for the active release of cisplatin only at the tumor site. Poly(ethylene glycol) diacrylate (PEGDA) hydrogels were made with crosslinks containing pendant MMP-sensitive peptides. Cisplatin was either entrapped in the hydrogels (without peptide) or complexed to the MMP-sensitive peptides within the hydrogels. With this scheme, cisplatin was released from the hydrogels as the free, native drug whereas when peptides were incorporated in the hydrogel, it was released as both free cisplatin and cisplatin-peptide complex. This system was the first reported for locally retaining a chemotherapeutic as a hydrogel-prodrug that can be activated by naturally occurring extracellular proteases available in cancer cells.

Sol-gel hydrogels are systems that act as aqueous polymer solutions (usually at room temperature) but form a more solid hydrogel once injected in the body and/or when they are exposed to body temperature. Two such systems have been investigated for applications in cancer therapy. Poly(organophosphazine)-paclitaxel conjugates were synthesized via covalent ester linkage between paclitaxel (PTX) and a carboxylic acid-terminated poly(organophosphazine) for their use in antitumor applications (Chun 2009). Aqueous solutions of these conjugates showed a sol-gel transition dependent on external temperature and after local injection at the tumor site. Upon release from the hydrogel, the polymer-drug complex was taken up by the cells where lysosomal enzymes cleave the PTX-polymer complex releasing the active free PTX. These hydrogels were shown to inhibit tumor growth more effectively than paclitaxel and saline alone. Similarly, aqueous poly(organophosphazine) solutions containing DOX were transformed into hydrogels at body temperature due to hydrophobic interactions. The release of DOX was sustained over 20 days and *in vitro* studies with mouse lymphoblast cells showed the efficacy of DOX released from the gels (Kang 2006). Overall, these systems are beneficial as they are able to increase the solubility of hydrophobic anticancer drugs such as paclitaxel. The polymer surrounds the drug in such a way as to prevent it from attaching with water molecules, while the hydrophilic part of the polymer has positive interactions with surrounding water molecules increasing solubility of the system (Kang 2006).

Stimuli-responsive hydrogels have also been used to deliver chemotherapeutics. For example, Kang and co-workers synthesized thermosensitive [$Np(IleOEt_{)1.20}(AMPEG550)_{0.80]n}$] hydrogels (Kang 2006) where AMPEG500 is α-amino-ω-methoxy-poly(ethylene glycol) and IleOEt is L-isoleucine ethyl ester. The release of the DOX using the hydrogels was analyzed over 20 days, showing control of the drug release. The delivery effect was further observed using cancer cell line of mouse lymphoblast of P388D1, and it was observed that this drug release remained constant over 30 days with no initial burst release. Similarly, a synthetic

pH/temperature-sensitive block copolymer was used for the sustained delivery of PTX over 36 days with various drug loadings (Shim 2007). The PTX-loaded polymer was injected subcutaneously into tumor-bearing mice and the systems showed good anti-tumor effect for 2 weeks and induced strong apoptosis in tumor tissue.

pH-responsive, psyllium and polyacrylic acid-based hydrogel networks were prepared by radiation-induced crosslinked polymerization and showed successful delivery of 5-fluorouracil (Singh 2008). This system may be ideal to use for delivery of drug to the colon as they could act as a double potential drug delivery device because psyllium itself has therapeutic importance in reducing colon cancer risk. Additionally, the vasculature of tumors is often insufficient to supply enough oxygen and nutritional needs for the expanding tumor. The production of lactic acid under hypoxic conditions and the hydrolysis of ATP in an energy-deficient environment contribute to an acidic micro-environment surrounding the tumor cells. Because of this, it has been proposed that such pH-induced release of anti-cancer drugs from pH-sensitive hydrogels could be a good mode of cancer treatment.

Hydrogel composites are systems that combine conventional hydrogels with particulate materials improving on the characteristics of the hydrogel systems. An example of this type of system is a two-phase hydrogel containing topotecan (TPT)-loaded liposomes entrapped in a PEG-based hydrogel (Lalloo 2006). The physically entrapped TPT released rapidly from the pure hydrogel system whereas controlled release was demonstrated for the two-phase system. Rats inoculated with MAT B III breast cancer cells treated with this system had longer tumor growth suppression and did not exhibit body mass loss in comparison to other treatment modalities. Overall, bulk hydrogels may be easy to implement and characterize, but they often lack the ability to degrade and therefore the necessity for post-treatment surgery may be necessary for their removal so other systems must be utilized.

2.3.2 Hydrogels from Natural Polymers

Hydrogels from natural polymers are also of great interest for cancer therapy. Of these, chitosan is the most commonly studied and Ta and coworkers recently provided an excellent review of chitosan hydrogels for cancer therapy (Ta 2008). Chitosan is both biocompatible and biodegradable. Obara and coworkers developed a photocrosslinkable chitosan hydrogel that successfully delivers paclitaxel (Obara 2005). The paclitaxel remaining in the hydrogel retained its biological activity for at least 21 days and was released *in vivo* upon degradation of the hydrogel. The paclitaxel incorporated gel inhibited the growth of subcutaneously induced tumors with Lewis lung cancer (3LL) cells more effectively than those treated with the chitosan hydrogel, free paclitaxel, and the non-treated control group. Similarly, fibroblast growth factor (FGF)-2 and paclitaxel were released from photocrosslinkable chitosan hydrogels for applications in wound repair, angiogenesis, and tumor growth (Ishihara 2006). PTX was released from the hydrogel in a controlled fashion via bulk degradation of the hydrogels and these systems were shown to effectively inhibit tumor growth and angiogenesis in mice. On the other hand, the release of FGF-2 caused an induction of angiogenesis showing the potential use in wound healing. An *in situ* gelling chitosan hydrogel system was designed to deliver doxorubicin in a sustain time period for the treatment of primary and secondary osteosarcoma in mice. The hydrogel system inhibited the growth of osteosarcoma as well as lung metastasis and also reduced the side effects of DOX in mice (Ta 2009).

Other natural polymers such as human serum albumin (HAS), alginate, and agarose have also been studied. An *in situ* forming drug delivery system consisting of DOX in a human serum albumin/tartaric acid derivative (HAS-TDA) tissue adhesive gel was developed by Kakinoki and coworkers which showed an anti-tumor effect in mice (Kakinoki and Taguchi 2007; Kakinoki 2007). WiDr (human colon carcinoma) were implanted subcutaneously into mice and the tumors grew up to approximately 1 cm in diameter.

Aqueous solution of DOX and HSA-TDA was injected around the tumor via a syringe pump and the gel was shown to reduce tumor volume in comparison to free DOX. Bouhadir and coworkers developed sophisticated alginate-based hydrogels capable of delivering several anti-cancer agents with different types of release (Bouhadir 2001). Methotrexate was incorporated within the pores of the gel, doxorubicin was covalently attached to the polymer backbone of the gel, and mitoxantrone was ionically complexed to the polymer. This resulted in diffusion-controlled release, release via chemical hydrolysis, and release after dissociation from the hydrogels, respectively. A sodium dodecyl sulfate (SDS) micellar/agarose hydrogel nanocomposite was developed for the delivery of the chemotherapeutic drug, camptothecin (CPT) (Liu and Li 2005). CPT was first incorporated into the micelles from SDS and the micellar drug solution was then used in the preparation of the agarose hydrogel. The CPT diffusion from the hydrogels was shown to be Fickian and the SDS prolonged the drug release by reducing the diffusion coefficient of CPT in the gel systems.

2.3.3 Biodegradable Hydrogels

The use of biodegradable hydrogels in the design of novel drug-delivery systems has attracted interest and attention due to the many advantages associated with these systems. These include controlled drug release via degradation as well as the ability to tailor the balance of the hydrophilicity and hydrophobicity of the carriers allowing for the release of different types of drugs (Guo and Chu 2007)). These materials are especially beneficial in cancer therapy as they allows for the implementation of the hydrogel at the tumor site without removal post-therapy. Several of these systems are discussed below. Shikanov and coworkers investigated a poly(sebacic acid-co-ricinoleic acid ester anhydride) biodegradable release implant for the delivery of paclitaxel to tumors in mice. The polymeric formulation with paclitaxel was injected intratumorally (Shikanov 2008) and this was shown to inhibit the growth of the tumors. Casadei and coworkers developed a pH-sensitive and biodegradable

composite hydrogel of methacrylated and succinate derivative of dextran for use in colon specific drug delivery (Casadei 2008). The hydrogel system showed pH-responsive swelling, chemical resistance in simulated gastrointestinal fluids, and yet degradation was shown in dextranase and esterase. The gels were able to effectively release 2-methoxyestradiol. Daunomycin was incorporated into a poly(aldehyde gluronate) hydrogel via labile covalent bonds and showed release from the hydrogel system after the hydrolysis of the linkage between the drug and polymer. These biodegradable devices were shown to successfully release daunomycin in a range from 2 days to 6 weeks while maintaining the biological activity of the drug (Bouhadir 2000). Additionally, fumerate-based unsaturated poly(ester amide) and poly(ethylene glycol) diacrylate systems were used to deliver PTX (Gou 2008) and biodegradable gelatin-based hydrogels were used to deliver cisplatin (CDDP) and adriamycin (ADM).

2.3.4 Microgels and Hydrogel Nanoparticles (Nanogels)

As previously mentioned, hydrogel particles are advantageous in that they exhibit features of both the hydrogels they are made up from and of particulate systems (Hamidi 2008). Microgels have been studied for oral delivery of chemotherapeutics. For example, Bromberg and colleagues evaluated the possibility of using a pH- and temperature-sensitive gel microparticles for this application (Bromberg and Alakhov 2003; Bromberg 2003). Gels made using free-radical polymerization of poly(acrylic acid) (PAA), poly(ethylene oxide) (PEO) and poly(propylene oxide) (PPO) were used. pH-sensitive microgels are useful in this type of delivery due to their ability to stay collapsed in low pHs in the stomach and the ability to swell in higher pHs in the small intestine, allowing for localized delivery. Human colorectal carcinoma (Caco-2) cells were used as the gastrointestinal model. P-glycoprotein (P-gp) is a transmembrane protein known to be overexpressed in Caco-2 cells and other tumor cell lines that pumps drugs out of the cell. The microgels were shown to inhibit P-gp-

mediated doxorubicin efflux from the cells, enhancing passive influx and the overall absorption of the drug by the cells. This group also developed microgels comprised of loosely crosslinked poly(acrylic acid) on which poly(ethylene oxide)-b-poly(propylene oxide)-b-poly(ethylene oxide) (PEO-PPO-PEO, Pluronic) copolymer segments were grafted. These gels showed tailorable surfaces, structures, and ion-exchange capacity depending on the type of Pluronic moiety grafted into the microgels. Studies were done to show the ability of these microgels to uptake various anti-cancer drugs such as mitomycin, doxorubicin, and camptothecin. These materials could potentially be used in oral delivery of anti-cancer drugs due to the strong mucoadhesive properties of the system which allows them to adhere longer onto mucosal tissues, thus providing the potential for sustained release of the loaded drugs by diffusion.

Numerous other microgel systems may be used in cancer therapies via chemotherapeutic delivery. One such systems include ferrogels consisting of hydrogel microspheres synthesized using irradiation of the emulsion of poly(N-vinylpyrrolidone) PVP/ferromagnetic granule with cobalt γ-ray (Chen 2005). These self-assembled PVP/PVA magnetic hydrogel microspheres were used to deliver bleomycin A5 to rabbit auricular VX2 tumors in New Zealand white rabbits in the presence of a 0.5 Te permanent magnet both during and 24 hours after drug perfusion. The microspheres, in conjunction with the permanent magnet, successfully locally delivered the drug which shows the potential for their use in magnetic drug targeting (Adriane 2006). Poly(vinyl alcohol (PVA) hydrogel microparticles were investigated and showed effective delivery of DOX to LoVo colon cancer cells (Cavalieri 2008). Cisplatin was complexed with and released from poly(acrylic acid-co-methyl methacrylate) microparticles where a burst release (40%) was shown in the first day followed by zero-order kinetics. The cisplatin had slightly lower activity and the microparticles themselves exhibited low *in vivo* acute toxicity (Yan 2005). Also, biocompatible chitosan-based microgels were fabricated and loaded with methotrexate

disodium (MTX) and then conjugated to the targeting molecule apo-transferrin. Upon intracellular delivery of the release vehicle, the microgel was exposed to low pH environments that caused the pH-responsive chitosan to swell and release the drug (Zhang 2006).

There are many types of hydrogel nanoparticles that are able to deliver chemotherapeutics. Paclitaxel was successfully delivered from the following systems: PEG-PLA-PEG and PLA-PEG-PLA triblock nanoparticles which give a range of release profiles from 90% total released after 12 days to only 20% released after 14 days (He 2007), poly(ethylene oxide)-modified poly(β-amino ester) nanoparticles (100 - 150 nm) (Potineni 2003), and poly(ε-caprolactone)/Poloxamer 188 (PCL-PXA 188) nanoparticles which were examined to determine their potential to overcome multidrug resistance (MDR) in a paclitaxel-resistant human breast cancer cell line (Zhang 2009). Overall, the PCL-PXA 188 nanoparticles caused a significantly higher cytotoxicity than commercial PCL and free paclitaxel. Doxorubicin has been delivered from multiple nanogel systems. These include pH-responsive PEGylated nanogels comprised of 2-(N,N-diethylamino)ethyl methacrylate used against breast and hepatoma cells (Oishi 2007), pH-sensitive hydrophobized pullulan (PUL)-Nα-Boc-L-histidine (bHis) conjugates which increased *in vitro* cytotoxicity of MCF-7 breast cancer cells (Na 2007), dextran-doxorubicin (DEX-DOX) conjugates encapsulated in chitosan hydrogel nanoparticles which resulted in biodegradable, biocompatible, long circulating system (Mitra 2001), and cholesterol pullulan (CHP) hydrogel nanoparticles conjugated with folic acid (FA) (Hidaka 2006). As the folate receptor (FR) is elevated in many cancers, the FA-CHP nanoparticles exhibited greater cellular uptake in human epidermal carcinoma (KB) cells that overexpress FR. *In vivo* studies indicated tumor volume in nude mice was significantly suppressed by these nanoparticles (Hidaka 2006).

Other hydrogel nanoparticle systems used to deliver chemotherapeutics include PVP/PVA-based hydrogel nanospheres to deliver bleomycin (Guowei 2007), core-shell nanoparticles prepared from block copolymer of methoxy poly(ethylene glycol)-

polycaprolactone (mPEG-PCL) to enhance the circulation time of cisplatin and treat BGC823 (human gastric cancer) and H22 (murine hepatoma) cells (Li 2008), PNIPAAm nanogels for the controlled release 5-FU, methotrexate, and mitomycin C (Blanco 2008), and carboxylic acid-functionalized poly(β-amino ester)-graft-PEG nanogels which delivered cisplatin and showed lower *in vitro* cytotoxicity to SKOV-3 ovarian cells versus free cisplatin (Jin 2007). Additionally, 300 nm self-assembled hydrogel nanoparticles capable of specific targeting were synthesized by Na and coworkers from carboxymethylated (CM)-curdlan, substituted with a sulfonylurea (SU) as a hydrophobic moiety for self-assembly. All-trans retinoic acid (ATRA) was used as their model anti-cancer drug and the nanoparticles were conjugated with lactobionic acid (LBA) due to the ligand-receptor interactions between this moiety and HepG2 hepatic carcinoma cells. It was determined that these hydrogel nanoparticles are useful for the treatment of liver cancer because of the ligand-receptor mediated specific interactions between the particles and HepG2 cells and the controlled release of ATRA (Na 2000).

A very unique utilization of hydrogels for cancer therapy was completed by Lee and coworkers who utilized nanogels in a novel manner to induce necrotic cell death in cancer cells (Lee 2009). Nanogels were fabricated via light crosslinking of oligo(L-lactic acid)-poly(ethylene oxide)-poly(propylene oxide)-poly(ethylene oxide)-oligo(L-lactic acid) and poly(ethylene glycol) grafted poly(L-lysine). The nanoparticle exhibited a drastic volume expansion from 150 nm diameter at 37 °C to 1.4 μm at 15 °C upon a brief cold-shock treatment. The expansion of the nanogels severely damaged the cancer cells through the disruption of the cytoskeleton and vesicular membranes as well as physically rupturing cellular membrane structures which resulted in necrotic cell death.

Overall, there are numerous hydrogel systems that can be used for the delivery of chemotherapeutic agents. These systems have the potential to overcome the limitations of systemic chemotherapy delivery in that the drug may be released locally by a hydrogel depot or the cancer cells may be specifically targeted via hydrogel nanoparticles. Additionally,

these systems may provide advantages to free drug by increasing the delivery, solubility and circulation of the drug while not requiring a continuous intravenous injection of the treatment agent. Fortunately, the use of hydrogel systems is not limited to just the delivery of chemotherapeutic agents and this will be outlined in the remainder of this review.

2.4 Radiation Delivery via Hydrogels

Conventional external radiation therapy is another one of the major treatment modalities used as a first-line treatment of cancer. It is often used in conjunction with chemotherapy and/or surgical resection of a tumor. Despite the wide-spread use of radiation to treat cancer it has several disadvantages including inconvenience (patients are often required to undergo daily treatments for several weeks), local limitations (no systemic delivery), and tissue tolerance, which limits the amount and location of radiation exposure. Brachytherapy, the local delivery of radioactive seeds, is also commonly used, but it has its own disadvantages including complicated implementation and the need to remove the seeds after treatment. Hydrogels that deliver radionucleotides may have the ability to overcome some of these limitations. The radiation would need to be delivered locally from the hydrogel without effecting surrounding healthy tissue and if degradable, there would be no need for removal post-treatment. There are several radionucleotides currently used for the treatment of cancer, the most common being beta-emitters which induce DNA damage in cells (Hamoudeh 2008).

One such radionucleotide is Rhenium-188 (^{188}Re), which decays by beta emission and 15% gamma emission which makes it suitable for both therapeutic and diagnostic purposes. Also, ^{188}Re is suitable because of its deep tissue penetration (11 mm maximum, 3.8 mm average) (Huang 2009). A biodegradable hydrogel comprised of sodium alginate and calcium chloride was fabricated for the delivery of cisplatin (CDDP) and Rhenium-188 for combined regional radiochemotherapy. This therapy was achieved in rats via *in situ* delivery of the

hydrogel system into Fischer-344 rats to treat breast adenocarcinoma induced tumors. Tumor volume measurements were lower after treatment with the CDDP/^{188}Re-loaded hydrogels as compared to various controls with limited changes in kidney function of the rats. Also, the ^{188}Re in the hydrogels allowed for the imaging of the hydrogel location and ^{188}Re distribution throughout the animals (Azhdarinia 2005).

Chitosan hydrogels have been investigated for the delivery of radionucleotides to cancerous tissue. Huh and coworkers developed a Holmium-166 (^{166}Ho)-chitosan hydrogel complex which were injected into Wistar rats with cultured C6 glioma cells. A 97% reduction in the tumor growth rate was shown in these animals and their survival rate was greater than those in the control group (Huh 2005). These materials were then utilized in a phase IIB clinical study with forty patients with hepatocellular carcinoma. The complex was administered percutaneously and after two months, 31 of the patients experienced complete tumor necrosis with survival rates of 87.2, 71.8, and 65.3 % for 1, 2, and 3 years, respectively (Cho 2005; Kim 2006). Crosslinked chitosan implants were also developed as a potential biodegradable device to be used in brachytherapy (Azab 2006). ^{131}I-Norcholesterol was incorporated into the chitosan/gluteraldehyde-based hydrogels, and 80% of the material was released within a month after implantation. Histological examination of the implants without ^{131}I-norcholesterol indicated negligible tissue response to the implants in comparison to degradable sutures (Azab 2006). Chitosan and β-glycerophosphate (β-GP) were used in the preparation of thermosensitive hydrogel (C/GP) nanoparticles for a novel internal radiation therapy (IRT) method for the controlled delivery of ^{188}Re-Tin colloids. Studies showed that the ^{188}Re-Tin colloids within the hydrogel nanoparticles were approximately 12 nm in diameter and these nanoparticles were localized around the injection site for up to 48 hours after injection. This type of IRT could be an effective treatment method for regional radiotherapy (Huang 2009). Azab and coworkers used chitosan-norcholesterol hydrogels to treat a mammary mouse tumor model which prevented 69% of tumor recurrence and

metastatic spread of the disease (Azab 2007). Overall these systems are a promising alternative to current radiation therapy.

2.5 Immunotherapy, Gene Delivery, and Hormone Delivery via Hydrogels

Although these therapies are not yet widely used in conventional cancer treatment, immunotherapy, gene therapy, and hormone therapy have been investigated for cancer therapy applications via hydrogels. Immunotherapy aims to exploit the body's natural anti-tumor defenses by stimulating immunity above a threshold level necessary to overcome tolerance, and thus leading to tumor regression (Havranek 2002). Using the protective mechanisms naturally occurring in the body is attractive for numerous reasons, including low toxicity, a high degree of specificity and the avoidance of cytotoxic drugs. Immunotherapy may provide an additional treatment modality for malignancies that are resistant to conventional cancer therapy. There are a variety of cytokines that have proven to be potentially effective in inducing immune responses in the body to eliminate tumor cells. Interleukin-12 (IL-12) is one of the most feasible cytokines to be utilized in immunotherapy. It induces the Th1 immune response, promotes maturation of cytotoxic T lympohcytes, and promotes stimulation of natural killer cells (Shimizu 2008).

For effective cytokine immunotherapy of cancer, a delivery system that ensures the slow release of cytokines is necessary due to the short half-life of the molecules involved (Shimizu 2008). As such, Shimizu and coworkers have developed cholesterol-loaded pullulan-based hydrogel nanoparticles that are able to encapsulate and stabilize various biological molecules. These nanoparticles were used for the *in vivo* administration of IL-12 for the treatment of fibrosarcoma in mice. The IL-12-loaded nanoparticles were subcutaneously injected into the mice which resulted in the prolonged elevation of IL-12 in the blood serum. Repetitive administration of the nanoparticles resulted in a drastic growth retardation of subcutaneous fibrosarcoma in the mice without causing any serious toxic effects

(Shimizu 2008). Similarly, two types of therapeutic devices were created and tested for the delivery of IL-2 in a mouse tumor model. IL-2-containing macroscopic cylinder-shaped hydrogels and injectable microspheres comprised of methacrylated dextran were investigated and the therapeutic activity was tested in DBA/2 mice with SL2 lymphosarcoma. IL-2 was slowly released from the hydrogel systems over a period of 5 to 10 days and the therapeutic effects were very good or comparable to that of free IL-2. This systems was more advantageous than free IL-2, however, due to continuous delivery after one implantation of the hydrogels versus 5 days of invasive treatments of free IL-2 (De Groot 2002).

GMCSF (granulocyte-macrophage colony-stimulating factor) is a potent cytokine that has been demonstrated to improve the function of antigen presenting cells. Cancer immunotherapeutics involving this agent have resulted in long-lasting and specific anti-tumor immune responses in animal models (Seo 2009). Seo and coworkers developed biodegradable chitosan (CH)-based hydrogels loaded with GMCSF and various anticancer drugs (doxorubicin, cisplatin, or cyclophosphamide) as a chemoimmunotherapeutic agent. The hydrogel system was tested on mice using TC-1 cervical tumor cells, which express the tumor-specific antigen, HPV-16 E7. Delivering both the anticancer drug and GMCSF from the CH hydrogel resulted in synergistic anti-tumor effects via the induction of a tumor antigen-specific CD8+ T cell-mediated anti-tumor immunity. Also, a chitosan-based hydrogel system which contained both doxorubicin and vaccinia virus vaccine expressing Sig/E7/LAMP-1 inhibited tumor growth in mice when injected intratumorally. The result was synergistic when the combined therapy was performed and the survival of the tumor-bearing mice was dramatically improved (Han 2008). Additionally, injectable matrices capable of delivering immunomodulatory factors were obtained by mixing alginate microspheres with soluble alginate solutions. The soft macroporous gels that formed were able to be loaded effectively with IL-2 which were delivered into bone marrow cells (Hori 2009).

Gene therapy has emerged as a new method of cancer therapy targeted at the level of cellular gene expression (Gomez-Navarro 1999). In this approach, the complex cancerous physiological state is changed by delivering nucleic acids to tumor or normal cells where these nucleic acids may be genes, portions of genes, oligonucleotides, or RNA. The delivery of DNA for this application is difficult because once the vector-plasmid DNA is injected into the body, gene expression cannot always been achieved due of the fast diffusion away from the injection site. Therefore, the application of delivery depots such as hydrogels containing plasmid DNA can be used to achieve controlled release over an extended period of time (Fukunaka 2002). Megeed and co-workers investigated the influences of DNA molecular weight, DNA conformation, and hydrogel shape on DNA release from silk-elastin like protein polymer hydrogels (SELP). *In vivo* studies using mice showed that supercoiled DNA was the main form released from the hydrogels (Megeed 2004). Fukunaka and coworkers developed a biodegradable hydrogel through the cationization of gelatin for carriers of plasmid DNA. ^{125}Iodine-labeled plasmid DNA incorporated in cationized gelatin hydrogels were implanted into the femoral muscle of mice and it was found that the intramuscular implantation of the plasmid DNA-incorporated hydrogel enhanced the expression of the plasmid DNA around the implantation site (Fukunaka 2002).

Hormone therapy is also effective in treating and preventing certain cancer, the most prevalent of these being prostate cancer. An implant that delivers histrelin for testosterone suppression has already been shown to decrease prostate cancer incidences (Schlegel 2009). Histrelin-based hydrogels were investigated for the effectiveness of the implants in suppressing testosterone production in men with prostate cancer. Gonadotropin-releasing hormone agonist, histrelin, was reliably released from the gel systems and successfully suppressed testosterone production in male patients with prostate cancer for 12 months after hydrogel implantation. Prostate cancer is very hormone-sensitive and responds to androgen

withdrawal leading to tumor regression and relief of symptoms from metastatic disease (Schlegel 2001).

2.6 Hyperthermia Therapy via Hydrogels

As mentioned previously, hyperthermia is becoming more prevalent in the treatment of cancer when used in conjunction with conventional therapies such as radiation and surgical resection of tumor tissue. Mild hyperthermia is effective in increasing the radiation response of tumors, as it oxygenates both diffusion-limited chronically hypoxic and perfusion-limited acutely hypoxic cells (Song 2001). Additionally, although the role of hyperthermia alone as a cancer treatment may be limited, there is extensive pre-clinical data showing that in combination with radiation it is one of the most effective radiation sensitizers known (Horsman and Overgaard 2007). Similarly, hyperthermia enhances the cytotoxicity of various antineoplastic agents. Applications of selected chemotherapeutic drugs at elevated temperatures has been shown to enhance the inhibition of clonogenic cell growth in both *in vitro* and in animal studies (Hildebrandt 2002). Some of the limitations of some of the current methods of implementing hyperthermia were mentioned previously.

Magnetic fluid hyperthermia (MFH) involves the introduction of magnetic particles into the tumor tissue and exposing the tissue to an external alternating magnetic field (AMF) to increase the temperature in the tumor (Wang 2005). The heating occurs due to the presence of magnetic nanoparticles which heat upon exposure to the AMF. The heating mechanism for superparamagnetic particles is based on Brownian relaxation (rotation of the particle as a whole according to external magnetic field) and Neel effect (reorientation of the magnetization vector inside the magnetic core against an energy barrier) (Babincova 2001). When superparamagnetic particles are used for localized hyperthermia therapy, only a weak magnetic field is needed to generate heat compared to the strong field needed for ferromagnetic particles. The superparamagnetic particles are economical and have been

shown to be biocompatible in many cases (Yang 2007). One of the biggest disadvantages of MFH is the fact that the magnetic nanoparticles are often in an aqueous solution and even if injected directly at the tumor site, there is no method to ensure the particles remain in that location. Hydrogel nanocomposites that can physically entrap nanoparticles in the hydrogel matrix may be used to deliver iron oxide nanoparticles directly to tumor sites so that hyperthermia treatment is locally restricted. Along with delivering heat, these systems would have the ability to deliver other therapeutic agents (chemotherapeutics, radionucleotides, immunotherapeutics) outlined previously for a multi-modality treatment. A handful of systems have already shown potential for this.

For example, temperature-responsive magnetic PNIPAAm hydrogels were synthesized by Ang and coworkers incorporating micron-sized iron and iron oxide nanoparticles. The gels were shown to heat in an alternating magnetic field at a frequency of 375 kHz and field strength range of 1.7 to 2.5 kA/m (Ang 2007). Le Rendard and coworkers developed a magnetic particle-loaded, injectable, *in situ* gelling system for the local delivery of hyperthermia. The gels entrapped magnetic particles within human cancer tumors xenografted in mice. Various systems were studied including a hydrogel, single-solvent organogel, and cosolvent organogel formulation. A poly(ethylene-vinyl alcohol) system in DMSO formed the most suitable system in terms of gel formation and heat delivery (Le Renard 2010). These materials have also shown the ability to remotely delivery drugs through the combination of temperature-responsive materials and the ability of these materials to respond in an AMF because of the heat generated by entrapped iron oxide nanoparticles. Such magnetically-responsive materials offer the benefit of controlling drug release in either a single or multiple pulse formulation which benefits the patient by reducing the total amount of drug required to reach the effective dose, reducing the frequency of administration (Brazel 2009). Satarkar has demonstrated this phenomenon with PNIPAAm gels loaded with iron oxide nanoparticles to deliver a model drug (Satarkar and Hilt 2008). Pulsatile release of the

drug was successful because upon exposure to the AMF, the PNIPAAm gels collapsed, releasing the drug, whereas the amount released was less with the field turned off. Overall, magnetic hydrogel nanocomposites are a promising avenue for multi-modality treatment of cancer and should be investigated further to show their *in vivo* effectiveness.

2.7 Miscellaneous Uses of Hydrogels in Cancer-Related Applications

In addition to using hydrogels for the treatment of cancer, these systems have been used in other cancer-related applications including tumor embolization, three-dimensional cell culture to mimic the tumor microenvironment, tumor imaging, and biosensors. A few examples of these are outlined below.

Dextran hydrogel and Holmium-166 poly(L-lactic acid) microspheres were investigated for their use in tumor embolization of Vx2 rabbit heat and neck cancers. Vx2 auricular tumors in rabbits were embolized via the caudal artery with these microspheres and it was determined that the particles are potential candidates for the embolization of head and neck cancer (van Es 2001). Regarding biosensors, hybridization on a polyacrylamide hydrogel microarray was developed by Fedorova and coworkers for the identification of point mutations in BRCA1 (Fedorova 2006). BRCA1 mutations are associated with a higher risk of breast and ovarian cancer in women (accounting for 56-80% of the total risk during the lifetime) and testing for such mutations allows for better breast cancer prognosis, selection of individual treatment strategy, and prevention of recurrence. The microarray was designed to detect five-point mutations and was tested with 36 control specimens with known genotypes and was then used to examine 65 breast cancer patients. The results demonstrated were that the microarray detects about 90% of all BRCA1 mutations.

Unfortunately, solid tumors are often undetectable with most imaging techniques until they grow to a substantial size. The difficulties in the fluorescent labeling of tumors may be overcome through the use of quantum dots (QDs) which have higher molar extinction

coefficients, increased light emission, better stability, and sustained luminescence in comparison to conventional fluorophores. They also exhibit broad excitation but narrow emission spectra, making them suitable for multi-modal detection. Cancer cells can be tagged with QDs causing them to fluoresce when excited with light allowing for the determination of the location of tumors (Nair 2008). As such, Nair and coworkers developed PNIPAAm hydrogel nanoparticles with embedded quantum dots (QDs) for use as a functional device for tumor imaging (Nair 2008). The hydrogel-encapsulated QDs and QD-PNIPAAm were taken into JHU-31 (prostate) cancer cell lines and tumors in mice. Additionally, in a melanoma model, they also preferentially accumulated in the tumor tissue compared to normal tissue and also showed a 16-fold uptake in comparison to non-derivatized QDs.

The most common application of hydrogels in cancer applications is their use in 3-D cell culture of cancer cells. There are numerous limitations in using 2-D cell culture experiments including the inability to reproduce physiological patterns of cell adherence, cytoskeletal organization, migration, signal transduction, proliferation, differentiation, and response to external stimuli (Hutmacher 2009). It has been demonstrated that 3-D models demonstrate cell-extracellular matrix (ECM) interactions that enhance cell biological activities making them more relevant to living organisms than simple 2-D *in vitro* adhesions (Dainiak 2008). The ECM environment should be mimicked by immobilizing cell adhesive proteins, such as fibronectin, collagen, laminin, or other biomolecules, or by developing synthetic polymers which have some key characteristics of ECM (Dainiak 2008). Hydrogels can allow this to occur. Also, three-dimensional cultures have become more popular for evaluating the therapeutic potential of anti-cancer agents. There are several examples of 3-D cell models including multi-layer cell systems cultured on porous membranes, matrix-embedded cultures of single cells or aggregates using various extracellular matrix compounds, or hollow fiber bioreactors with cell cultured within networks of perfused capillaries (Friedrich, Ebner et al. 2007). Hydrogels have the potential to expand these types of systems.

The establishment of cell-based assays to rapidly detect active drug candidates is an important stage in the testing of anti-tumor therapeutics. For example, a 3-D model for the evaluation of anti-cancer drug sensitivity was developed using hyaluronan hydrogels (David 2008). The crosslinked hydrogel provided a 3-D matrix in which three cell lines (SA87, NCI-H460, and H460M) were able to grow resulting in clusters and colonies of cells within the hydrogel system. When exposed to doxorubicin and 5-fluorouracil, the cancer cells were more resistant in the 3-D model than monolayer cell systems. The 3-D culture allows the cancer cells to adopt behavior similar to what is observed in the natural tissue matrix and mimics *in vivo* behavior better than monolayer cultures. Also, Dainiak and co-workers synthesized macroporous hydrogels using NIPAAm, abRGDm, and abRDGm-NIPAAm (Dainiak 2008). Cells were grown in 3-D cultures in these functionalized materials and further developed by matching cell types with appropriate extracellular matrix components, allowing for the potential of using these 3-D models for more realistic *in vitro* studies. Similarly, an alginate-based hydrogel system was used to examine the role of the transition from 2-D to 3-D cell culture on cancer cell angiogenic capability (Fischbach 2009). It was found that the 3-D integrin engagement within the tumor microvasculature regulates cancer cell angiogenic signaling, making them more valid for use in cancer therapy applications.

2.8 Future Work and Applications

The applications of hydrogels for cancer therapy can definitely be expanded upon in the future. For the combination of radiotherapy and hyperthermia, the effect is greatest for simultaneous application, but this is not necessarily feasible in clinical practice (Wust 2002). Hydrogels could potentially overcome this through the combined delivery of heat and radiotherapeutics. Other future directions include further development of *in situ* gelation, *in vivo* biocompatibility studies on the effect of hydrogels, looking into the treatment of metastasis, using hydrogels for the prevention of recurrence, delivery of other agents such as

plasmids, short oligonucleotides, hormones, antibodies, and peptidic agents (Ta 2008). Further studies also need to focus on hydrogel nanocomposites capable of delivering heat for hyperthermia applications. These materials have been widely investigated for chemotherapeutic delivery and the effectiveness of hyperthermia is well-established so this should be a priority in those studying hydrogels for cancer therapy.

2.9 Conclusions

Hydrogels have been successfully implemented for the treatment of cancer in numerous *in vitro* and *in vivo* applications. This includes using hydrogels and hydrogel particle systems comprised of many types of polymeric materials as implantable or injectable materials to deliver therapeutics. These materials can deliver therapeutics such as chemotherapeutic agents, immunotherapetics, radiotherapeutic agents, and heat. Hydrogels offer great potential to improve upon current conventional cancer therapies which are often limiting. They may also be utilized in non-therapy cancer applications such as biosensors, 3-D cell culture, tumor imaging, and tumor embolization. More *in vivo* studies will be necessary for the future development of these applications.

References

All references are located at the end of the dissertation.

CHAPTER 3

Poly(ethylene glycol)-Based Magnetic Hydrogel Nanocomposites for Hyperthermia Cancer Therapy

(Modified from article published in Acta Biomaterialia, 2009, 6, 1039-1046.)

Hyperthermia, the heating of cancerous tissues to between 41 and 45°C, has been shown to improve the efficacy of cancer therapy when used in conjunction with irradiation and/or chemotherapy. Here, a novel method for remotely administering heat is presented, which involves the heating of tumor tissue using hydrogel nanocomposites containing magnetic nanoparticles which can be remotely heated upon exposure to an external alternating magnetic field (AMF). Specifically, this research explores the use of hydrogel nanocomposites based on poly(ethylene glycol) methyl ether methacrylate and dimethacrylate (PEGMMA/PEGDMA) with iron oxide as implantable biomaterials for thermal cancer therapy applications. Swelling analysis of the systems indicated a dependence of ethylene glycol (EG) content and crosslinking density on swelling behavior where greater EG amount and lower crosslinking resulted in higher volume swelling ratios. Both the entrapped iron oxide nanoparticles and hydrogel nanocomposites exhibited high cell viability for murine fibroblasts indicating potential biocompatibility. The hydrogels were heated in an AMF, and the heating response was shown to be dependent on both iron oxide loading in the gels and the strength of the magnetic field. For proof-of-concept of these systems as a thermal therapeutic, the ability to selectively kill M059K glioblastoma cells *in vitro* with hydrogel nanocomposites exposed to an AMF was demonstrated.

Keywords

Hydrogel nanocomposite, poly(ethylene glycol), hyperthermia, thermoablation, magnetic, thermally-responsive material.

3.1 Introduction

The development of cancer therapeutics is an important component of biomedical research today because even though much has been done to overcome and treat the disease, there are still many types of cancer, such as glioblastoma and pancreatic (Sneed, Stauffer et al. 1998) that have extremely poor treatment success rates. Therefore, multiple-modality treatment has become the preferred treatment approach. Hyperthermia, the heating of cancer tissues to between 41 and 45°C, has been proven to have the potential to provide a straightforward way of treating cancer in combination with well-developed therapeutics such as irradiation and chemotherapy (Falk and Issels 2001). Extensive pre-clinical data has shown that the combination of hyperthermia with radiation and/or chemotherapy improves the efficacy of the prescribed treatment without affecting additional systemic toxicity (Horsman and Overgaard 2007; Issels 2008). Aside from having a cytotoxic effect on cancerous tissue, hyperthermia has been shown to increase tumor blood flow which induces hypoxia, acidosis, and energy deprivation at the tumor site, thereby increasing therapy efficacy (Hildebrandt, Wust et al. 2002).

Thermoablation, the thermal destruction of cells at temperatures above at least 50°C, is another potential cancer therapy method involving heat therapy (Jordan, Scholz et al. 1999). Currently, there are a number of obstacles hyperthermia treatment faces including restriction of local heating into the tumor without damaging surrounding tissue (Moroz, Jones et al. 2002), and the inability to heat the cancer tissue locally without using invasive and uncomfortable heating probes (Guedes, Sadeghiana et al. 2005). This can potentially be overcome through the development of systems which can be delivered to and/or implanted at

tumor sites and remotely heated from outside the body as seen in Figure 3.1. The hydrogel nanocomposite composed here will be fixed in place due to compression by the surrounding tissue, hence, providing local heating and overcoming less-specific whole-body and regional heating. A novel class of biomaterials based on nanocomposite hydrogels, specifically systems composed of PEG and iron oxide, has the potential to be used in such hyperthermia applications. The exposure of the gels to a high-frequency magnetic field will lead to remote heating due to the magnetic particles in the nanocomposite.

Hydrogels are three-dimensional, hydrophilic, polymeric networks that can absorb up to thousands of times their dry weight in water or biological fluids (Peppas 1987; Corkhill 1989; Peppas 2006). They consist of polymeric chains with either physical or chemical crosslinks preventing their dissolution while allowing swelling upon interaction with aqueous solutions. Hydrogels are advantageous for many biomedical applications due to their resemblance of natural living tissue and inherent biocompatibility, which can be partially attributed to their soft, flexible nature and high water content (Peppas 2006). They have been utilized in a wide variety of biomedical and pharmaceutical applications such as drug delivery, contact lenses, and tissue engineering (Peppas 1987; Peppas 2000; Frimpong and Hilt 2007). In particular, poly(ethylene glycol) (PEG)-based hydrogels have been widely investigated and are considered "stealth" systems due to their high water content and the presence of PEG chains which exhibit high biocompatibility. The biocompatibility of PEG stems from its ability to repel protein absorption, due to the hydrophilic nature of the polymer (Nagaoka 1984; Jeon 1991). The PEG polymer component in this research shows the ability to shield iron oxide nanoparticles incorporated in the polymer matrix.

Despite the many advantages of using conventional hydrogels, their applications are often limited due to their poor mechanical strength and somewhat limited response and actuation properties (Xiang 2006). In recent years, hydrogel nanocomposites have received increased interest as a result of their unique properties and expanded applications

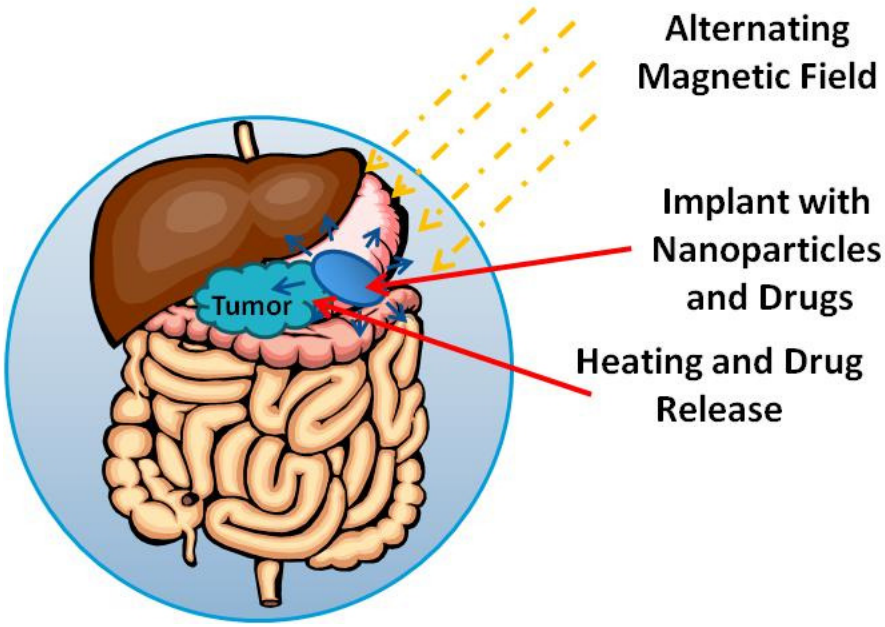

Figure 3.1. Schematic of hydrogel nanocomposites placed near tumor and heated via an external alternating magnetic field.

(Brazel 2009; Hawkins 2009; Satarkar 2009; Schexnailder and Schmidt 2009). Hydrogel nanocomposites involve the incorporation of various nanoparticulate materials within a hydrogel matrix which provides easy, straightforward methods for enhancing the properties of hydrogels. Thus far, a number of nanoparticulates have been utilized in nanocomposite hydrogel systems including metallic nanoparticles, carbon nanotubes, clay, ceramics, magnetic nanoparticles, hydroxyapatite, and semiconducting nanoparticles (Degirmenbasi 2006; Frimpong 2006; Okada and Usuki 2006; Zhang 2006; Meenach 2009; Meenach 2009). The incorporation of magnetic nanoparticles such as iron oxide nanoparticles into hydrogels can create tunable nanocomposites that can be remotely controlled by a magnetic field (Frimpong 2006; Satarkar and Hilt 2008). In recent work by Satarkar and coworkers (Satarkar and Hilt 2008; Satarkar and Hilt 2008), remote-controlled heating and drug release using hydrogel nanocomposites based on N-isopropylacrylamide (NIPAAm) and Fe_3O_4 nanoparticles have been successfully demonstrated. This controlled release was due to the thermally-responsive nature of the NIPAAm, and the remote-controlled heating by applying an alternating magnetic field (AMF) which heated the magnetic nanoparticles present in the hydrogel matrix. Similarly, PEG methyl methacrylates demonstrate a thermal response with tunable lower critical solution temperature (LCST) values depending on the PEG chain length which may also allow them to be used in drug delivery applications (Lutz 2008). At temperatures below the LCST, hydrogel systems are swollen whereas above this temperature the polymer matrix collapses. For these studies, iron oxide nanoparticles (20-30 nm diameter) were incorporated into a PEG methyl ether methacrylate/dimethacrylate hydrogel matrix. Upon exposure to an alternating magnetic field, superparamagnetic iron oxide nanoparticles have the ability to heat primarily due to Brownian movement (frictional losses) and Neel relaxation losses (Babincova 2001; Bahadur and Giri 2003) .

In regards to the biocompatibility of hydrogel nanocomposites, a limited amount of cytocompatibility or hemocompatibility studies have been reported. However, a wide variety

of literature is available regarding the biocompatibility of the hydrogels and nanoparticulate components that make up a hydrogel nanocomposite (Meenach 2009). One of the advantages of hydrogel nanocomposites is that hydrogels can provide increased biocompatibility over exposed, uncoated nanoparticulates because they encapsulate the particulate matter in the composite matrix and providing a barrier between the sensitive tissues and the more harmful nanoparticulates. In a recent publication, the encapsulation of uncoated iron oxide nanoparticles within a poly(N-isopropylacrylamide) hydrogel (Meenach 2009) was shown to exhibit a more favorable cell viability than the nanoparticles themselves. As more hydrogel nanocomposites are fabricated and characterized for various applications, it is important that biocompatibility issues and safety of these materials are examined.

The objective of this research was to develop biocompatible magnetic hydrogel nanocomposites that exhibit favorable swelling and cytotoxicity properties, and these novel biomaterials have the ability to be remotely-heated via an alternating magnetic field. Swelling analysis showed the thermal-responsive nature of the hydrogels, which exhibited deswelling behavior at higher temperatures. In addition, murine fibroblasts exposed to the nanocomposites showed viability similar to that of the control on polystyrene. Also, it was shown that the thermal response of the nanocomposites can be controlled through the AMF field strength so that they exhibit temperatures for either hyperthermia and thermoablative treatment. For proof-of-concept of these systems as a thermal therapeutic, the ability to selectively kill M059K glioblastoma cells *in vitro* with hydrogel nanocomposites exposed to an AMF was demonstrated. Ultimately, these hydrogel systems have the potential to more effectively treat localized tumor via both drug delivery and thermal therapy via hyperthermia.

3.2 Materials and Methods

3.2.1 Materials

The macromers poly(ethylene glycol) (N=200) methyl ether methacrylate (PEG200MMA) and poly(ethylene glycol) (N=1000) methyl ether methacrylate (PEG1000MMA) and crosslinkers tetra(ethylene glycol) dimethacrylate (TEGDMA) and poly(ethylene glycol) (N=400) dimethacrylate (PEG400DMA) were obtained from Polysciences (Warrington, PA). The Fe_3O_4 nanoparticles (20-30 nm diameter, 0.2% PVP-coated) were obtained from Nanostructured and Amorphous Materials (Los Alamos, NM). The initiator, ammonium persulfate (APS), accelerator, N,N,N',N'-tetramethylethane-1,2-diamine (TEMED), and ethanol (95%) were obtained from Sigma Aldrich (St. Louis, MO) at 99 and 98% purity, respectively. All materials were used as received.

3.2.2 PEGMMA-PEGDMA hydrogel fabrication

Magnetic hydrogel nanocomposites were fabricated via free-radical polymerization with various macromer (PEGMMA) and crosslinking (PEGDMA) amounts as seen in Table 3.1, resulting in various crosslinking densities. The structure of these compounds can be seen in Figure 3.2. A schematic describing the fabrication can be seen in Figure 3.3. Ethanol was added to the macromer solution in a 1:1 by weight basis based on the macromer and crosslinker. For hydrogels with iron oxide nanoparticles, the particles were added at 5 weight % based on the macromer and crosslinker and were exposed to an ultrasonic bath for 30 minutes to facilitate dispersion of the iron oxide nanoparticles throughout the solution. After sonication, 2 weight % APS and 4 weight % TEMED were then added to the mixture to initiate the free-radical polymerization. This solution was then sonicated further for 2 minutes before being loaded into a template consisting of two 15 cm by 15 cm glass plates with a 1.5 mm thick Teflon spacer. The gels were kept in this template for

Table 3.1. Hydrogel nanocomposite systems fabricated. For the nanocomposite system column, the numbers before the PEG constituents refers to the mole% added to the feed solution. All gels were made with 5 weight% iron oxide nanoparticles based on the mass of the macromer and crosslinker.

Nanocomposite System	**Abbrev**	**Macromer Feed**	**Crosslinker Feed**
50PEG200MMA-50PEG400DMA	AM	50 mol% PEG200MMA	50 mol% PEG400DMA
80PEG200MMA-20PEG400DMA	BM	80 mol% PEG200MMA	20 mol% PEG400DMA
95PEG200MMA-5PEG400DMA	CM	95 mol% PEG200MMA	5 mol% PEG400DMA
50PEG200MMA-50TEGDMA	DM	50 mol% PEG200MMA	50 mol% TEGDMA
50PEG1000MMA-50PEG400DMA	EM	50 mol% PEG1000MMA	50 mol% PEG400DMA
50PEG1000MMA-50TEGDMA	FM	50 mol% PEG1000MMA	50 mol% TEGDMA

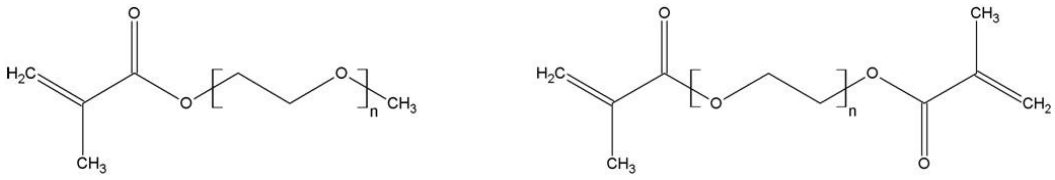

Figure 3.2. Poly(ethylene glycol) methyl methacrylate and poly (ethylene glycol) dimethacrylate structures. n refers to the number of ethylene glycol groups present in the chain.

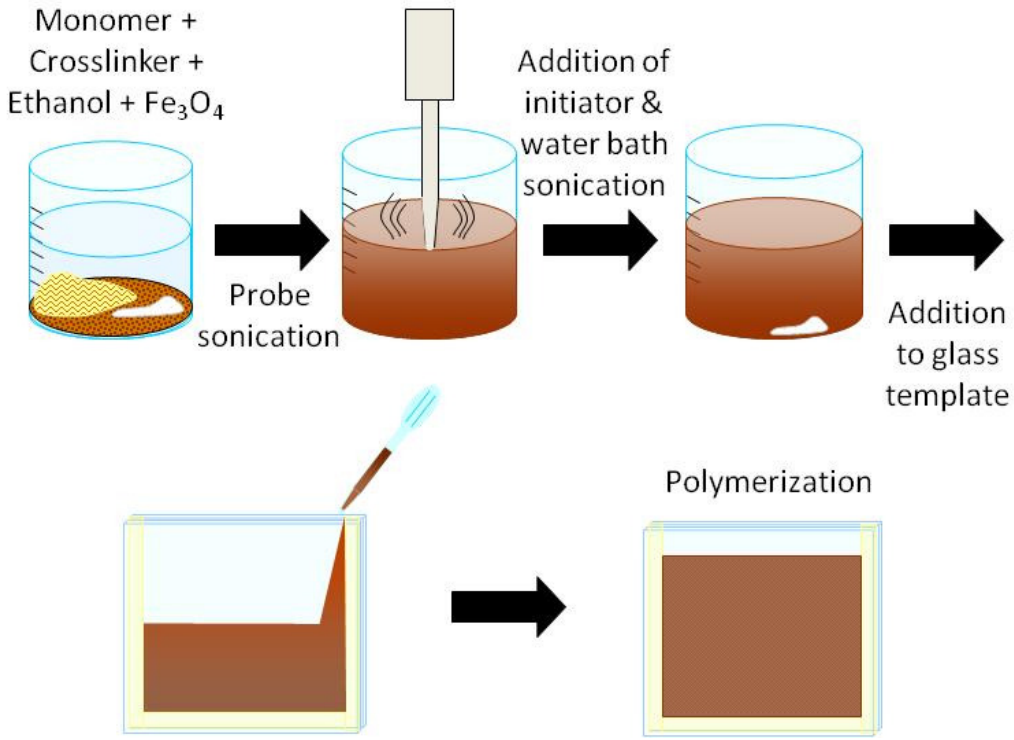

Figure 3.3. Schematic of how magnetic hydrogel nanocomposites were fabricated via free-radical polymerization.

at least 2 hours (usually overnight) to allow for completion of polymerization. To remove any potentially unreacted and potentially toxic macromer, crosslinker, and initiator residues, the hydrogels were washed with deionized water for at least one week.

Attenuated Total Reflectance Fourier Transform Infrared (ATR-FTIR) analysis was performed to determine the conversion of available carbon-carbon double bonds present in the PEG constituents of the hydrogel using a Varian Inc. 7000e step-scan spectrometer. Upon addition of the initiator to the gel solution, a sample of the solution was placed on the diamond ATR crystal and IR spectra were obtained for 90 minutes at 2 scans per minute at 8 cm^{-1} spectral resolution between 700 and 4000 cm^{-1}. The data was analyzed using Varian Resolutions software.

3.2.3 Thermal gravimetric analysis (TGA) of hydrogel nanocomposites

TGA measurements were made to determine the actual iron oxide nanoparticle loading in the hydrogel nanocomposites using a TA Instruments Q500 thermogravimetric analyzer. A dry hydrogel sample of approximately 10 mg was exposed to heat at a rate of 20°C min^{-1} in nitrogen flow conditions. At 120°C the sample was heated isothermally for 10 minutes to vaporize residual water and other volatile compounds before being heated to a final temperature of 700°C. Final TGA data was obtained after normalizing the results with respect to the gel mass at 120°C.

3.2.4 Swelling characterization

Equilibrium swelling characteristics of the PEG-Fe_3O_4 hydrogel nanocomposites and pure PEG hydrogels were measured using a gravimetric method based on a comparison of the density measurements of both swollen and dry gels at equilibrium as described previously (Frimpong 2006). Upon the completion of synthesis and washing, hydrogel discs 13.8 mm in diameter were cut from the bulk hydrogel films. The discs were then placed in phosphate

buffered saline solution (PBS, pH 7.4) for at least 3 days to reach equilibrium. The mass of the discs were measured in air and then in n-heptane (non-solvent) in their swollen state at 22, 37, 43, and 63°C and in their dry state. Heptane was used for volumetric swelling studies as it interacts little if any, with water in the hydrogel system. The masses of the hydrogels both dry and swollen states in air and n-heptane then allowed for the calculation of the volume swelling ratio (Q) at equilibrium:

$$Q = \frac{V^s}{V^d} = \frac{\left(\frac{M^s_{air} - M^s_{heptane}}{\rho_{heptane}}\right)}{\left(\frac{M^s_{air} - M^s_{heptane}}{\rho_{heptane}}\right)} = \frac{M^s_{air} - M^s_{heptane}}{M^d_{air} - M^d_{heptane}} \quad (1)$$

where V is the volume of the sample, $\rho_{heptane}$ is the density of n-heptane, M_{air} is the mass of the sample in air, and $M_{heptane}$ is the mass of the sample in n-heptane. The subscripts s and d refer to the swollen and dry forms of the samples, respectively.

3.2.5 Cytotoxicity analysis of iron oxide nanoparticles and hydrogel nanocomposites

The iron oxide nanoparticles and hydrogel nanocomposites were analyzed for tissue cytotoxicity using NIH 3T3 murine fibroblasts (American Type Culture Collection, ATCC Manassas, VA). Fibroblasts were cultured in Dulbecco's Modified Eagle's Medium supplemented with 10% v/v calf bovine serum, 100 I.U/ml penicillin, 100 µg/ml streptomycin (ATCC), and 1 µg/ml antimycotic Fungizone® (Invitrogen, Carlsbad, CA) at 37°C and 5% CO_2 in a humidified incubator. The cells were used from passages 5 to 8.

For iron oxide nanoparticle analysis, fibroblasts were seeded at 2500 cells/cm^2 in a polystyrene 12 well plate. After 24 hours, the media was aspirated and 1 ml of nanoparticles suspended in complete medium (at 100, 500, and 1000 µg/ml) was added to each well. The well plates were then returned to the incubator for 24 and 48 hour exposure time periods after

which the fibroblasts were assayed for cell viability. A two-color fluorescence Live/Dead Viability Assay® (Molecular Probes, Carlsbad, CA) was used to assess the cell viability of both attached and unattached fibroblasts. A schematic of this process can be seen in Figure 3.4. Stained samples were observed using a NIKON Eclipse 80i microscope at 50x magnification. The percent cell viability (live cells/total cells) was determined by manually counting the live and dead cells imaged with NIS-Elements software. Both attached and unattached fibroblasts were analyzed in three separate samples with ten images (5 live and 5 dead) taken for each.

For hydrogel analysis, the gels were cut into discs (12.5 mm diameter), placed in complete fibroblast medium and incubated at 37°C for 48 hours as seen in Figure 3.5. NIH 3T3 murine fibroblasts were seeded at 2500 cells/cm^2 for 24 hours in 12 well-plates. The medium was then aspirated from the wells and discarded. Next, the medium that the hydrogels were soaked in was placed over the fibroblasts. The well plates were then returned to the incubator for 24 and 48 hours. Afterward, both the attached and unattached cells were assayed for cell viability using the method described above.

3.2.6 Remote-controlled heating of nanocomposite hydrogels

Prior to heating, hydrogel nanocomposites were cut into discs (8.2 mm in diameter) and equilibrated in PBS at room temperature (22°C). Remote-controlled heating of the hydrogel nanocomposites was completed using an alternating electromagnetic field induced by a Taylor Winfield induction power supply (model MMF-3-135/400-2) equipped with a solenoid with a 15 mm diameter and 5 turns. The hydrogel discs at their equilibrium swollen state were covered with Saran wrap, placed on top of the solenoid coil and exposed to the alternating magnetic field. Two types of thermal analyses were performed. First, all six hydrogel nanocomposite systems were exposed to the same magnetic field power at 297 kHz and 25 kA/m. Then, the hydrogel systems were heated to either hyperthermia temperature

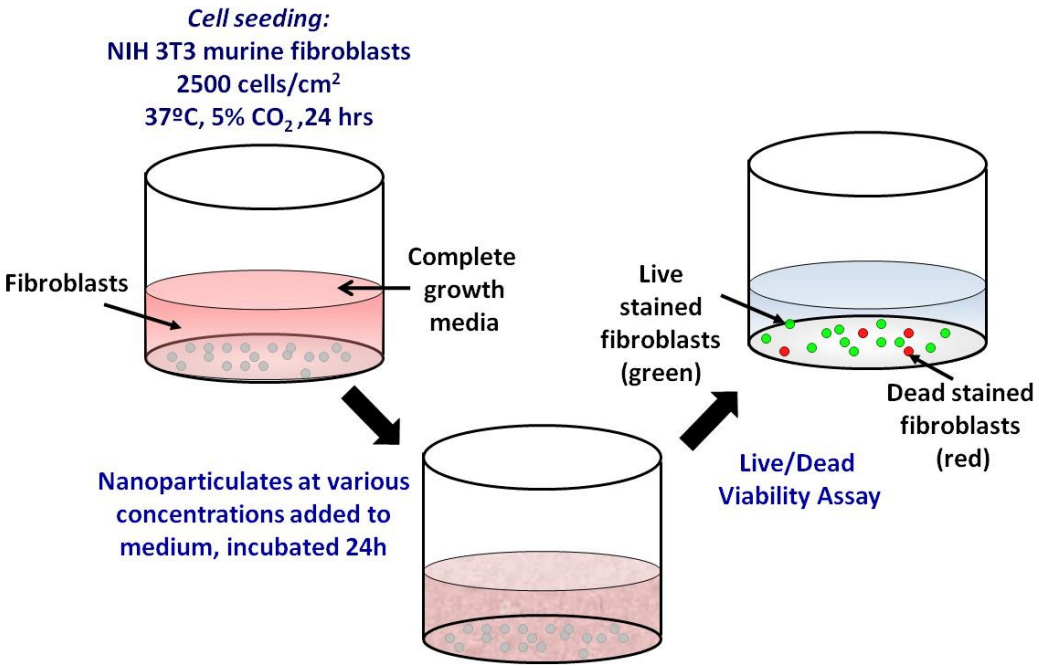

Figure 3.4. Schematic showing the cytotoxicity analysis of iron oxide nanoparticles. NIH 3T3 murine fibroblasts were exposed to the nanoparticles in solution then stained with a Molecular Probes Live/Dead stained and imaged for viability.

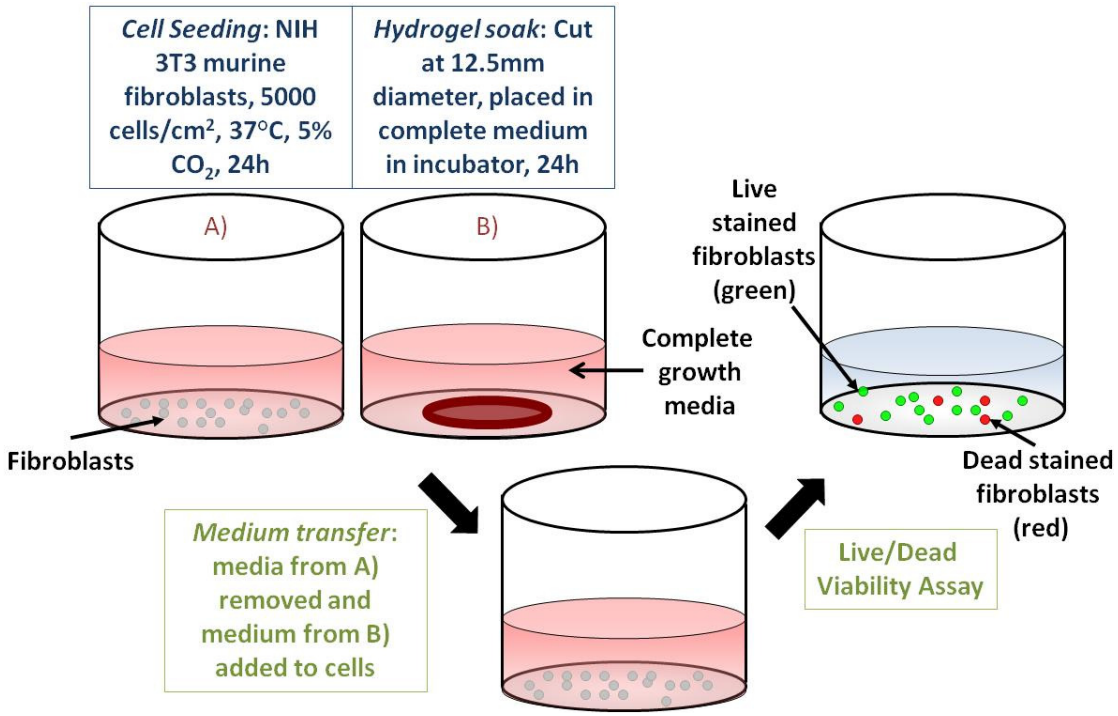

Figure 3.5. Schematic of the cytotoxicity analysis of magnetic hydrogel nanocomposites soaked in complete medium for 24 hours. NIH 3T3 cells were exposed to the media wash solution and stained with a Live/Dead stain prior to fluorescence imaging to determine cell viability.

range (41-44°C) or thermoablative temperature range (61-64°C) by controlling the magnetic field strength. Thermal images and data were acquired using an infrared camera (AGEMA Thermovision 470) which recorded the surface temperature of the hydrogels. The surface temperature was recorded continuously for 5 minutes.

3.2.7 M059K glioblastoma cell thermoablation via hydrogel heating

PEG-based magnetic hydrogels were used to demonstrate that cancer cells can be killed by heat generated by hydrogel nanocomposites upon exposure to an alternating magnetic field (via thermoablation). As seen in Figure 3.6, M059K glioblastoma cells (ATCC) were cultured in DMEM/Ham's F-12 medium supplemented with 0.05 mM non-essential amino acids and 10% fetal bovine serum at 37°C and 5% CO_2 in a humidified incubator. The cells were then seeded in 35mm culture dishes at 20,000 cells/cm^2 and incubated for 24 hours. 50 mole% PEG400MMA/50 mole% TEGDMA hydrogel nanocomposites were cut at 8.2 mm and equilibrated in PBS overnight at room temperature. Prior to heating, the gels were placed in Saran wrap to prevent water loss, and then placed on the AMF coil. M059K cells were removed from the incubator, medium was aspirated from the culture dish, and the dish was placed directly on the hydrogel for heat treatment. The gel and cells were then exposed to the AMF (297 kHz, 18 kA/m) for 5 minutes. An IR camera was used to collect still IR images at the end of the heating experiment to show the actual temperature of the cells after exposure. Controls were done with the cells only (with no hydrogel) exposed to the AMF and with cells exposed to no field, both with medium removed for 5 minutes. Upon heat and AMF exposure, the cells were returned to the incubator for 2 hours to allow time for cellular response to the heat treatment and then assayed using the Molecular Probes Live/Dead Assay and fluorescence imaging.

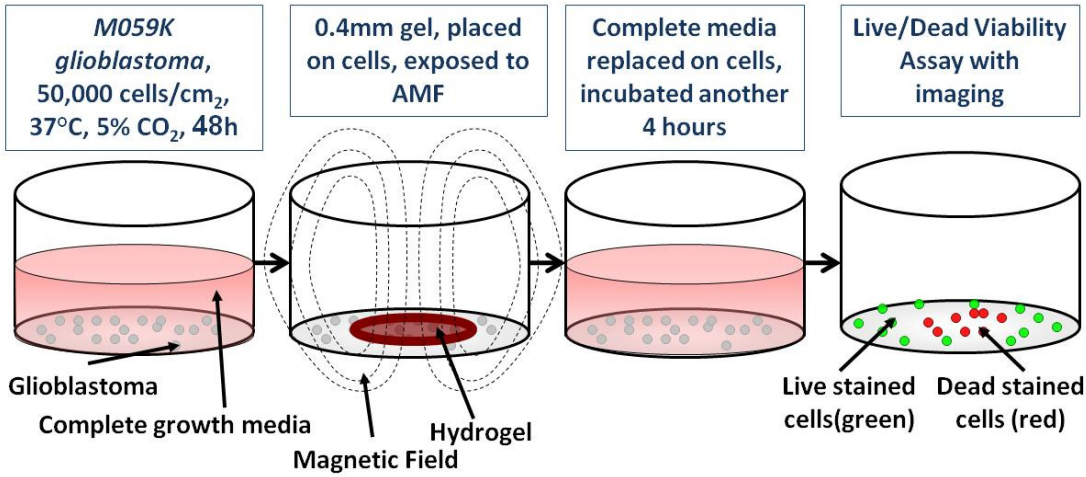

Figure 3.6. Schematic of how M059K glioblastoma cells were exposed to heat from magnetic hydrogel nanocomposites exposed to an AMF to induce cell death via thermoablation. The cells were exposed for 5 minutes, returned to the incubator for 2 hours, then assayed via a Live/Dead stain for fluorescence imaging.

3.2.8 Statistical analysis

All experiments were performed at least in triplicate. MYSTAT 12 for Windows (12.02.00) was used for t-tests (paired t-test with unequal variances) to determine any significance in observed data. A p-value of <0.05 was considered statistically significant.

3.3 Results

3.3.1 Polymerization analysis and TGA characterization of hydrogel nanocomposites

ATR-FTIR was used to determine the conversion of carbon-carbon double bonds present in the hydrogels. Both PEGMMA and PEGDMA have C=C bonds which undergo free radical polymerization to form the crosslinked hydrogel systems which decreases the amount of C=C bonds available. The conversion of the double bonds of the PEG constituents was determined using standard baseline techniques from the peak area of 1637 cm^{-1} for C=C vibration and using the area of 1713 cm^{-1} for C=O stretching as a reference. The C=C conversion data can be found in Appendix A, Figure A.3.1. The percent conversion of the double bonds was calculated from:

$$\%\ Conversion = \left(1 - \frac{R_f}{R_0}\right)\ x\ 100\% \qquad (2)$$

where R_f is the ratio of the peak area of the C=C to the reference peak area of C=O at the final time (90 minutes) and R_0 is the ratio of the same peak at the initial time. The conversion for all of the hydrogel nanocomposites after 90 minutes was at least 93% as seen in Table 3.2 indicating that the majority of the hydrogels were nearly completed reacted.

TGA was performed to determine the actual iron oxide nanoparticle loading in the hydrogel nanocomposites. For all hydrogel nanocomposites, the iron oxide loading was found

Table 3.2. Summary of characterization results for C=C conversion via ATR-FTIR, murine fibroblast % cell viability for iron oxide nanoparticles and hydrogel nanocomposites at 24 and 48 hours, final temperature values for the gels exposed to AMF at constant field strength, calculated iron oxide mass for the heated gels and AMF strengths needed for hyperthermia and thermoablative temperatures.

System	C=C % Conv.	Fibroblast % Cell Viability (24h)	Fibroblast % Cell Viability (48h)
50PEG1000MMA-50TEGDMA	96.3	95.7 ± 1.4%	97.2 ± 3.3%
95PEG200MMA-5PEG400DMA	94.2	97.3 ± 0.9%	97.4 ± 2.5%
50PEG1000MMA-50PEG400DMA	99.4	97.9 ± 0.5%	96.8 ± 0.8%
80PEG200MMA-20PEG400DMA	97.3	96.0 ± 2.0%	97.8 ± 2.2%
50PEG200MMA-50PEG400DMA	93.3	97.0 ± 2.5%	97.8 ± 2.5%
50PEG200MMA-50TEGDMA	95.0	96.9 ± 1.0%	98.0 ± 2.1%
100 μg/ml Fe_3O_4	---	98.3 ± 0.5%	99.1 ± 0.1%
500 μg/ml Fe_3O_4	---	98.1 ± 0.4%	98.1 ± 0.6%
1000 μg/ml Fe_3O_4	---	98.0 ± 0.2%	98.0 ± 0.5%
Control	---	97.9 ± 0.6%	98.3 ± 1.3%

Table 3.2 (con't). Summary of characterization results for C=C conversion via ATR-FTIR, murine fibroblast % cell viability for iron oxide nanoparticles and hydrogel nanocomposites at 24 and 48 hours, final temperature values for the gels exposed to AMF at constant field strength, calculated iron oxide mass for the heated gels and AMF strengths needed for hyperthermia and thermoablative temperatures.

System	**Final T at 25 kA/m (°C)**	**Fe_3O_4 Mass/Gel Volume (mg/cm^3)**	**Hyper. AMF Strength (kA/m)**	**Thermo. AMF Strength (kA/m)**
50PEG1000MMA-50TEGDMA	60.7 ± 0.7	1.58	17.3	25.3
95PEG200MMA-5PEG400DMA	59.5 ± 1.1	1.92	17.4	25.9
50PEG1000MMA-50PEG400DMA	65.7 ± 1.7	2.74	16.5	24.2
80PEG200MMA-20PEG400DMA	66.1 ± 0.7	5.32	14.7	22.0
50PEG200MMA-50PEG400DMA	73.8 ± 0.8	7.24	14.3	23.0
50PEG200MMA-50TEGDMA	79.6 ± 1.3	7.93	12.7	17.4
100 μg/ml Fe_3O_4	---	---		
500 μg/ml Fe_3O_4	---	---		
1000 μg/ml Fe_3O_4	---	---		
Control	---	---		

to have a range of 5.48 ± 0.65 weight % (raw data shown in Appendix A, Figure A.3.2) which is close to the initial loaded amount.

3.3.2 Characterization of hydrogel nanocomposite swelling behavior

The analysis of swelling behavior of hydrogels is necessary for determining the ability of the gels to retain fluids for drug delivery applications. Hydrophobic drugs such as estradiol and insulin (DiRamio, Kisaalita et al. 2005) and protein (bovine serum albumin) (Mellott, Searcy et al. 2001) have already been successfully delivery from PEG-based hydrogels. The swelling behavior of the nanocomposite gels was analyzed to determine the effects of iron oxide nanoparticle loading, crosslinking ratio, crosslinking and macromer types, and temperature. Mesh size of the hydrogel systems was calculated using the Flory-Rehner equation which incorporates the Peppas-Merrill modification (Flory 1953; Peppas and Merrill 1976). The mesh size was determined to be on the order of 10-20 angstrom, which is an order of magnitude smaller than the iron oxide nanoparticles incorporated into the hydrogel matrix. As such, it is hypothesized that the nanoparticles are physically entrapped in nanocomposite and therefore particle loss from the systems is negligible (nor has it been observed).

The following descriptions apply for the hydrogels at 22°C. For the PEG200MMA/PEG400DMA systems, the amount of crosslinking varied from 5 to 50 mole%, and as the amount of crosslinking increased, the swelling ratio decreased as seen in Figure 3.7. As the amount of crosslinking is increased, the mesh structure of the hydrogel is tighter which does not allow as much water into the system. For 50 mole % PEG200MMA crosslinked with 50 mole % PEG400DMA or TEGDMA, the volume swelling ratio was the same irrespective of the crosslinker used. For 50 mole % PEG1000MMA systems with either crosslinker, the volume swelling ratio was higher for the gel with TEGDMA versus the system with PEG400DMA. This is contradictory to what was expected. TEGDMA has a much shorter PEG chain length in comparison to PEG400DMA (approximately 4.5 versus 9 PEG groups,

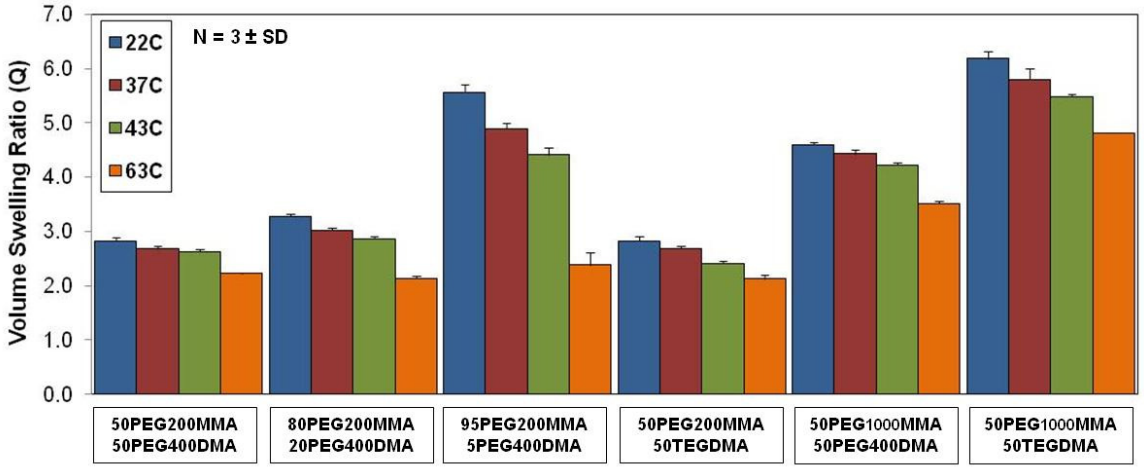

Figure 3.7. Swelling analysis results for all PEG hydrogel nanocomposites at 22, 37, 43, and 63°C showing the volume swelling ratio (Q) for each system.

respectively), and it is expected that a system crosslinked with TEGDMA would exhibit a tighter gel mesh and therefore have a smaller swelling ratio. It is hypothesized that in this case, primary chain cyclization may have an effect on the structure of the hydrogel. This occurs when a propagating radical reacts intramolecularly with a pendant double bond on the same chain, (Elliott 2001). This results in a decrease in the crosslinking density and an increase in the space between crosslinks. For these systems, the solvent (ethanol) concentration was relatively high (1:1 by weight of the macromer and crosslinker) which is known to increase the probability of primary cyclization.

For the PEG200MMA and PEG1000MMA systems crosslinked with PEG400DMA, the volume swelling ratio was smaller for the system containing the PEG200MMA macromer. This is because the ethylene glycol (EG) content of PEG200MMA is much less than that of PEG1000MMA (by a factor of 5) which makes the system less hydrophilic. For the same macromers crosslinked with TEGDMA, the swelling ratio for PEG200MMA versus PEG1000MMA was also lower resulting from the decreased EG content. Iron oxide nanoparticle loading had a slight effect on the swelling of the PEG-based hydrogel nanocomposites. The gels with iron oxide nanoparticles exhibited slightly higher volume swelling ratios than those without nanoparticles (data not shown). This may be attributed to the particles interfering with the macromers and crosslinkers to cause less effective crosslinking during the polymerization.

The PEG-based hydrogels were shown to be thermally-responsive as seen by the change in their swelling properties when exposed to various temperatures. The swelling ratios for all systems decreased as they reached their approximate LCST. For the PEG200MMA hydrogels, the volume swelling ratio was approximately 2.2 at 63°C which is above the LCST (Lutz 2008) of this compound explaining the partial collapse of the hydrogel structure. This attribute of the hydrogels may allow them to be used in controlled drug delivery applications

when switching the temperature of the system from below their LCST at room temperature to above it in the body.

3.3.3 Cytotoxicity analysis of Fe_3O_4 nanoparticles and hydrogels

The effects of iron oxide nanoparticles on the cell viability of fibroblasts after 24 and 48 hours are shown in Table 3.2. For all nanoparticle concentrations, the cell viability was statistically insignificant in comparison to the control sample regardless of the amount of nanoparticle loading in the medium ($p > 0.05$). This indicates that the iron oxide nanoparticles have the potential to be biocompatible (most likely due to their polymeric coating) and thus should not be recognized by the body as foreign objects should they leach from the hydrogel nanocomposites.

After the hydrogels were soaked in complete fibroblast medium for 48 hours, the medium was transferred to fibroblasts for 24 and 48 hours. The results determined whether or not any harmful substances leached from the hydrogels into the medium. As seen in Table 3.2, for all hydrogel systems, the cell viability was favorable and close to that of the control ($p > 0.05$). This indicates minimal or no leaching of substances from the hydrogels, which was as expected. Figure 3.8 shows the favorable response of the fibroblasts exposed to both the nanoparticles and gel-exposed medium in comparison to a control on polystyrene. The cells have good morphology and look similar to those of the control. Similar cell morphology was seen for cells exposed to all nanoparticle concentrations and hydrogel systems (results not shown). Overall, these results indicated that magnetic PEG-based hydrogel nanocomposites have the potential to be biocompatible.

3.3.4 Characterization of the remote-controlled heating of nanocomposite hydrogels

Swollen hydrogels equilibrated at 22°C were exposed to an alternating magnetic field for 5 minutes at 297 kHz and 25 kA/m to induce heating within the system. As seen in Figure

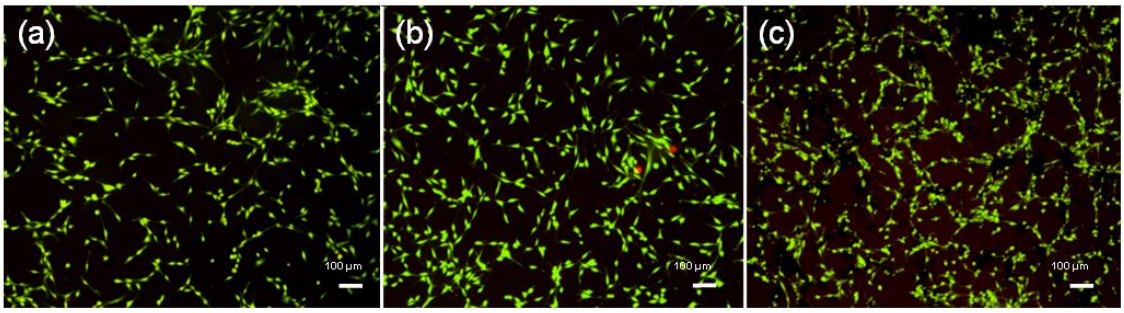

Figure 3.8. Fluorescent microscopy images of NIH 3T3 after Molecular Probes Live/Dead assay was performed to show live and dead cells. The images are fibroblasts exposed to: (a) 80 mole % PEG200MMA, 20 mole% PEG400DMA , 5 weight % Fe_3O_4 hydrogel nanocomposite, (b) control on polystyrene, and (c) 1000 µg/ml Fe_3O_4 nanoparticles. The scale bar represents 100 µm.

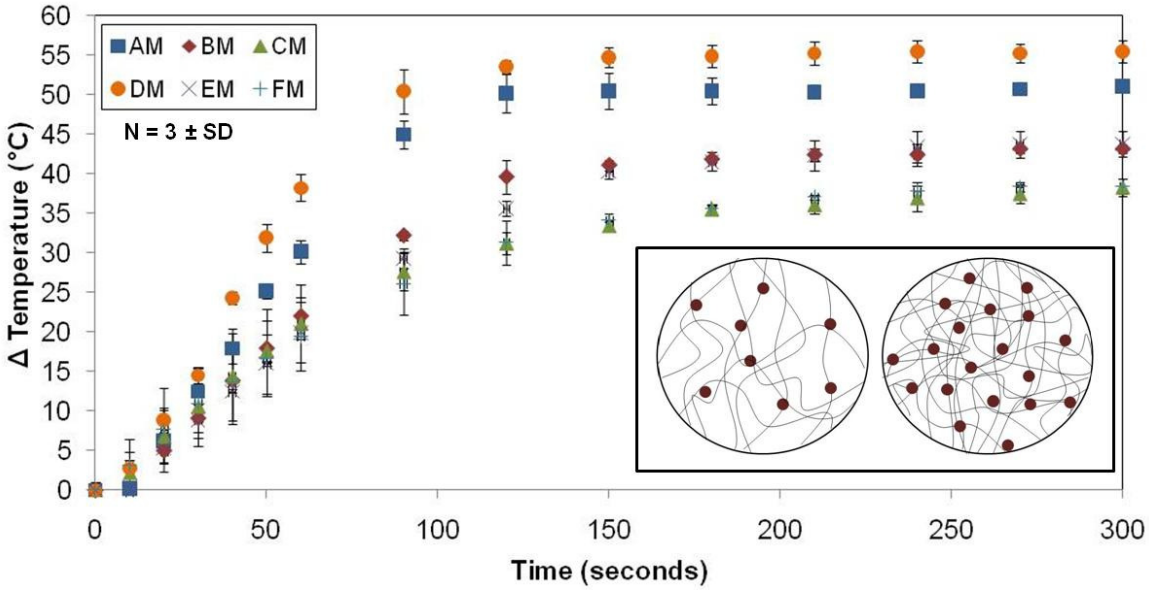

Figure 3.9. Thermal response of hydrogel nanocomposites exposed to AMF at 297 kHz and 25 kA/m for 5 minutes. AM through FM gel abbreviations are defined in Table 1. The insert represents hydrogel mesh structure and iron oxide particles for a gel with a higher volume swelling ratio (left) and lower swelling ratio (right).

3.9, the hydrogel nanocomposites reached their maximum temperature after 180 seconds. Hydrogels without magnetic particles were also exposed to the alternating magnetic field (data not shown) and exhibited minimal heating confirming that the heat generation was due to the Fe_3O_4 nanoparticles. The amount of heating of the hydrogel systems was dependent on the swelling ratio of the gel and subsequently the iron oxide nanoparticle loading per gel volume. The estimated amount of Fe_3O_4 nanoparticles for a given swollen nanocomposite disc was calculated from the following:

$$Fe_3O_4\ mass = \frac{M_s^{heat}}{q} w_f = M_s^{heat} \left(\frac{M_d^{is}}{M_s^{is}}\right) w_f \quad (3)$$

where Ms refers to the gels in the swollen state, Md in their dry state, and the superscripts heat and subscript is refers to the gels prior to heating and data from the initial swelling data, respectively. q is the mass swelling ratio calculated from the mass of swollen gels over dry gels and wf refers to the initial weight % of the iron oxide loaded into the gels. The volume for a swollen nanocomposite disc prior to heating was then determined from:

$$V_{disc} = \left(\frac{M_{air}^{heat} - M_{heptane}^{heat}}{\rho_{heptane}}\right) \quad (4)$$

where M_{air} and $M_{heptane}$ are the mass of the gels prior to heating in air and in n-heptane, respectively. The iron oxide mass per hydrogel volume was then calculated by taking the ratio of the iron oxide mass and gel volume calculated above. As expected, as the amount of iron oxide per volume in the gels increases, the final maximum temperature of the systems increased as seen in Table 3.2. The variance in heating can be attributed to the fact that the gels with a higher volume swelling ratio have a looser mesh and less particles present when

cut at the same size as a gel with a lower Q value that has a tighter mesh and more particles. A demonstration of this phenomenon can be seen in the insert of Figure 3.10.

For hyperthermia applications, the temperature of cancerous tissue needs to reach 42 - 45°C for effective therapy whereas temperatures above 50°C cause damage to cancer cells via thermoablation. It was demonstrated that the temperature of the hydrogels can be controlled by changing the alternating magnetic field strength so that the gels either reached hyperthermia (42 to 45°C) or thermoablative (60 to 63°C) temperatures. Figure 3.10 demonstrates that the final temperature the hydrogel nanocomposites reach can be tailored to either one of these temperature ranges. The insert shows IR images of the gels heating at hyperthermia temperatures (a-c) and thermoablative temperatures (d-e) for 15 seconds, 1 minute, and 5 minutes respectively. The variance in the temperatures reached by the hydrogels was directly controlled by the strength of the AMF as seen in Table 3.2. As expected, for the hydrogel nanocomposites with less iron oxide per hydrogel volume, the AMF strength needed to heat to the appropriate temperature range increased. This was true for both the hyperthermia and thermoablative temperature ranges and the field strength needed to heat gels for thermoablation was higher than that for hyperthermia.

3.3.5 Thermoablation demonstration with M059K glioblastoma cells exposed to hydrogels heated in AMF

M059K glioblastoma cells were heated with hydrogel nanocomposites exposed to AMF to both demonstrate the ability of the gels to kills cells via thermoablation and prove the safety of exposure to the field. Figure 3.11 (top) shows the heating set up where the hydrogel was placed in Saran wrap on the solenoid with the Petri dish containing cells on top of the gel/wrap. Previous studies showed negligible heat loss through the Petri dish so that the cells received direct heat through the polystyrene. An 8.2 mm hydrogel was placed under a 35 mm dish so that only the center area of cells was affected by the heat. This resulted in an acute

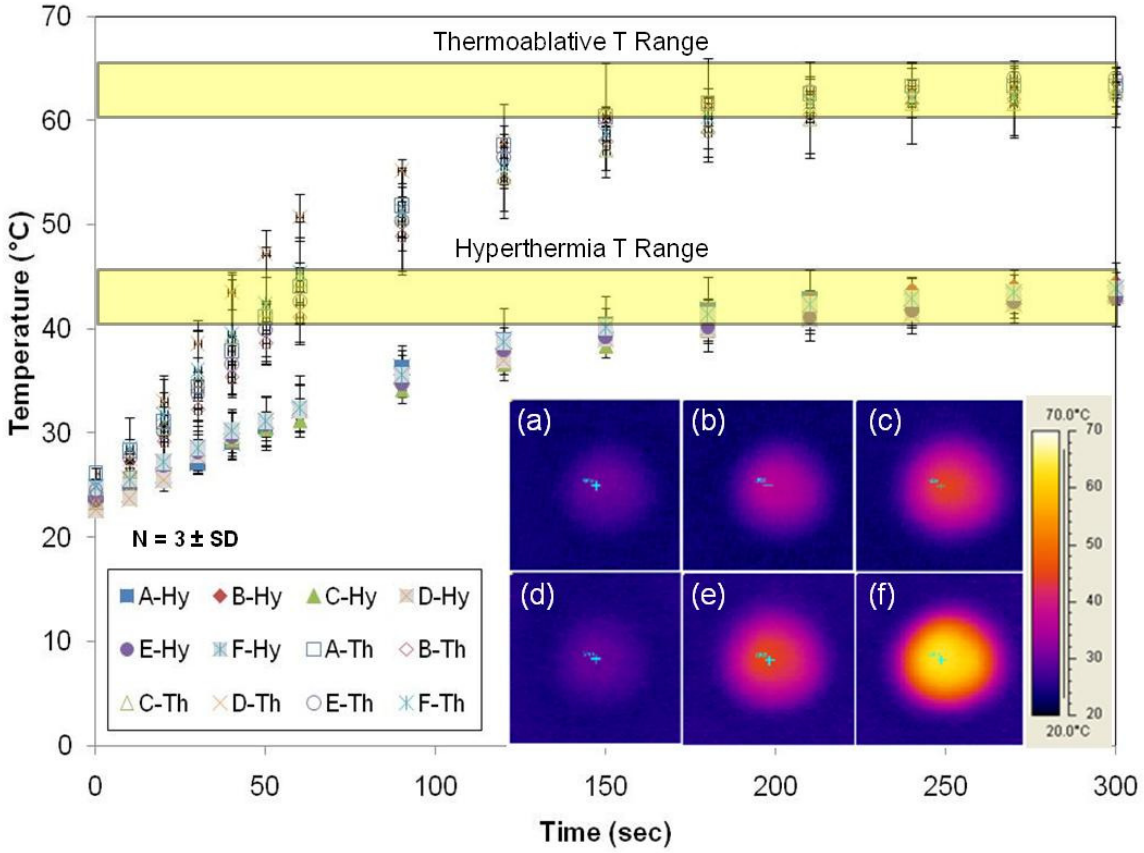

Figure 3.10. Thermal analysis of hydrogel nanocomposites exposed to varied AMF strengths to control gel temperatures in the hyperthermia and thermoablative temperature ranges where the Th and Hy after the gel abbreviations represents thermoablative and hyperthermia heating, respectively. Transparent boxes represent the thermoablative (top) and hyperthermia (bottom) temperature range goals for heating. The insert show IR images of gels for hyperthermia (a-c) and thermoablation (d-f) at 15 seconds, 1 minute, and 5 minutes.

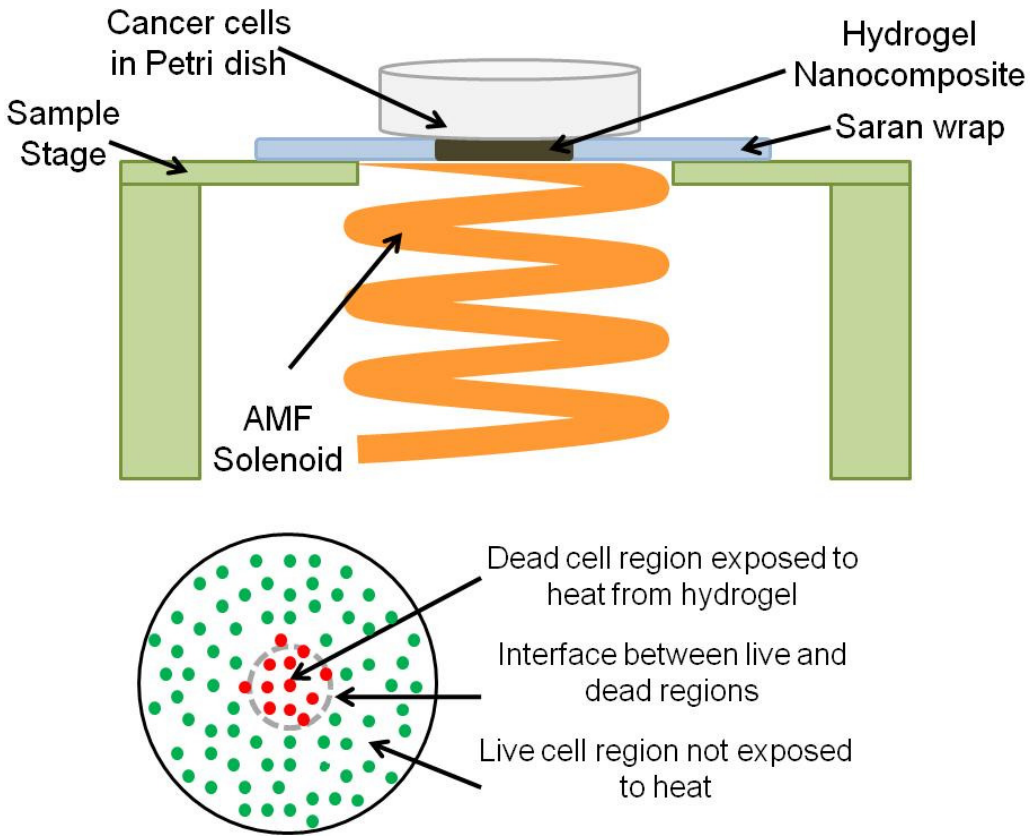

Figure 3.11. (Top) schematics of M059K glioblastoma multiforme/hydrogel heating apparatus (top) with hydrogel in Saran wrap on the solenoid then covered by the cancer cells present in the Petri dish. (Bottom) schematic of cancer cells in Petri dish and their response after exposure to gels heated in AMF. The gels cause acute cell death (red) at the center of the dish with a distinct interface where outer cells are unaffected (green).

cellular response as indicated in Figure 6 (bottom) where the center cells were killed by the heat and outer cells were unaffected with a distinct interface between the live and dead cells. A 50 mole% PEG200MMA, 50 mole% TEGDMA hydrogel was used as it showed the ability to heat the highest with the lowest field strength. Figure 3.12 confirms the success of these experiments where the left column of images are the M059K heated by the gel, the center is the cells exposed to the field only, and the right is the control. The cells heated with the gel showed distinct cell death at the center and interface whereas both of the controls showed favorable cell morphology. The IR images show the final temperature the cells were exposed to (63°C for thermoablation, j, and 24°C for AMF control, k). Overall, these results show the ability of the gels to kill cancer cells without harming them with the magnetic field.

3.4 Conclusions

It was demonstrated that PEGMMA/PEGDMA magnetic hydrogel nanocomposites can potentially be used in thermal cancer therapy through remote heating via application of an alternating magnetic field. Swelling analysis of the hydrogels indicated a dependence of swelling properties on both the EG content in the gels and crosslinking density of the system. As either the amount of EG increased or crosslinking decreased, the volume swelling ratio of the hydrogels increased. The hydrogel systems were shown to be slightly temperature-responsive. Increasing the temperature of the hydrogels decreased their volume swelling ratio upon reaching the LCST. The exposure of murine fibroblasts to the hydrogel nanocomposites and iron oxide nanoparticles was carried out and favorable cell viability was seen for both the gels and particles indicating their safe use as in vivo systems. This is due to both the high EG content and high water content of the hydrogels. Both hyperthermia and thermoablation are therapies that increase the efficacy of both radiation and chemotherapy. Upon exposure to an AMF, the hydrogels showed the ability to heat at both hyperthermia and thermoablative temperatures which can be controlled by the content of the iron oxide in the hydrogel or

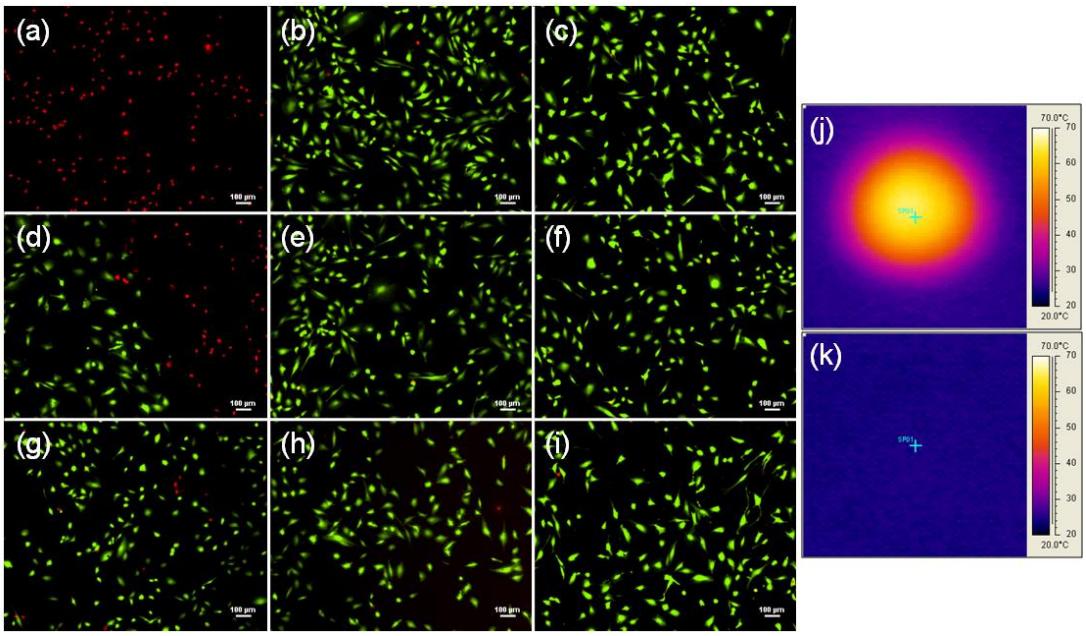

Figure 3.12. M059K glioblastoma multiforme/hydrogel heating results. Images a through i represent fluorescent microscopy images after live/dead assay of M059K cells where a-b are at the center of the Petri dish, d-f at the interface between live and dead cells, and g-I at the outer edge unaffected by heat. The first column of images are for the cells exposed to a DM gel (50 mol% PEG200MMA, 50 mol% TEGDMA) at 297 kHz and 25 kA/m for 5 minutes, the middle column are of cells exposed to AMF only at 297 kHz and 25 kA/m for five minutes, and the right column is of cells not exposed to gels or AMF. Images j and k represent IR images after the cells heated with the gel for 5 minutes (j) and exposed to AMF for 5 minutes (k).

changing the strength of the applied alternating magnetic field. For gels with higher iron oxide content, lower field strength was needed to get the desired temperature and as the field strength was increased for a particular system, the temperature was also increased.

A proof-of-point demonstration was done to show the ability of these hydrogel nanocomposites to kill M059K glioblastoma *in vitro* by exposing the cells to hydrogels at thermoablative temperatures. This concept can be further extended to systems for the delivery of heat at hyperthermia temperatures with the delivery of chemotherapeutics as a dual-delivery system for cancer therapy. These systems could potentially be used to target cancer in two primary applications including implantation after surgical resection of a tumor for prevention of metastasis or recurrence and injection for *in situ* formation of the hydrogels in difficult-to-reach locations. For this to occur, *in vivo* testing of these materials must be completed including those demonstrating the biocompatibility of the nanocomposites (before and after heating), potential iron oxide nanoparticle release during implantation, and overall efficacy of the heating on surrounding tissues. The limitations of these systems that must be overcome may include but are not limited to non-specific formation of the hydrogels during *in situ* implementation, encapsulation of the hydrogel system, the need to surgically remove the implant after its useful life, and the possible need for long-term drug delivery.

References

All references are located at the end of the dissertation.

CHAPTER 4

Synthesis and Characterization of Thermoresponsive Poly(ethylene glycol)-Based Hydrogels and Their Magnetic Nanocomposites

Temperature-responsive hydrogels are one of the most widely-studied types of stimuli-responsive hydrogel systems. Their ability to transition between their swollen and collapsed states makes them attractive for controlled drug delivery, microfluidic devices, and biosensor applications. Recent work has shown that poly(ethylene glycol) methacrylate (PEGMA) polymers are temperature-responsive and exhibit a wide range of lower critical solution temperatures based on the length of EG units in the macromer chain. The addition of iron oxide nanoparticles into the hydrogel matrix can provide the ability to remotely heat the gels upon exposure to an alternating magnetic field (AMF). In this work, diethylene glycol methyl ether methacrylate and poly(ethylene glycol) (n = 4.5) methyl ether methacrylate copolymers were polymerized into hydrogels with 5 mole % poly(ethylene glycol) (n = 13.6) dimethacrylate as the crosslinker along with 5 weight % iron oxide nanoparticles. Volumetric swelling studies were done from 22 to 80 °C and confirmed the temperature-responsive nature of the hydrogel systems. The ability of the gels to collapse in response to rapid temperature changes when exposed to an alternating magnetic field was demonstrated showing their potential use in biomedical applications such as controlled drug delivery and hyperthermia therapy.

Keywords

PEG, hydrogels, nanocomposites, temperature-responsive, magnetic.

4.1 Introduction

Stimuli-responsive hydrogels are one class of polymers that have been studied extensively due to their ability to respond to external stimuli such as light, heat, pH, electric fields and ionic strength (Peppas 2000). These stimuli allow for the control of the swelling and deswelling behavior of the hydrogel matrices. These types of hydrogels have been utilized in many biological applications such as drug delivery, artificial muscle, chemical valves, immobilization of enzymes and cells, and in bioseparation applications (Qiu and Park 2001). Temperature-responsive hydrogels are among the most commonly studied types of stimuli-responsive polymer systems. Negative temperature-responsive hydrogels exhibit a lower critical solution temperature (LCST) at which they undergo a deswelling phenomenon at this temperature due to thermodynamically-driven interactions between the polymer and its surrounding media. Typical LCST polymers that have been widely studied in hydrogel applications include N-isopropylacrylamide (NIPAAm), as well as other types of acrylamides and methacrylates (Fournier 2007). When such hydrogels are exposed to an aqueous solution at a temperature that is below their LCST, solvent (water)-polymer interactions dominate and the hydrogel swells, whereas above the LCST, hydrophobic interactions between the polymer chains dominate and the hydrogel structure collapses, releasing water from the hydrogel matrix. LCST hydrogels have been used successfully in drug delivery applications as they can undergo triggered drug release by squeezing-controlled release as described by Brazel (Brazel 2009).

Poly(ethylene glycol) (PEG) is one of the most widely studied polymers for biomedical applications. It is nontoxic, non-immunogenic, and approved by the US Food and Drug Administration for various clinical uses (Peppas 1999; DiRamio 2005). Despite this, PEG macromolecules and hydrogels have only recently been studied as temperature-responsive polymeric systems. In particular, PEG methacrylate (PEGMA) macromolecules have exhibited temperature-responsive behavior in physiological temperature ranges and are

appealing to use because many PEGMA macromolecules are available commercially. Lutz and coworkers have done extensive work synthesizing and characterizing the temperature-responsive behavior of PEG methacrylate macromolecules (Lutz 2006; Lutz and Hoth 2006) through the copolymerization of PEGMA oligomers with various EG unit lengths. In particular, random copolymers of diethylene glycol methacrylate (DEGMA, M_w = 188) and PEG400 methacrylate (PEG400MA, M_w = 475) were shown to exhibit LCST values between 26 and 90 °C where this value can be precisely tuned by varying the comonomer composition during the macromolecule synthesis. Similarly, LCST values of 32, 37, and 39 °C was observed in pure water for these copolymers possessing an average 5, 8, or 10 % of DEGMA units to PEG200MA (M_w = 300) units per chain(Lutz and Hoth 2006). This group has also developed thermoresponsive P(DEGMA-co-PEG400MA) hydrogels (Lutz 2008), and they exhibited LCST values comparable to those measured for their single-chain analogues (42-45 °C for a gel with 10 mole % DEGMA and 51-53 °C for a 20 % DEGMA). Preliminary evaluation of the deswelling kinetics of these systems indicated that their thermally inducted shrinkage is extremely fast which is important for drug delivery applications.

Hydrogel nanocomposites involve the incorporation of various nanoparticulate materials within a hydrogel matrix which can provide easy, straightforward methods for enhancing the properties of hydrogels. Thus far, a number of nanoparticulates have been utilized in nanocomposite hydrogel systems including metallic nanoparticles, carbon nanotubes, clay, ceramics, magnetic nanoparticles, hydroxyapatite, and semiconducting nanoparticles (Meenach 2009). In particular, the incorporation of magnetic nanoparticles, such as iron oxide nanoparticles, into hydrogels can create tunable hydrogel nanocomposites that can be remotely heated by an electromagnetic field. Potential applications of such systems range from controlled drug release applications to hyperthermia treatments in cancer patients. By combining iron oxide nanoparticles with LCST polymers, an alternating magnetic field (AMF) can be used to trigger localized heating of the nanoparticles within the

hydrogel, which in turn causes the deswelling of the system (Brazel 2009). The heating mechanism for paramagnetic iron oxide nanoparticles exposed to an AMF is based on Brownian relaxation (rotation of the particle) and Néel effect (reorientation of the magnetization vector inside the magnetic core) (Babincova 2001). This type of AMF-controlled, temperature-responsive behavior of hydrogel nanocomposites has been utilized with poly(N-isopropylacrylamide) (PNIPAAm)-iron oxide hydrogels for remote-controlled pulsatile drug delivery (Satarkar and Hilt 2008) and as remote-controlled microvalves (Satarkar 2009).

This current work utilizes both magnetic iron oxide (Fe_3O_4) nanoparticles and LCST PEG-based polymers to create a hydrogel that will heat upon exposure to an AMF causing a rapid deswelling of the hydrogel matrix. This type of system could be applied for use as magnetothermally-responsive nanomaterials to be used for drug delivery and hyperthermia applications as described recently in a comprehensive review of these systems by Brazel (Brazel 2009). The properties of the hydrogels can be controlled by the amount and type of PEG macromer constituent as demonstrated by the heating, swelling, and mesh size analysis of the systems. These particular hydrogels, comprised of PEGMA macromers, exhibited broad swelling responses to a wide temperature range and exhibited tunability in their swelling response depending on the amount of EG units present in the polymer matrix. This is the first demonstration of PEG-based, easy-to-fabricate hydrogel nanocomposites that exhibit such behavior.

4.2 Materials and Methods

4.2.1 Materials

The macromers diethylene glycol methyl ether methacrylate (DEGMA, $M_w = 188$) and poly(ethylene glycol) (n = 4.5) methyl ether methacrylate (PEG200MA, $M_w = 300$) and the

crosslinker poly(ethylene glycol) (n = 13.6) dimethacrylate (PEG600DMA, M_w = 754) were obtained from Polysciences (Warrington, PA). Fe_3O_4 nanoparticles (25 nm diameter, 0.2% polyvinylpyrrolidone-coated) were obtained from Nanostructured and Amorphous Materials (Los Alamos, NM). The free-radical initiator, ammonium persulfate (APS), accelerator, N,N,N',N'-tetramethylethane-1,2-diamine (TEMED), and ethanol (95%) were obtained from Sigma Aldrich (St. Louis, MO) at 99 and 98% purity, respectively. All materials were used as received.

4.2.2 Fabrication of Poly(ethylene glycol)-Iron Oxide Hydrogel Nanocomposites

Magnetic hydrogel nanocomposites were fabricated via free-radical polymerization with various macromer ratios (DEGMA to PEG200MA). The structures of these compounds can be seen in Figure 4.1. Ethanol was added to the macromer solution in a 1:1 by weight basis based on the macromer and crosslinker amounts. For hydrogels with iron oxide nanoparticles, the particles were added at 5 weight % based on the macromer and crosslinker and were exposed to an ultrasonic bath for 30 minutes to facilitate dispersion of the iron oxide nanoparticles throughout the solution. After sonication, 2 weight % APS and 4 weight % TEMED were then added to the mixture to chemically initiate the free-radical polymerization. This solution was then sonicated further for 2 minutes before being loaded into a template consisting of two 15 cm by 15 cm glass plates with a 1.5 mm thick Teflon spacer. The gels were kept in this template for at least 2 hours (usually overnight) to allow for completion of polymerization. To remove any potentially unreacted and potentially toxic macromer, crosslinker, and initiator residues, the hydrogels were washed with deionized water for at least one week. The systems fabricated were comprised of 0, 25, 50, 75, and 100 mole % PEG200MA to DEGMA based on the macromer amounts and were abbreviated 100DEGMA, 25PEG200MA, 50PEG200MA, 75PEG200MA, and 100PEG200MA, respectively.

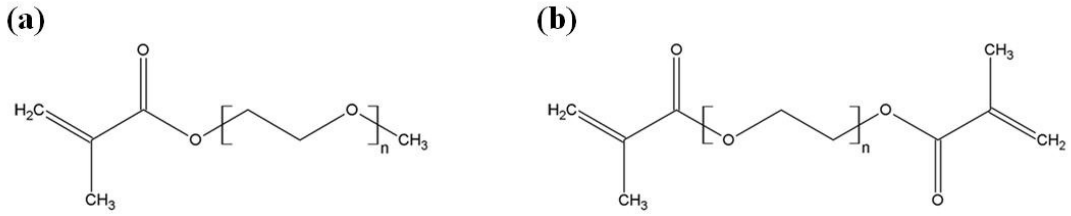

Figure 4.1. Schematic representations of (a) PEGMA and (b) PEGDMA structures.

4.2.3 Swelling Analysis and Mesh Size Calculations

The equilibrium swelling characteristics of the PEG-Fe_3O_4 hydrogel nanocomposites were measured using a gravimetric method based on a comparison of the density measurements of both swollen and dry gels at equilibrium as described previously (Frimpong 2006). Upon the completion of synthesis and washing, hydrogel discs 13.8 mm in diameter were cut from the bulk hydrogel films. The discs were then placed in phosphate buffered saline solution (PBS, pH 7.4) and allowed to reach equilibrium for at least 72 hours. The mass of the discs were measured in air and then in *n*-heptane (non-solvent) in their swollen state at 22, 37, 43, and 60 and 80 °C and in their final dry state. The masses of the hydrogels in both dry and swollen states in air and *n*-heptane were used to calculate of the volume swelling ratio (Q) at equilibrium:

$$Q = \frac{V^s}{V^d} = \frac{\left(\frac{M^s_{air} - M^s_{heptane}}{\rho_{heptane}}\right)}{\left(\frac{M^d_{air} - M^d_{heptane}}{\rho_{heptane}}\right)} = \frac{M^s_{air} - M^s_{heptane}}{M^d_{air} - M^d_{heptane}} \quad (1)$$

where V is the volume of the sample, $\rho_{heptane}$ is the density of *n*-heptane, M_{air} is the mass of the sample in air, and $M_{heptane}$ is the mass of the sample in *n*-heptane. The superscripts s and d refer to the swollen and dry forms of the samples, respectively.

The bulk structure of hydrogels is important in determining their suitability for various biomedical applications, especially drug delivery (Peppas 2006). The most important parameters used to characterize the network structure of hydrogels are the molecular weight of the polymer chain between two adjacent crosslinking points ($\bar{M}_c$) and the hydrogel mesh size (ξ). The molecular weight between crosslinks and corresponding mesh size are measures of the degree of crosslinking of the system. For poly(ethylene glycol) methyl ether methacrylate (PEGMA) and poly(ethylene glycol) dimethacrylate (PEGDMA) hydrogels, the hydrogel

mesh will be an amorphous mesh with PEGDMA acting as the "backbone" with PEGMA incorporated into the hydrogel acting as a tether/brush throughout the system. The structural characterization can be done by either equilibrium swelling theory or rubber-elasticity theory. Traditionally, hydrogels that do not contain ionic moieties have been analyzed using Flory-Rehner theory (Flory 1953). Elbert and coworkers have described another method of hydrogel mesh analysis (Elbert 2001) and this was compared to the Flory-Rehner method. $\bar{M}_c$ can be calculated from the Flory-Rehner equation which incorporates the Peppas-Merrill modification (Peppas and Merrill 1976) for a neutral hydrogel prepared in the presence of a swelling agent:

$$\frac{1}{\overline{M_c}} = \frac{2}{\overline{M_n}} - \frac{\left(\frac{\bar{v}}{V_1}\right)\left[ln\left(1-v_{2,s}\right)+ v_{2,s}+ \chi_1 v_{2,s}^2\right]}{v_{2,r}\left[\left(\frac{v_{2,s}}{v_{2,r}}\right)^{1/3} - \frac{1}{2}\left(\frac{v_{2,s}}{v_{2,r}}\right)\right]} \qquad (2)$$

where $\bar{M}_n$ is the number average molecular weight of the uncrosslinked chains, $\bar{v}$ is the specific volume of the polymer/crosslinker, V_1 is the molar volume of water (18 cm^3/mol), $v_{2,s}$ is the polymer volume fraction in the swollen state (1/Q), χ_1 is the Flory polymer-solvent interaction parameter (0.43, (Merrill 1993)), and $v_{2,r}$ is the polymer fraction in the relaxed state (amount of total polymer in initial feed versus total polymer plus solvent amount, based on the assumption of complete reaction with no volume change). For these studies $\bar{M}_n$ was not determined experimentally and thus two values were used as a comparison. The first value used was 100,000, a value that has been assumed for lightly crosslinked systems (Brazel and Peppas 1995). Then $\bar{M}_n$ was calculated from the molecular weight of the PEGMA chains between each PEGDMA link (One PEGDMA plus 19 PEGMDA units). The number of C=C bonds between two crosslinks can be calculated from the following:

$$n = \frac{2\,\bar{M}_c}{M_r} \quad (3)$$

where M_r is the average molecular weight of the repeating (44 for ethylene glycol). The root mean squared end-to-end distance of the polymer chain in the unperturbed state is then calculated as:

$$(\bar{r}_0)^{1/2} = l(C_n n)^{1/2} \quad (4)$$

where l is the carbon-carbon bond length (1.54 Å) and C_n is the Flory characteristic ratio of the polymer (3.8, (Thomas 2007)). The mesh size (ξ) was then calculated as:

$$\xi = v_{2.s}^{-1/3}(\bar{r}_0)^{1/2} \quad (5)$$

It is important to note that the equations used to calculate $\bar{M}_c$ and mesh size are derived for polymer fractions up to 0.2 in solvent and therefore the values obtained for greater polymer fractions are approximations (Brazel and Peppas 1995; Mellott 2001). In the analysis method described by Elbert et al., the number of moles of elastically active chains in the hydrogel network (v_e) was calculated from:

$$v_e = -\frac{V_P}{V_0}\frac{[ln(1-v_{2,s}) + v_{2,s} + \chi_1 v_{2,s}^2]}{v_{2,r}\left[\left(\frac{v_{2,s}}{v_{2,r}}\right)^{1/3} - \frac{2}{f}\left(\frac{v_{2,s}}{v_{2,r}}\right)\right]} \quad (6)$$

where V_p is the volume of the dry polymer calculated from the dry mass of the hydrogel and the density of the polymer in the dry state (for PEG, 1.12 g/cm^3) and f is the functionality of

the crosslinks (assumed to be 2 for the case of the dimethacrylated crosslinker). $\bar{M}_c$ was then calculated from:

$$\bar{M}_c = \frac{m_p}{v_e} \quad (7)$$

where m_p is the total mass of PEG in the hydrogel. ξ was then calculated using equations 3 through 5. Further explanation for mesh analysis can be found in Appendix B, Section B.4.1.

4.2.4 Thermal and Swelling Analysis of Hydrogels Exposed to an Alternating Magnetic Field

Prior to heating, hydrogel nanocomposites were cut into discs (8.2 mm in diameter) and equilibrated in PBS at room temperature (22 °C). Remote-controlled heating of the hydrogel nanocomposites was completed using an alternating electromagnetic field induced by a Taylor Winfield induction power supply (model MMF-3-135/400-2) equipped with a solenoid with a 15 mm diameter and 5 turns. Prior to heating, the gels were weighed in air and *n*-heptane to determine their swelling characteristics. The hydrogel discs at their equilibrium swollen state were then covered with Saran wrap, placed on top of the solenoid coil and exposed to the alternating magnetic field to induce heating. The hydrogel nanocomposite systems were each exposed to the same magnetic field power at 291 kHz and 24.8 kA/m for 5 minutes. Thermal data was acquired using an infrared camera (AGEMA Thermovision 470) which recorded the surface temperature of the hydrogels. After heating, the gels were re-weighed then placed immediately back in PBS at room temperature. The swelling behavior of the hydrogel nanocomposites was characterized by evaluating the volume swelling ratio of the hydrogels at various time points. The mass of the gels in their swollen state were measured in air and *n*-heptane at the following times: before heating via the AMF, immediately after heating, and 5 minutes, 20 minutes, 60 minutes, 3 hours, 24 hours,

and 7 days after returning to PBS. The gels were then dried and re-weighed in air and *n*-heptane and their volume swelling ratios were calculated as described previously.

4.2.5 Statistical Analysis

All experiments were performed at least in triplicate. MYSTAT 12 for Windows (12.02.00) was used for t-tests (paired t-test with unequal variances) to determine any significance in observed data. A p-value of <0.05 was considered statistically significant.

4.3 Results and Discussion

4.3.1 Swelling and Mesh Size Analysis

The swelling of the PEG-iron oxide hydrogel nanocomposites was initially determined through a gravimetric analysis of the systems. The volume swelling ratio (Q) of the gels in their swollen state was measured at 22, 37, 43, 60, and 80 °C to determine their swelling-responsive behavior with respect to a change in temperature. Previously, Lutz and coworkers determined that DEGMA and PEG200MA have LCST values of 26 and 64 °C, respectively(Lutz and Hoth 2006). The LCST of PEGMA macromolecules can be tuned by varying the ratio of macromers with differing EG content. Ratios of DEGMA and PEG375MA (M_w = 475, LCST = 90 °C)-based macromolecules were synthesized by Lutz and coworkers, and it was shown that they exhibit LCST values of 32, 37, and 39 °C for 5, 8, and 10% of DEGMA units, respectively (Lutz 2008). It was hypothesized that by fabricating PEGMA-based hydrogels of DEGMA and PEG200MA that the swelling properties could be tuned according to the amounts of each macromer type in the hydrogels. Figure 4.2 shows the volume swelling data for all of the hydrogel systems from 22 to 80 °C. These results indicate that as the temperature is increased, the volume swelling ratio of all hydrogel systems decreases. These hydrogels, however, do not exhibit a sharp deswelling behavior around their

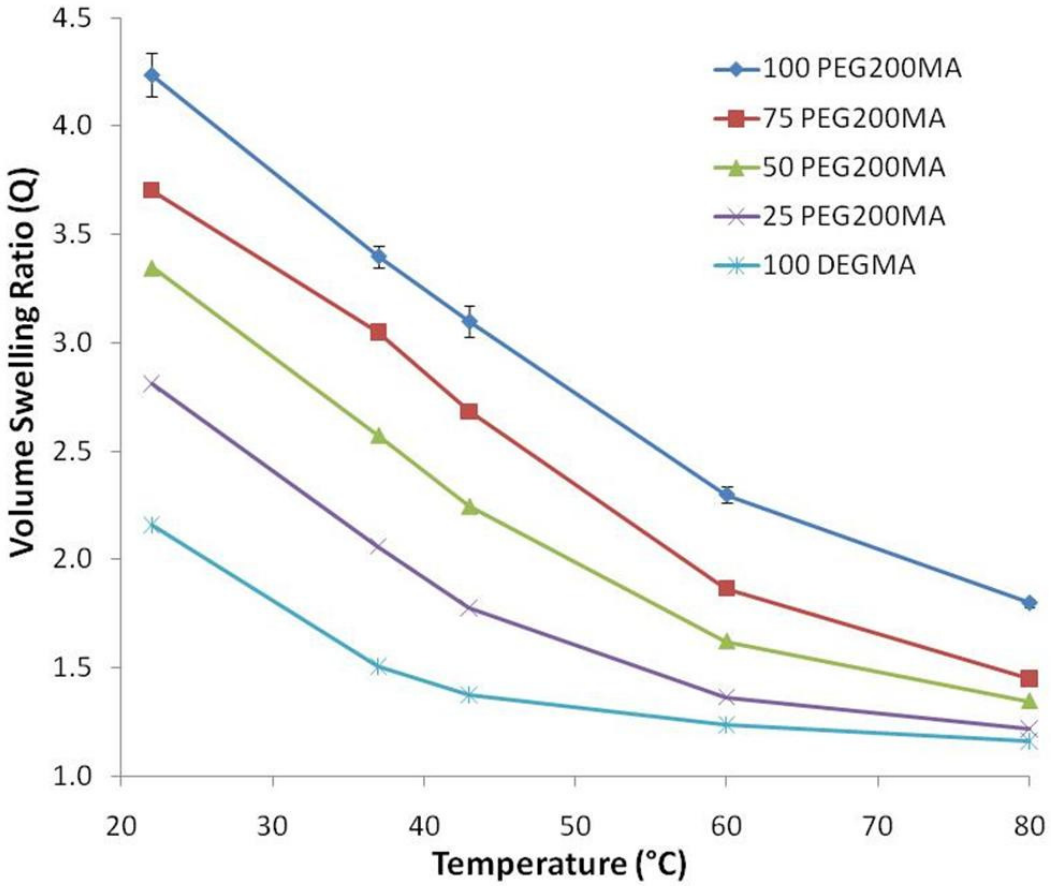

Figure 4.2. Volume swelling ratio data for all hydrogel systems at 22, 37, 43, 65, and 80°C at their swollen equilibrium state. N = 3 ± SE.

LCST. This could be due to the PEG600DMA crosslinker which is the backbone of the hydrogel matrix and could shift the LCST of the overall gel higher due to the increased EG content it provides. The other trend shown in this data is that as the amount of PEG200MA content of the gel increases, the volume swelling ratio also increases. This is because the higher molecular weight EG chains in the hydrogel matrix results in a lower crosslink density in the network.

The average molecular weight between crosslinks ($\bar{M}_c$) and mesh size (ξ) of the PEG hydrogels were determined via the modified Flory-Rehner and Elbert equations as described in the Experimental section. Table 4.1 shows these values for all hydrogels systems at 22 °C. For all methods of analysis, as the amount of PEG200MA in the hydrogel system increased, both the average molecular weight between crosslinks and mesh size increased. These theoretical values (especially mesh size) can allow for the approximation of the size of drugs or other molecules that could potentially be loaded and delivered from these hydrogel nanocomposites. With the mesh size values ranging from 2.1 to 59.8 Å, a wide variety of different size molecules may potentially be released from these hydrogel systems. Also, the mesh size values indicate that the iron oxide nanoparticles are likely to be physically entrapped in the hydrogel matrix as their aggregated size (100-200 nm) is much larger than the reported mesh size values.

4.3.2 Remote-Controlled Heating of Hydrogels via AMF

Heating of the hydrogel nanocomposites is made possible by inducing heating of the iron oxide nanoparticles within the hydrogel matrix via an AMF. Although the diameter of the nanoparticles is small (approximately 25nm), they are known to form into 100-200 nm aggregates as described by the company that provides them. As such, the nanoparticles are believed to be physically entrapped within the hydrogel matrix as the theoretical mesh sizes of the gels are much smaller than the size of these aggregates. The hydrogel systems were

Table 4.1. Average molecular weight between crosslinks ($\bar{M}_c$) and mesh size (ξ) of the PEG hydrogels as determined via the Flory-Rehner equation. The values were tabulated using the volume swelling ratio of the hydrogels at 22 °C.

System	Peppas-Merrill Method (M_n = 100,000)		Peppas-Merrill Method (M_n = calculated)		Brandl Method (No M_n, perfect gel)	
	$\bar{M}_c$ (g/mol)	Mesh Size (Å)	$\bar{M}_c$ (g/mol)	Mesh Size (Å)	$\bar{M}_c$ (g/mol)	Mesh Size (Å)
100PEG200MA	2324.2 ± 58.7	59.8 ± 1.0	1388.2 ± 21.1	46.2 ± 0.5	888.1 ± 26.7	35.4 ± 0.7
25DEGMA	453.7 ± 6.2	21.1 ± 0.2	401.0 ± 4.9	19.8 ± 0.2	128.0 ± 2.2	11.0 ± 0.1
50DEGMA	345.2 ± 4.1	17.8 ± 0.1	313.8 ± 3.4	17.0 ± 0.1	80.8 ± 1.1	8.4 ± 0.1
75DEGMA	210.0 ± 2.3	13.1 ± 0.1	197.9 ± 2.0	12.7 ± 0.1	34.8 ± 0.7	5.2 ± 0.1
100DEGMA	91.6 ± 1.4	7.9 ± 0.1	89.3 ± 1.3	7.8 ± 0.1	6.5 ± 0.2	2.1 ± 0.0

exposed to the alternating magnetic field at 291 kHz and 24.8 kA/m for 5 minutes, and the resulting temperature profiles can be seen in Figure 4.3. For all systems, the equilibrium temperature was reached after approximately 3 minutes. Also, the change in temperature increased with increasing DEGMA content. This can be attributed to the swelling properties of the hydrogels. Hydrogels with the highest DEGMA content swelled the least and therefore had a tighter hydrogel mesh. Figure 4.4 is a representation of two hydrogel discs cut at the same diameter. The gel on the left has a higher volume swelling ratio and looser mesh which results in less iron oxide nanoparticles per swollen polymer, and therefore, these gels heat less in the AMF. It is important to note that even for the hydrogel that heated the least (65°C), all temperature values are well above what would be needed to induce a collapse in the hydrogel matrices as seen by the temperature-responsiveness of the gels through their initial swelling analysis.

One potential application of temperature-responsive biomaterials is their use as magnetothermally-responsive materials where the hydrogels deswell as a result of the heating of magnetic nanoparticles embedded in the polymer matrix. This could allow for remote-controlled release of a drug via a "squeezing effect" as seen in Figure 4.5. Therefore, the swelling properties of the PEG hydrogel nanocomposites were characterized for all systems immediately before and after their heating in the AMF for 5 minutes. Figure 4.6 shows that the volume swelling ratios of the gels change drastically before and after their heating in the AMF. All systems exhibited very fast deswelling (visually observed to occur almost immediately after the gels neared their equilibrium temperature after approximate 2 minutes of inducing heating), and their swelling decreased at least by half. As the gels are exposed to the AMF, they heat because of the nanoparticles and deswell as the overall temperature increases as seen in the schematic in Figure 4.7. This figure shows representative views of the gel at the individual particle, microscopic, and macroscopic view of the hydrogel systems in the field where localized heating of the nanoparticles affects the overall temperature of the

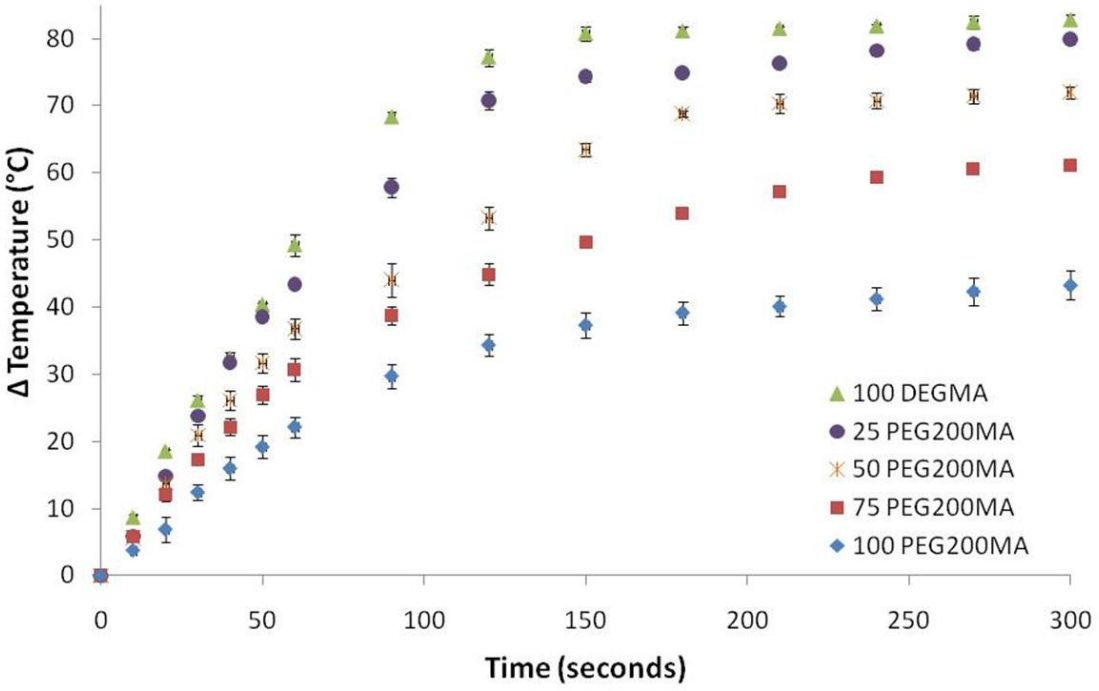

Figure 4.3. Temperature profile of hydrogel nanocomposites upon exposure to AMF for 5 minutes. The initial temperature was 22 °C for all systems. N = 3 ± SE.

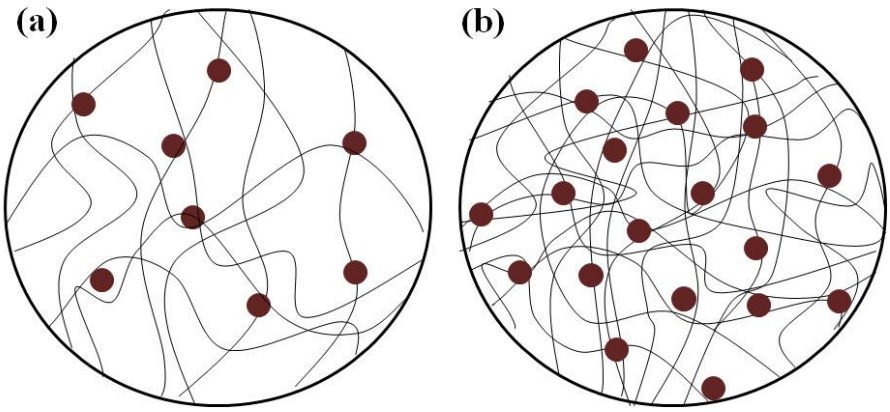

Figure 4.4. Representations of magnetic hydrogel nanocomposites at various crosslinking densities. The black lines represent the polymer chains present in the hydrogel matrix where as the small brown circles represent iron oxide nanoparticles embedded in the system. (a) represents a gel with a higher volume swelling ratio and loose hydrogel mesh, whereas (b) represents a gel with a lower volume swelling ratio and tighter hydrogel mesh. The looser mesh results in less polymer, less iron oxide, and more water which results in lower heating of the gels when heated in an AMF.

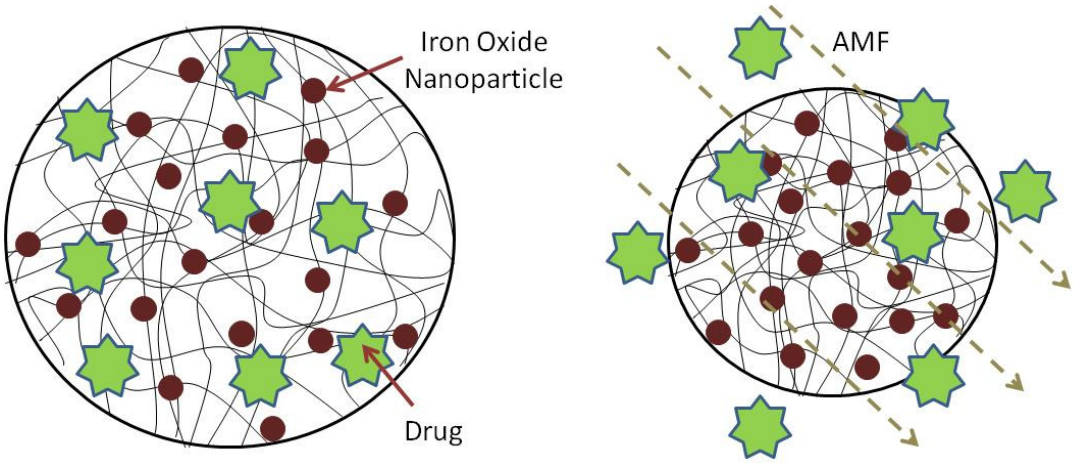

Figure 4.5. Hydrogel nanocomposite with iron oxide and loaded drug before and after AMF exposure. Heat from the iron oxide nanoparticles causes the nanocomposite to collapse due to the temperature-responsive nature of the polymer which causes drug to be expelled from the gel via a squeezing effect.

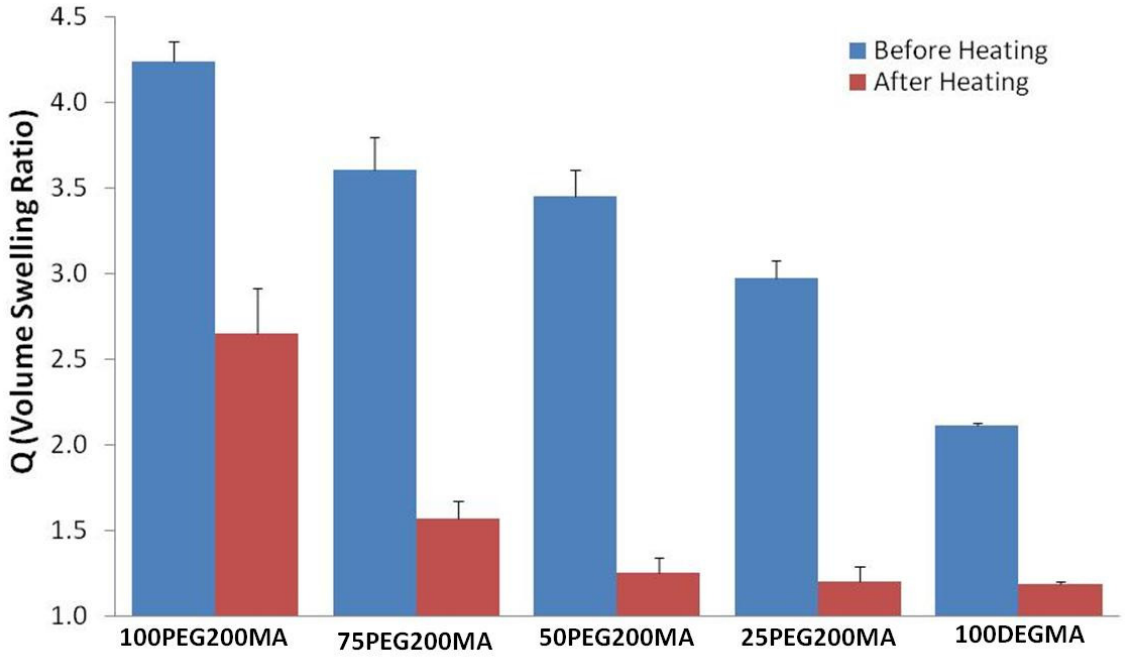

Figure 4.6. Volume swelling ratio of PEG hydrogel nanocomposites before and after heating due to exposure to an AMF for 5 minutes. N = 3 ± SE.

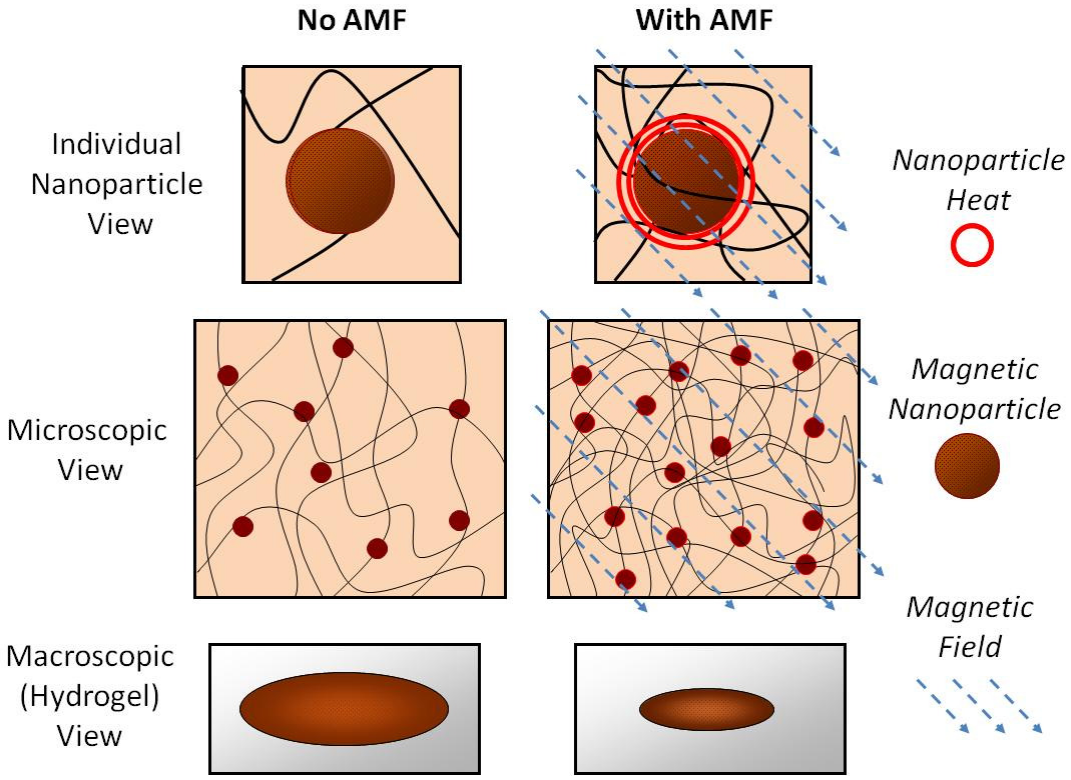

Figure 4.7. Schematic representation of magnetic hydrogel nanocomposites at their individual particle, microscale, and microscale view. The left images show the gel now exposed to AMF whereas those on the left are exposed to an AMF which results in localized heating of the nanoparticle at the nanoscale level which results in the collapse of the hydrogel at the macroscale level.

hydrogel system. The final volume swelling ratio after heating decreased with increasing DEGMA content. This is due to the final heating properties of the gels. For the 100PEG200MA system, the final temperature reached 65 °C whereas for the DEGMA system, the final temperature was 104 °C. Therefore, the DEGMA system collapsed more due to this increased temperature as would be expected due to the temperature-responsive effect seen in the initial swelling profiles.

Although the deswelling behavior of the hydrogels is very important, their reswelling behavior after heating is equally important for determining the usefulness of these gels in various applications. After being heated in the AMF, the volume swelling ratio of the hydrogels was also measured 5 minutes, 20 minutes, 60 minutes, 3 hours, 24 hours, and 7 days after the gels were allowed to reswell in PBS at 22 °C. Figure 4.8 shows the deswelling and reswelling profile of the 100PEG200MA and 100DEGMA systems up to 3 hours after the gels were heated in the AMF. The gels initially deswell due to their heating in the AMF where they reach their lowest volume swelling ratio (time = 5 minutes). After 5 minutes of reswelling in PBS at 22° C the gels begin to reswell (time = 10 minutes), however, their final equilibrium swelling ratio is not reached until after 3 hours (time = 185 minutes). The volume swelling ratios at the 24 hour and 7 day time points were not included in this graph as they were not statistically significant in comparison with the 3 hour time point. For both systems, the final volume swelling ratio after reswelling was found to be the same as the initial volume swelling ratio indicating that they can potentially maintain multiple cycles of deswelling and swelling.

4.4 Conclusions

PEG/iron oxide-based hydrogel nanocomposites show the potential to be used as magnetothermally-responsive materials in various biomedical applications. PEGMA hydrogels are temperature-responsive polymer systems that collapse due to their LCST

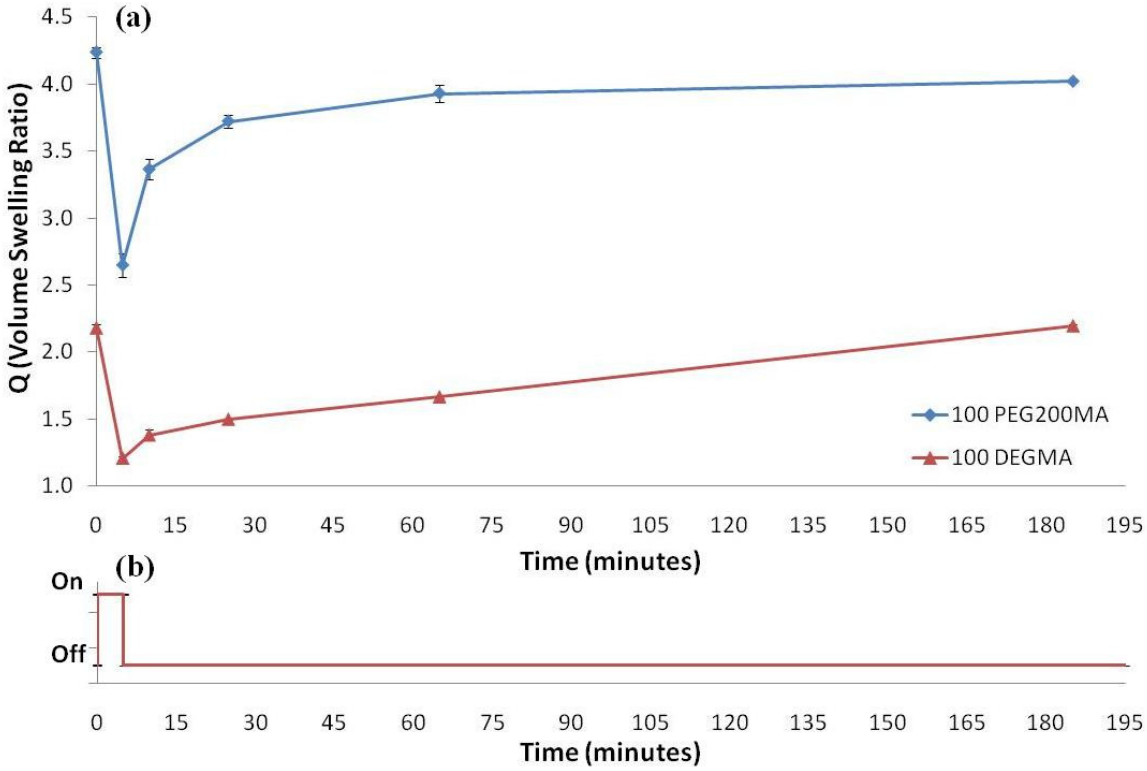

Figure 4.8. a) Volume swelling ratio (Q) of 100PEG200MA and 100DEGMA hydrogel nanocomposites with respect to time before, during, and up to 3 hours after their remote heating in an AMF. Q was measure for the gels: initially, before heating (time = 0 minutes), immediately after heating (time = 5 minutes), and after reswelling in PBS at 22°C for 5 minutes (time = 10 minutes), 20 minutes (time = 25 minutes), 60 minutes (time = 65 minutes), and 3 hours (time = 185 minutes). b) denotes the on/off cycle of the AMF the hydrogel nanocomposites were exposed to. N = 3 ± SE.

behavior where polymer-polymer thermodynamic interactions become more favorable as their surrounding temperature increases. PEG200MA and DEGMA-based hydrogels were made with various ratios and the same crosslinking amount with PEG600DMA. The gels exhibited temperature-responsive behavior as their volume swelling ratios decreased as the surrounding temperature increased. Also, the systems behaved as magnetothermally-responsive materials when they were exposed to an AMF. The iron oxide nanoparticles in the gels allowed for heating in the AMF which caused rapid deswelling of the hydrogels due to the resulting rapid localized heating. Overall, these systems have the potential to be used in various biomedical applications such as drug delivery, hyperthermia, and as remote-controlled valves.

References

All references are located at the end of the dissertation.

CHAPTER 5

Characterization of PEG-Iron Oxide Hydrogel Nanocomposites for Dual Hyperthermia and Paclitaxel Delivery

Hyperthermia, the heating of tissue to 41 to 45°C, has been shown to improve the efficacy of cancer therapy when used in conjunction with irradiation and/or chemotherapy. In this work, hydrogel nanocomposites have been developed that can control the delivery of both heat and a chemotherapeutic agent (e.g., paclitaxel). The nanocomposites studied involve a stealth, poly(ethylene glycol) (PEG)-based system comprised of PEG (n = 1000) methyl methacrylate and PEG (n = 400) dimethacrylate with iron oxide nanoparticles physically entrapped within the hydrogel matrix. The capability of the hydrogels to be heated in an alternating magnetic field was demonstrated. The heating of the hydrogel systems was dependent on the crosslinking of the hydrogel network where hydrogels with lower swelling ratios were found to heat to a greater extent than those with higher ratios. In addition, paclitaxel was shown to exhibit non-Fickian release from the hydrogel systems, with the rate of release dependent on the hydrogel network structure. Three cell lines: M059K (glioblastoma), MDA MB 231 (breast carcinoma), and A549 (lung adenocarcinoma) were exposed to paclitaxel only, hyperthermia heat only, and both paclitaxel and hyperthermia to determine if a synergistic effect was possible for the cell lines. The efficacy of paclitaxel was greater with hyperthermia for the A549 cells, however, the M059K and MDA MB 231 did not show the same response.

Keywords

PEG, hydrogel nanocomposites, hyperthermia, paclitaxel.

5.1 Introduction

Currently, cancer is the second leading cause of death in the United States. In 2009 alone, there were an estimated 1.5 million new cases diagnosed (ACS 2009). Conventional treatment methods of cancer include surgery, radiation, and chemotherapy where chemotherapy is often administered systemically or regionally. During systemic chemotherapy, drug delivery is dependent upon distribution through vasculature, transport across microvessel walls, and diffusion into the tumor tissue. Regional chemotherapy relies on injecting the drug directly into the tumor or peritumoral space, with diffusion through the space between tumor cells as the primary mode of transport (Obara 2005). However, these treatments are not always effective or possible due to the health of the patients, cancer types, and severity of side effects. Therefore, it is necessary to develop novel, noninvasive, and effective approaches to treat cancer. One such approach is the combination of treatment modalities. Specifically, hyperthermia can be used in combination with chemotherapy and radiation to more effectively treat cancer.

Hyperthermia is the controlled heating of cancerous tissues to between 41 and 45 °C (Issels 2008). Depending on the type of cancer and implementation, current clinical treatment options involving hyperthermia include devices for local, regional, and whole body hyperthermia (Falk and Issels 2001). Local hyperthermia may be superficial, where heating arrays are placed above shallow tumors in the skin, interstitial, or endocavitary, where a heating probe is inserted into the skin, tissue or body cavity, respectively. Regional hyperthermia may involve external heating of a large area, or perfusion, where blood from the region surrounding the tumor is removed, heated, and then pumped back into the area. Whole body hyperthermia often utilizes equipment where tubes of heated water blanket the patient, while simultaneously entrapping the heat and preventing sweating in order to quickly elevate the patient's body temperature (Babincova 2000). While some systemic toxicity has been reported (Hergt 2006), generally, toxicity due to hyperthermia treatment is low and does not

limit treatment, though treatment may result in burns or pain in the treated area. Tumors often contain chaotic vasculature, which creates regions of low oxygenation and perfusion, and higher acidity. These environmental factors can make the cells less susceptible to chemotherapy and radiation treatments. However, when hyperthermia is applied, perfusion and oxygen levels in the tumor increase, thus increasing the effectiveness of chemotherapy or radiation. Additionally, direct tumor cytotoxicity from hyperthermia is possible and is considered a result of denaturation of proteins in the nucleus, cytoplasm, or cell membrane (Issels 2008). Additional mechanisms for improved efficacy of combined treatment include an increased rate of drug alkylation, prevention of repair from drug-induced damage, and increased uptake of drug. Enhanced drug delivery is thought to be a result of improved perfusion in the tumor and surrounding area, and increased vascular permeability (Wust 2002).

Paclitaxel (PTX, MW = 853.91) is a plant alkaloid, the structure of which is depicted in Figure 5.1 (a). It effectively disrupts mitosis during the G2 phase of the cell cycle by binding with the beta subunit of tubulin dimers, interfering with the dynamic instability of the microtubules in the cytoskeleton and thus forming highly stable, rigid microtubules (Obara 2005; Michalakis 2007). In addition to preventing proliferation, paclitaxel also inhibits angiogenesis, cell migration, and collagenase production (Obara 2005). At micromolar doses, paclitaxel has also been shown to initiate the release of cytokines and promote the expression of certain genes, including those that encode tumor suppressors (Michalakis 2007). When used in combination with hyperthermia, paclitaxel has been shown to have a complex effect that is cell-line dependent, and effective in the range of 41.5 to 43°C. PTX has been commonly used to treat human carcinomas, with considerable antineoplastic activity specifically against ovarian, head, and neck carcinoma (Issels 2008). As a chemotherapeutic, paclitaxel has also been effective treating lung cancer, breast cancer, acute leukemia and other solid tumors. Currently, the most common formulation of paclitaxel used clinically is

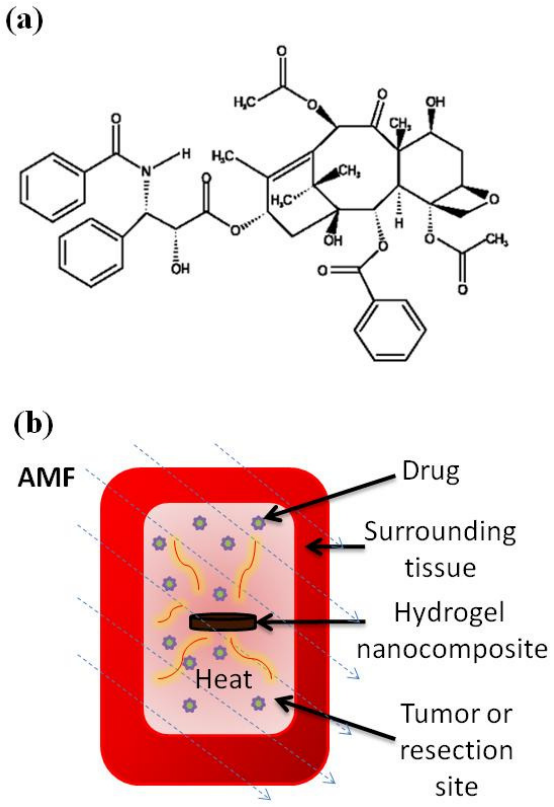

Figure 5.1. (a) Chemical structure of paclitaxel (Mw = 853.91) and (b) schematic showing the use of hydrogel nanocomposites to treat cancer. The nanocomposite would be injected or implanted within a tumor or at a tumor resection types. It would then release a chemotherapeutic agent and upon exposure to an alternating field, release heat to increase the efficacy of the drug treatment.

Taxol®, which uses a solution of Cremophor® EL and ethanol to combat the drug's high hydrophobicity. Because of paclitaxel's poor solubility in water, it is necessary to create vehicles that can effectively deliver the chemotherapy treatment.

Hydrogels are three-dimensional, polymeric networks that are hydrophilic and able to absorb large amounts of water, while remaining insoluble due to their crosslinked structure (Lin and Cheng 2001; Hilt and Byrne 2004; DiRamio 2005). As such, hydrogels are able to mimic human soft tissues and are thus suited for a variety of biomedical applications. Hydrogels have been used as drug delivery devices, as scaffolds for tissue engineering, and in biosensors (Peppas 2000; Peppas 2006). When nanoparticles are incorporated into the hydrogel matrix, a nanocomposite is formed. The nanoparticles can strengthen the hydrogel structure and/or enhance certain properties of the hydrogel (Meenach 2009). For instance, hydrogel nanocomposites containing iron oxide (Fe_3O_4) have the ability to heat when placed in an alternating magnetic field. This has lead to the use of magnetic nanocomposites in remote-controlled heating (Meenach 2009; Meenach 2009), valves (Satarkar 2009), drug release (Satarkar and Hilt 2008), and degradation applications (Hawkins 2009). The heating mechanism of superparamagnetic magnetic materials via AMF is a combination of Brownian and Néel relaxations. Brownian relaxation results from the random motion of the nanoparticles, which produce frictional energy losses. Néel relaxation can be attributed to the reorientation of the magnetic dipole moments of the particles when exposed to the alternating magnetic field (Babincova 2001). This release of heat from the hydrogel nanocomposite can be used as a method for local or regional hyperthermia, and depending on the coating, iron oxide particles can be well tolerated in the body (Bahadur and Giri 2003).

Because of their large swelling capabilities, hydrogels are able to release molecules with a wide range of molecular weights, including chemotherapeutics. Obara and coworkers were able to imbibe and release hydrophobic paclitaxel from chitosan-based hydrogels successfully (Obara 2005). Additionally, DiRamio and coworkers used poly(ethylene glycol)

methacrylate and poly(ethylene glycol) dimethacrylate polymers to create gels able to imbibe and release hydrophobic estradiol and insulin (DiRamio 2005) indicating the potential use of hydrogels to deliver various therapeutic agents.

Poly(ethylene glycol) (PEG) is known as a "stealth" material because of its limited interaction with biological molecules, including proteins (Peppas 2006). During hydrogel synthesis, Fe_3O_4 nanoparticles can be incorporated into the PEG matrix, resulting in a hydrogel that can be remotely heated by an alternating magnetic field. When imbibed with paclitaxel, the hydrogel nanocomposite has the capacity to release the chemotherapeutic simultaneously with hyperthermia treatment. For an improved therapy option, hydrogel nanocomposites loaded with chemotherapeutic agents could be implanted or injected into a tumor for treatment or implanted where a tumor has been resected to prevent recurrence. The nanocomposite hydrogel would release drug into a localized area, thus reducing systemic side effects and increasing regionally high concentrations of the drug. When exposed to an external alternating magnetic field, the hydrogel would be able to produce hyperthermia conditions in the area surrounding the implant as seen in Figure 5.1 (b). The overall objective of this work was to investigate magnetic PEG hydrogel nanocomposites that have the ability to control the release of both PTX and heat for the treatment of cancer. Three cancer cell lines were also evaluate *in vitro* for the effectiveness of their treatment with both PTX and hyperthermia.

5.2 Materials and Methods

5.2.1 Materials

The macromer poly(ethylene glycol) (N = 1000) methyl ether methacrylate (PEG1000MMA) and crosslinker poly(ethylene glycol) (N = 400) dimethacrylate (PEG400DMA) were obtained from Polysciences (Warrington, PA). Fe_3O_4 nanoparticles (20-

30 nm, 99.5% purity, 0.2% polyvinylpyrrolidone-coated) were purchased from Nanostructured & Amorphous Materials (Los Alamos, NM). The initiator, ammonium persulfate (APS), accelerator N, N, N', N'-tetramethylethane-1,2-diamine (TEMED), Cremophor® EL, and Tween® 20 were supplied by Sigma Aldrich (St. Louis, MO). Methanol was purchased from Fisher Scientific (Pittsburgh, PA) and paclitaxel (PTX) was obtained from LC Laboratories (Woburn, MA). Cells, cell medium, and DMSO were obtained from American Type Culture Collection (ATCC, Manassas, VA). The mammalian cell live/dead assay was from Molecular Probes/Invitrogen (Carlsbad, CA). All materials were used as received.

5.2.2 Magnetic Hydrogel Nanocomposite Fabrication

Three hydrogel systems were synthesized and characterized in these studies. 80PEG1000MA, 50PEG1000MA, and 20PEG1000MA gels were fabricated with 80, 50, and 20 mole % PEG1000MA macromer to PEG400DMA crosslinker, respectively. The structures of these compounds are shown in Figure 5.2. After the crosslinker and macromer were added to a glass vial, 25 weight % of methanol was added as a solvent. 5 weight % Fe_3O_4 nanoparticles were then added, and the mixture was placed in an ultrasonic bath for an hour to promote dispersion of the nanoparticles. Following this, 2 weight % APS and 4 weight % TEMED were added to the hydrogel solution to initiate free-radical polymerization of the hydrogels. This mixture was then vortexed for approximately 10 seconds and pipetted into a template of two 15 cm by 15 cm glass plates separated by 1.5 mm Teflon spacers. The hydrogel remained in the template for at least two hours prior to removal in order to ensure that the polymerization had gone to completion, and it was then washed for at least three days in deionized water to remove any unreacted components.

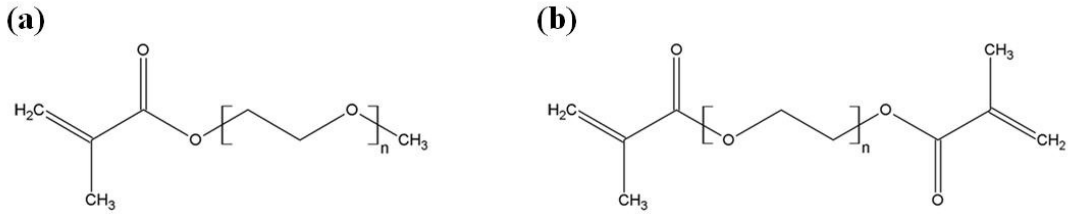

Figure 5.2. Chemical structures of (a) the macromer poly(ethylene glycol) (n = 1000) methyl methacrylate and (b) the crosslinker poly(ethylene glycol) (n = 400) dimethacrylate which were used to fabricated the PEG-based magnetic hydrogel nanocomposites.

5.2.3 Swelling Analysis of PEG Hydrogel Nanocomposites

The volumetric swelling ratios of the hydrogel nanocomposite systems were determined using a gravimetric density analysis method described previously (Frimpong 2006). Samples with 15 mm diameters were cut from each hydrogel system and were placed in PBS (pH 7.4), and these were allowed to equilibrate at 22, 37, 43 and 65 °C. Hydrogels were weighed in both air and n-heptane at each temperature. They were then completely dried and weighed again in air and n-heptane. The volume swelling ratio of each system (Q) was calculated using equation 1:

$$Q = \frac{V^s}{V^d} = \frac{\left(\frac{M^s_{air} - M^s_{heptane}}{\rho_{heptane}}\right)}{\left(\frac{M^d_{air} - M^d_{heptane}}{\rho_{heptane}}\right)} = \frac{M^s_{air} - M^s_{heptane}}{M^d_{air} - M^d_{heptane}} \quad (1)$$

where V is the volume of the sample, $\rho_{heptane}$ is the density of n-heptane, M_{air} is the mass of the sample in air, and $M_{heptane}$ is the mass of the sample in n-heptane. The superscripts s and d refer to the swollen and dry forms of the samples, respectively.

5.2.4 Remote-Controlled Heating of Nanocomposites by Exposure to Alternating Magnetic Field

Samples with 15 mm diameters were cut from each hydrogel system using a cork borer and placed in PBS and allowed to equilibrate at room temperature (22° C) overnight. Excess moisture was removed from the hydrogels before placing them into Saran wrap which was necessary to prevent evaporation of water during heating. The hydrogel and plastic wrap were taped to a stage situated over the alternating magnetic field induction power supply (Taylor-Winfield, MMF-3-135/400-2) equipped with a solenoid with a 15 mm diameter and 5 turns. An infrared camera (AGEMA Thermovision 470) positioned over the hydrogel measured the

surface temperature. The samples were exposed to the AMF for a period of 5 minutes at field strength of 15.1 kA/m and frequency of 298 kHz. The change in temperature recorded was the difference between the initial hydrogel surface temperature and the surface temperature during the heating.

5.2.5 Mechanical Testing to Determine Compressive Modulus

Samples that were 8.5 mm diameter discs were cut from each hydrogel system, placed in PBS, and allowed to equilibrate. Using a BOSE ElectroForce 3300 mechanical test instrument, a displacement method was performed to determine the compressive modulus of the materials. A 1 mm displacement length, displacement rate of 0.05 mm/s, and 500 N load were specified for each test. A stress versus strain curve was plotted for each system, and a strain range of 0.05 to 0.10 was analyzed. From this information, the compressive modulus was determined from the slope of the curve.

5.2.6 Paclitaxel Release from PEG Hydrogel Nanocomposites

Samples (8.5 mm diameter) from each hydrogel system were imbibed with drug by placing them into a solution of Taxol®, the formulation of paclitaxel most commonly used for cancer patient treatment. This consisted of 6 mg paclitaxel, 527 mg Cremophor® EL, and 49.7% (v/v) dehydrated ethanol, with each piece of hydrogel being placed in 1 ml of this solution for two days at room temperature at 100 rpm in an incubator shaker. Release studies were performed in a modified PBS medium comprised of PBS, 2.4 weight % Tween® 20, and 4 weight % Cremophor® EL where Tween and Cremophor® EL surfactants aided in the release of the hydrophobic paclitaxel into the water-based medium. Hydrogels were placed in 6 mL of release medium at 37 °C and 100 rpm, allowed to release over a period of time, then transferred to a fresh release medium to maintain infinite sink conditions. The release medium samples were prepared for high performance liquid chromatography (HPLC) by

adding 4 mL acetonitrile to each sample. Reverse phase-HPLC was carried out on a Thermo Finnigan Spectra System with ChromQuest 4.0 software. The mobile phase consisted of acetonitrile and water (50:50 v/v), the injection volume was 20 µL, and the mobile phase flow rate was 1.0 mL/min. The separation was achieved using a C_{18} Reverse Phase Column (4.6 × 150 mm, pore size 5 µm, Waters, Milford, MA). The mobile phase was monitored at a wavelength of 227 nm with a UV detector. A calibration curve of paclitaxel in acetonitrile and PBS (50:50 v/v) was used to determine the concentration of paclitaxel released.

5.2.7 Mathematical Analysis of Paclitaxel Release

The modeling of drug release from hydrogels has been extensively studied in literature. Higuchi (Higuchi 1961) developed a release model for a thin polymer slab of thickness, ℓ, assuming perfect sink conditions, using Fick's second law. For short times $0 < M_t/M_\infty < 0.6$ (where M_t is the mass of drug released at time, t, and M_∞ is the accumulated mass of drug released at infinity), the solution of this model can be written as:

$$\frac{M_t}{M_\infty} = 4\left(\frac{Dt}{\pi \ell^2}\right)^{1/2} \quad (2)$$

where D is the diffusion coefficient for short times and t is time. This model has its limitations as it assumes Fickian diffusion, and therefore the more general power law seen below is often used to better characterize drug release:

$$\frac{M_t}{M_\infty} = kt^n \quad (3)$$

where k is a constant that depends on the structural and geometrical characteristics and n is the release exponent indicating the mechanism of drug release. An n value of 0.5 indicates Case I

Fickian diffusion while values between 0.5 and 1 indicate anomalous diffusion, and a value of 1 indicates zero-order diffusion (Case II Fickian diffusion). A limitation of this model, however, is the fact that it does not account for an initial burst release or lag time during the initial phase of release. A more detailed description of Fickian drug release modeling is in Appendix B.5.1.

5.2.8 In Vitro Paclitaxel/Hyperthermia Cancer Cell Studies

Three cancer cell lines were evaluated for their response to the chemotherapeutic agent, paclitaxel, and hyperthermia temperatures induced in a humidified incubator. Three cell lines were evaluated, including glioblastoma (M059K), breast adenocarcinoma (MDA MB 231), and lung carcinoma (A549) cells which were all obtained from ATCC. The base cell culture medium for each cell line was as follows: M059K used Dulbecco's Modified Eagle's Medium and Ham's F-12 medium (1:1), A549 used F-12K medium, and MDA MB 231 cells used Leibovitz's L-15 medium. The complete medium for all cell lines contained the base medium supplemented with 10% v/v calf bovine serum, 100 I.U./ml penicillin, 100 µg/ml streptomycin, and 1 µg/ml antimycotic Fungizone® (Invitrogen). The cells were cultured at 37 °C and 5 % CO_2 in a humidified incubator and were used from passages 4 through 8. Initially, M059K were seeded at 10000 cells/cm^2, and A549, and MDA MB 231 cells were both seeded at 5000 cells/cm^2 in 12 well plates and were placed in an incubator for 24 hours. The cells were then exposed for two hours to the following: 10 µM PTX, 50 µM PTX, 10 µM PTX plus heat, 50 µM PTX plus heat, heat only, complete medium with 2% (v/v) DMSO with and without heat, and medium only. The medium with PTX also contained 2% (v/v) DMSO to increase PTX solubility and the DMSO control was used as a comparison to ensure no negative effects on the cells were due to the solvent. After 2 hours, the cells were washed and exposed to fresh medium for 4 hours, 1 day, and 3 days before they were analyzed for cytotoxicity. A two-color fluorescence Live/Dead Viability Assay® (Molecular Probes)

was used to assess the cell viability of the cells initially (corresponding to the PTX or heat treatment for one sample set) or after exposed to fresh medium for the determined times. Stained samples were observed using a NIKON Eclipse 80i microscope at 50x magnification. The number of live cells was determined by manually counting the live and dead cells imaged with NIS-Elements software. The cells were analyzed as three separate samples with ten images (5 live and 5 dead) taken for each. Results were reported as the ratio of the number of live cells for all samples exposed to treatment over the initial cell numbers counted prior to treatment.

5.2.9 Statistical analysis

All experiments were performed at least in triplicate. MYSTAT 12 for Windows (12.02.00) was used for t-tests (paired t-test with unequal variances) to determine any significance in observed data. A p-value of <0.05 was considered statistically significant.

5.3 Results and Discussion

5.3.1 Swelling, Remote-Controlled Heating, and Mechanical Analysis

Swelling studies were performed on the hydrogels in order to determine their capability for imbibing fluids. Figure 5.3 shows the volume swelling ratio (Q) for each hydrogel system at various temperatures. From this, it can be seen that for all systems, Q decreases from 22 to 37 °C (p-values < 0.05), Q is the same from 37 to 43 °C (p-value > 0.05), and Q decreases again from 43 to 65 °C. Additionally, as the crosslinking density increases, Q decreases. The volume swelling ratios for the 50PEG1000MA and the 20PEG1000MA hydrogels were close despite the difference in crosslinking density but were still statistically different (p-values were 0.016, 0.015, 0.011, and 0.020 for 22, 37, 43, and 65 °C, respectively). The Q values for each hydrogel system did not vary between 37 °C and 43 °C,

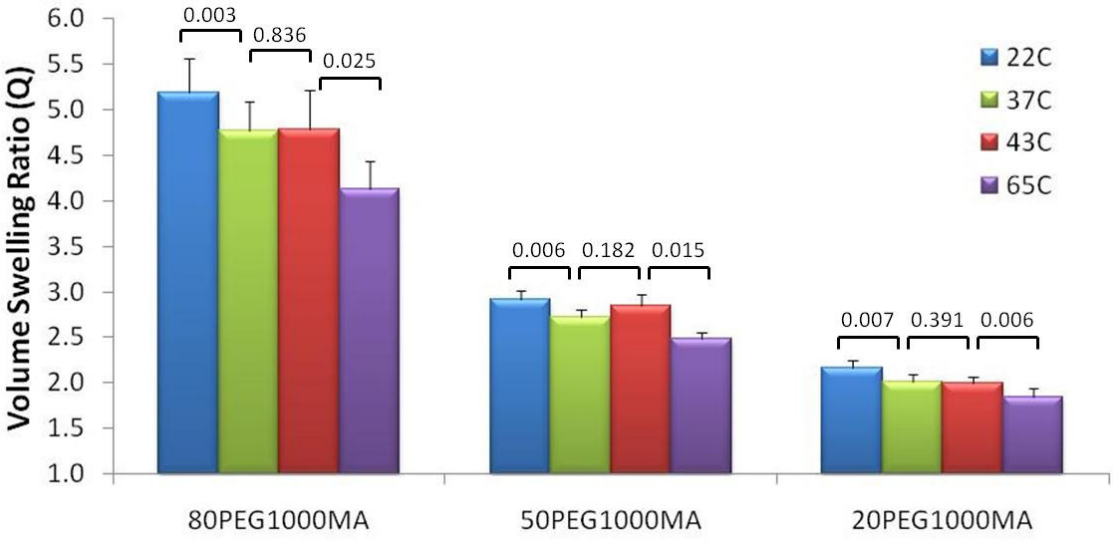

Figure 5.3. Volume swelling ratio (Q) for the hydrogel nanocomposites at various temperatures with corresponding p-values. N = 3 ± SE.

which are body and hyperthermia temperatures, respectively. This data may have implications should the hydrogel be implemented as a treatment device, since the hydrogel would not alter its swelling from being placed in the body or due to heating.

Remote-controlled heating data was analyzed by finding the change in temperature from the initial room temperature to the surface temperature of the hydrogel after five minutes of exposure to an AMF (ΔT). As seen in Figure 5.4, the higher crosslinked hydrogel (20PEG1000MA) had a greater change in temperature after exposure to the AMF. This is due to a higher iron oxide to hydrogel volume ratio (i.e., lower water content) in the gel. Because the hydrogel is more densely crosslinked, a greater amount of iron oxide nanoparticles per unit volume of the hydrogel are present in the swollen nanocomposite. The ΔT for the 50PEG1000MA system is similar to the ΔT for the 20PEG1000MA hydrogel, and this is in agreement with the swelling data which showed a significant difference between the lowest crosslinked hydrogel and the highest, but less of a difference between the 50PEG1000MA and the higher crosslinked 20PEG1000MA hydrogel. Importantly, each hydrogel was able to reach temperatures well above hyperthermia range, thus demonstrating that the temperature range for hyperthermia treatment can be reached using these hydrogel nanocomposite systems.

Compression testing was done on three samples from each hydrogel system. Figure 5.5 shows the compressive modulus for each hydrogel. As expected, the hydrogel with the lowest crosslinking density also had the lowest compressive modulus. As crosslinking density was increased, the compressive moduli increased.

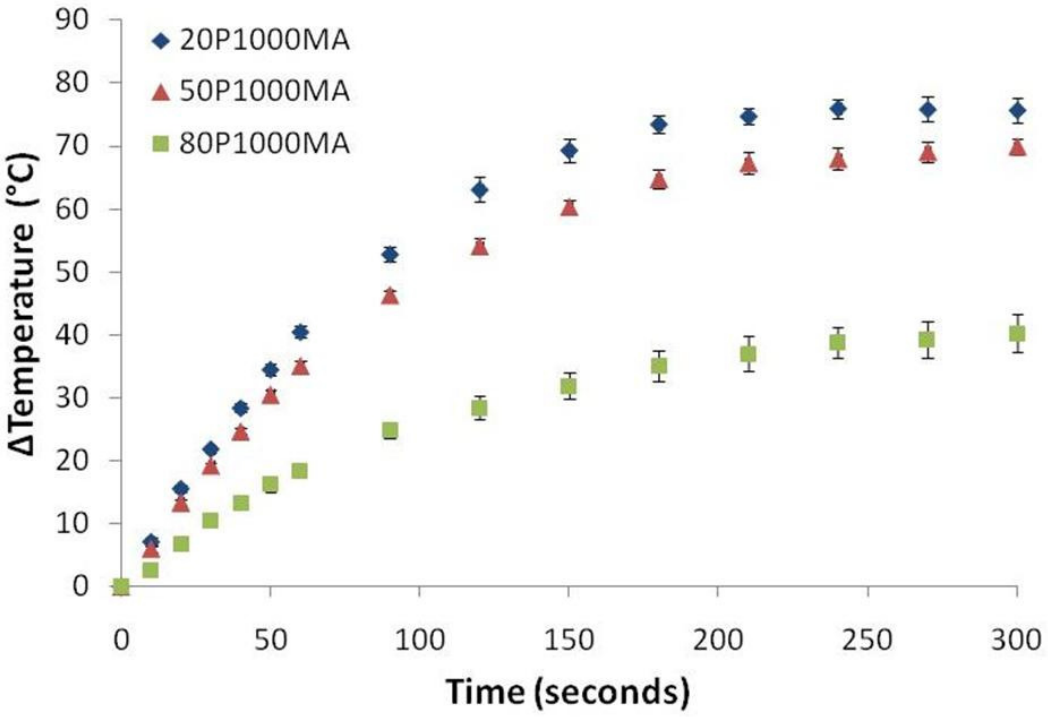

Figure 5.4. Heating analysis of nanocomposites exposed to an alternating magnetic field (15.1 kA/m, 298 kHz) for 5 minutes. The change in temperature (ΔTemperature) is relative to the initial temperature of the hydrogel at room temperature. N = 3 ± SE.

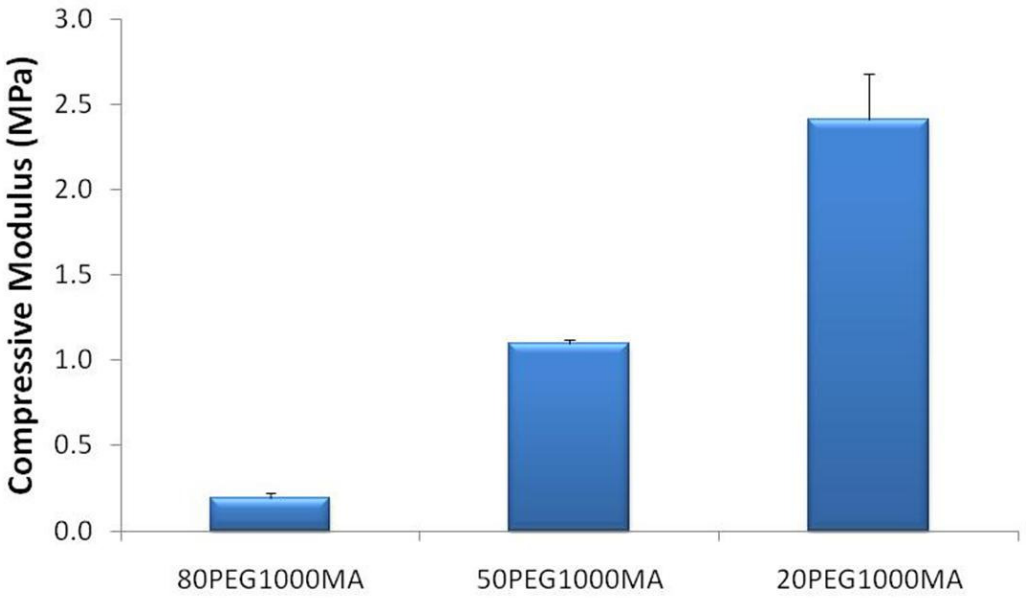

Figure 5.5. Compressive modulus of hydrogel nanocomposites after mechanical analysis of swollen hydrogels at room temperature using a displacement method. N = 3 ± SE.

5.3.2 Mathematical Analysis of Paclitaxel Release

For purely Fickian diffusion, a model for drug release has been developed by Higuchi which was described in equation 2. It is the power law, as seen in equation 3, however, which can be used to determine the drug release mechanism of the system, whether the release is Fickian or not. For this work, all three hydrogel systems were imbibed with PTX in a Taxol® formulation, and its release was studied in a modified PBS solution at 37 °C. Figure 5.6 (a) shows the fractional drug release with time, and PTX was released from all of the hydrogels by 22 days. This data was analyzed using the power law from $0 < M_t/M_\infty < 0.6$ and the corresponding n values can be found in Table 5.1. For all of the systems, the release exponent (n) was less than 0.5 indicating the release mechanisms are non-Fickian. It was hypothesized that this phenomenon was most likely due to the initial burst release from the hydrogels. In addition, since the hydrogels were not dried prior to the release studies, the Taxol® formulation loaded into the hydrogels increases the solubility of paclitaxel. The large initial concentration gradient of Taxol® to PBS would act as a strong driving force to release the paclitaxel quickly from the hydrogels.

The data indicates that the least crosslinked hydrogel system (80PEG1000MA) released the paclitaxel the fastest, with the most crosslinked system (20PEG1000MA) releasing the drug the slowest. This is due to the fact that hydrogel systems with less crosslinking exhibit a looser mesh and larger mesh size, allowing for the drug to diffuse more freely through the system. Additionally, Figure 5.6b shows the cumulative release of paclitaxel from the hydrogels. 80PEG1000MA was shown to imbibe and release more paclitaxel with less drug being released in the more crosslinked systems. Overall, these results indicate that paclitaxel can be release successfully from PEG hydrogel systems and this release can be tailored by the crosslinking density of the hydrogel systems.

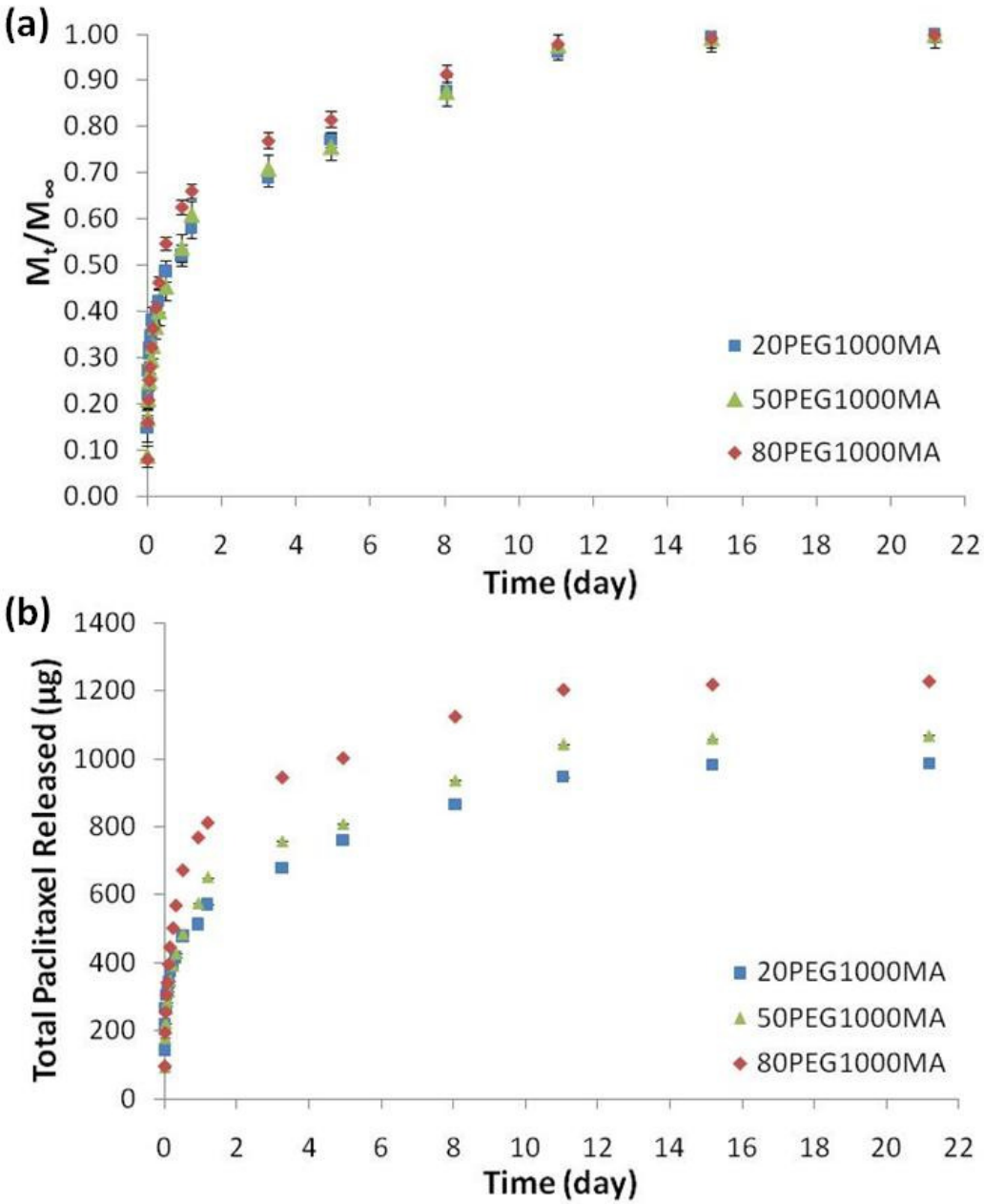

Figure 5.6. Paclitaxel release data from PEG hydrogel nanocomposites versus time. (a) is the fractional release of PTX whereas (b) is the total amount of paclitaxel released from the hydrogel nanocomposites. N = 3 ± SE.

Table 5.1. Drug release analysis values including the initial release exponent from the power law prior (n) and the thickness of the gels (ℓ).

System	n	ℓ (cm)
20PEG1000MA	0.19	0.16
50PEG1000MA	0.24	0.17
80PEG1000MA	0.25	0.21

5.3.3 Cancer Cell Response to Paclitaxel and/or Hyperthermia

In vitro studies were performed to determine the effect of paclitaxel and/or hyperthermia on three cells lines: M059K (glioblastoma), MDA MB 231 (breast adenocarcinoma), and A549 (lung carcinoma). The cells were exposed to micromolar concentrations of PTX and/or heat for 2 hours and then allowed to respond in fresh medium for 3 hours, 1 day, and 3 days. The number of cells counted for each sample was ratioed against the initial cell sample counted for each cell type. This then can show the effect the different treatments have on the various cell lines.

As seen in Figure 5.7, for MDA MB 231 cells after 3 hours, there was no change in the cells due to DMSO, heat, or PTX in comparison to the control (p-values > 0.05). 1 day after exposure, there was no effect due to DMSO ($p = 0.508$), however, 10 and 50 μM PTX and heat decreased the number of cells ($p = 0.023$, 0.001, 0.000, respectively). No synergistic effect was for 10 and 50 μM plus heat in comparison to PTX alone ($p = 0.362$, 0.729). Similar effects were seen 3 days with no DMSO effect ($p = 0.134$), a decrease in cells compared to the control for 10 and 50 μM PXL or heat ($p = 0.000$, 0.001, 0.023). There was no synergistic effect due to PXL and heat combines ($p = 0.086$ and 0.324 for 10 and 50 μM, respectively). Figure 5.8 supports this data showing a decrease in the number of cells for samples exposed to PTX or heat.

For the glioblastoma (M059K) cells 3 hours after exposure, there were no effects seen due to any treatments ($p > 0.05$) as seen in Figure 5.9. 1 day after exposure, however, there were no effects due to DMSO ($p = 0.377$) or heat (0.787), however, the cell number did decrease for 10 and 50 μM PTX treatment ($p = 0.015$, 0.003). There was no synergistic effect seen for 10 and 50 μM PTX plus heat ($p = 0.053$, 0.259). 3 days after treatment, M059K cells showed a negative response to DMSO with a vast decrease in cell numbers in comparison to the control ($p = 000$). Therefore, there was no was no way to determine what effect PTX or heat had on this cell line. Figure 5.10 shows the cell morphology of the M059K cells 3 days

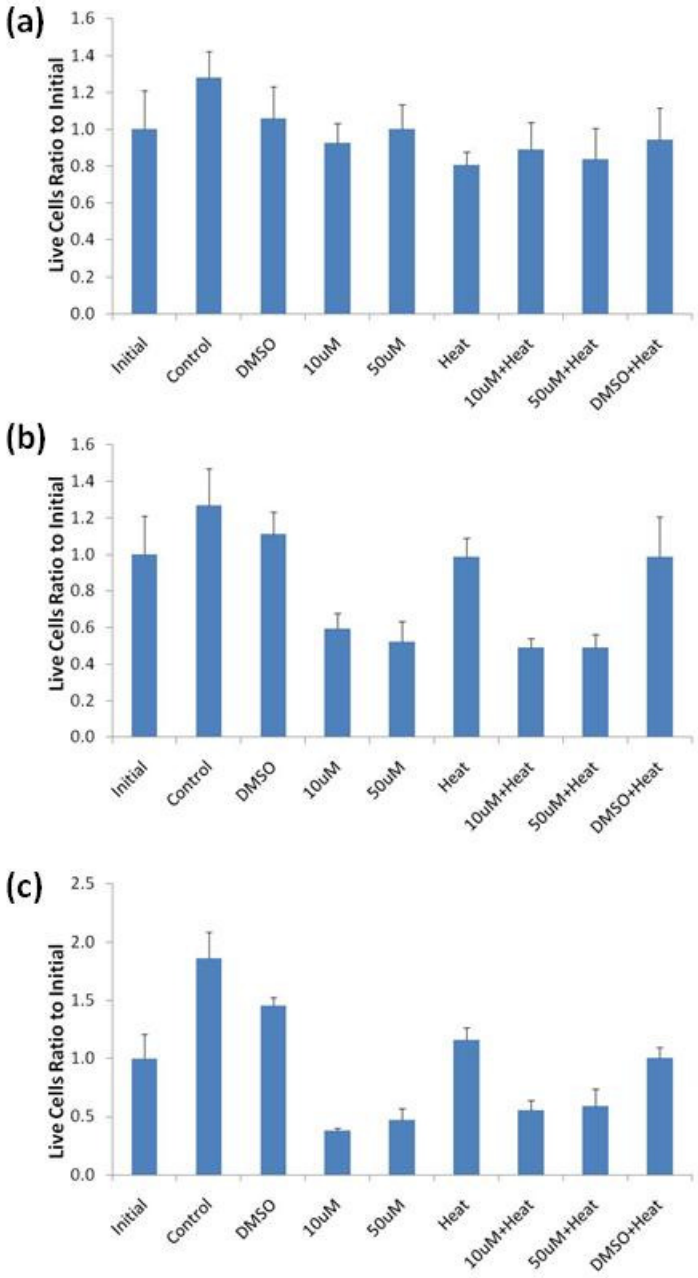

Figure 5.7. *In vitro* analysis of MDA MB 231 (breast adenocarcinoma) cells exposed to PTX and/or heat treatment for 2 hours and then analyzed (a) 3 hours, (b) 1 day, and (c) 3 days after PTX or heat exposure, respectively. N = 3 ± SE.

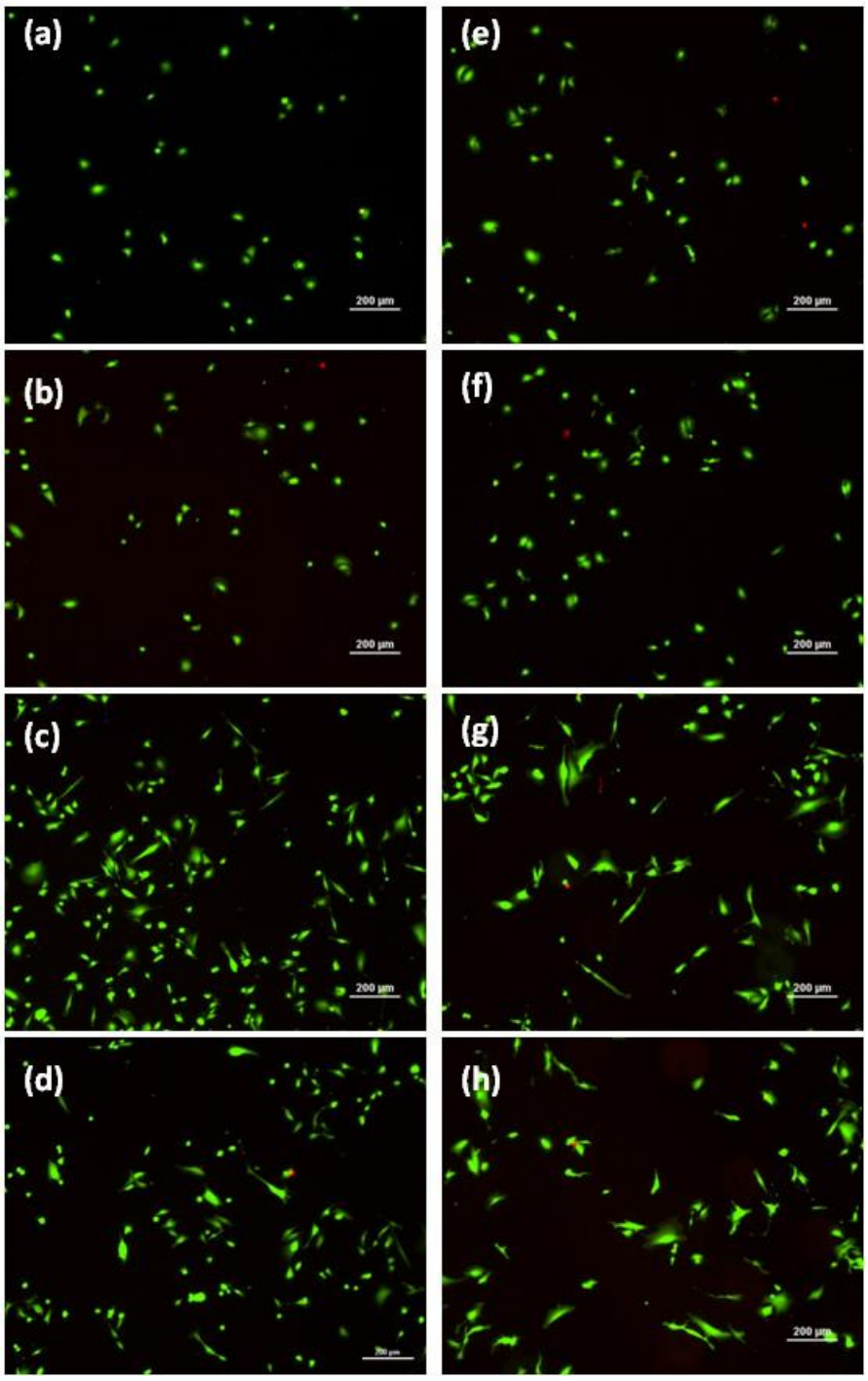

Figure 5.8. *In vitro* analysis of MDA MB 231 (breast adenocarcinoma) cells exposed to PTX and/or heat treatment for 2 hours with fluorescent images of the cells 3 days after exposure for the following conditions: (a) 10 μM PTX only, (b) 50 μM PTX only, (c) media only, (d) DMSO in media, (e) 10 μM PTX plus heat, (f) 50 μM PTX plus heat, and (g) heating only and (h) heat only with DMSO in media.

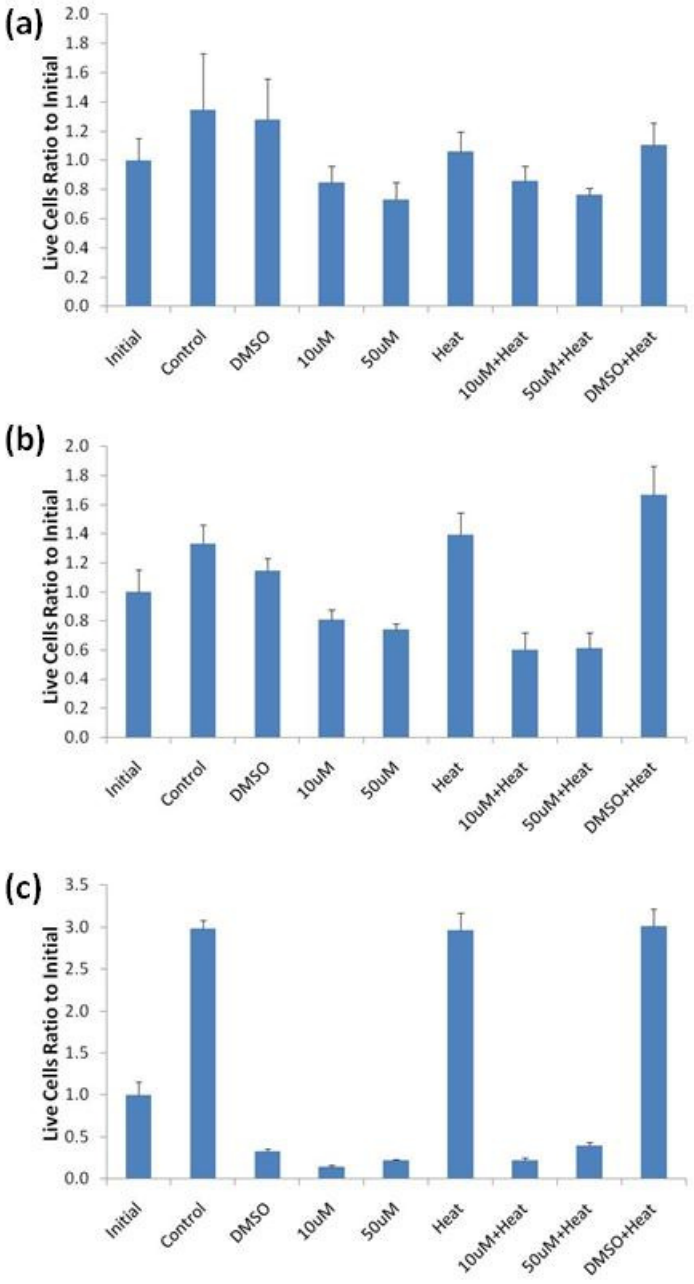

Figure 5.9. *In vitro* analysis of M059K (glioblastoma) cells exposed to PTX and/or heat treatment for 2 hours and then analyzed (a) 3 hours, (b) 1 day, and (c) 3 days after PTX or heat exposure, respectively. N = 3 ± SE.

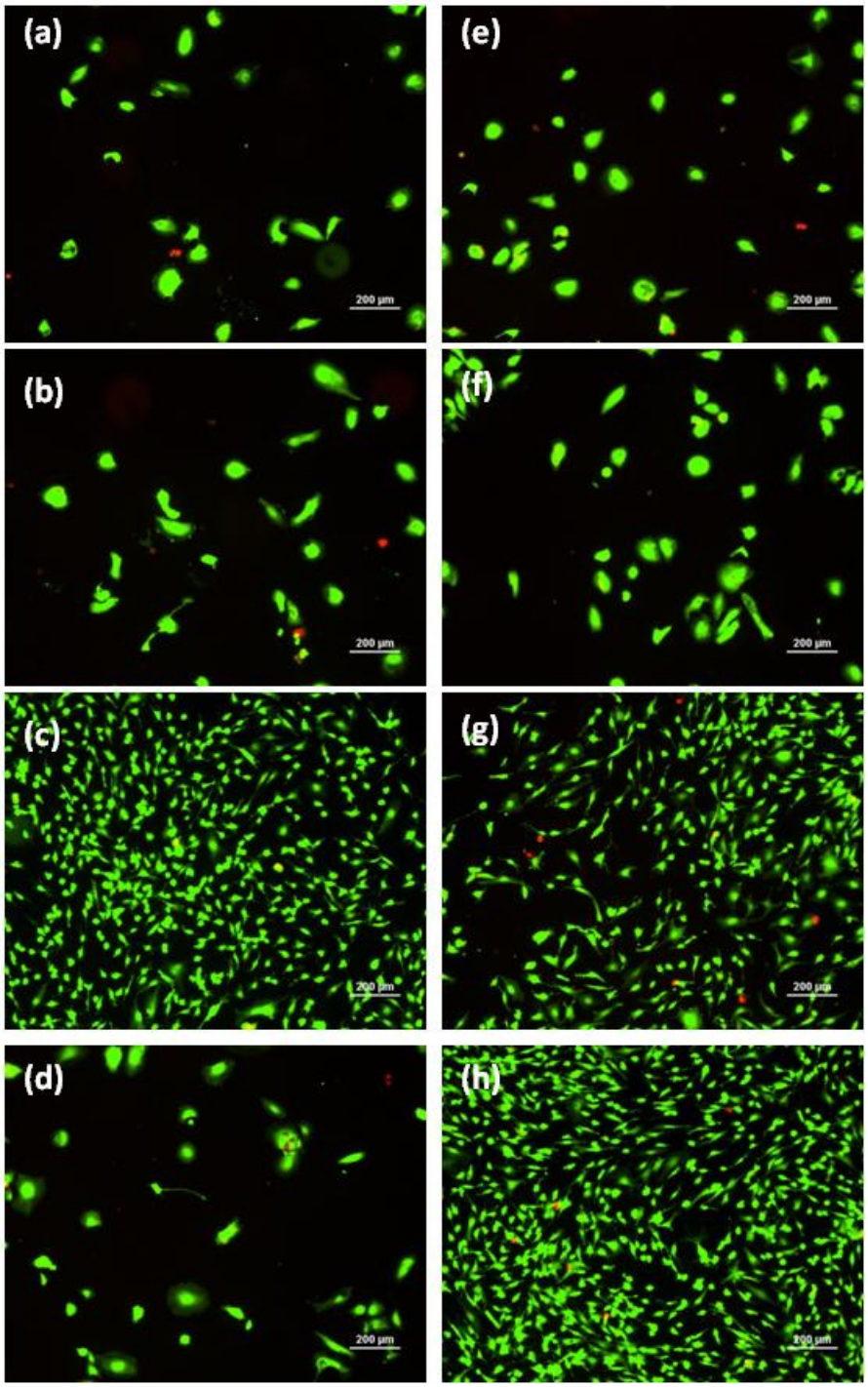

Figure 5.10. *In vitro* analysis of M059K (glioblastoma) cells exposed to PTX and/or heat treatment for 2 hours with fluorescent images of the cells 3 days after exposure for the following conditions: (a) 10 μM PTX only, (b) 50 μM PTX only, (c) media only, (d) DMSO in media, (e) 10 μM PTX plus heat, (f) 50 μM PTX plus heat, and (g) heating only and (h) heat only with DMSO in media.

after exposure and the effect of DMSO on the cells is evident with fewer cells which have abnormal morphology.

There are no studies that show that either PTX or hyperthermia are effective in treating M059K cell lines although PTX is effective in treating other types of glioblastoma cell lines (Langer, Ruffer et al. 2001; Zhan, Gu et al. 2010). Similarly, there is no data that supports the treatment of MDA MB 231 cells with PTX or heat. There are studies that illustrate the effectiveness of paclitaxel in treating other breast cancer cells lines both in vitro (Ito, Kuga et al. 2004) and in vivo (Cividalli, Cruciani et al. 1999). Overall, the data from the study in our current project shows that other types of breast adenocarcinoma and glioblastoma cell lines may need to be evaluated to show the efficacy of combined hyperthermia and paclitaxel treatment so that this work can be effectively translated into in vivo studies.

Figure 5.11 shows the effect of the PXL and heat treatments on A549 (lung adenocarcinoma) cells 3 hours, 1 day, and 3 hours after exposure. For the 3 hour samples, there was no effect on the cells in comparison to the control due to DMSO or 10 or 50 μM PXL ($p = 0.519, 0.598, 0.998$, respectively). The number of cells did decrease in comparison to the control ($p = 0.048$), however, there was no synergistic effect due to PXL plus heat compared to PXL alone ($p > 0.05$). 1 day after exposure, there was no effect on the cells due to DMSO, 10 or 50 μM PXL, or heat only in comparison to the control ($p = 0.223, 0.888, 0.553, 0.691$, respectively). There was, however, a synergistic effect when combining the PXL treatment with heat ($p = 0.014$ and 0.000 for 10 and 50 μM PXL plus heat, respectively). Similar effects were seen 3 days after exposure with no effect due to PXL, 10 or 50 μM PTX, or heat ($p = 0.123, 0.148, 0.103, 0.380$). For 10 and 50 μM PTX plus heat, however, the number of cells decreased significantly compared to the PTX only treatment ($p = 0.000$ for both PTX concentrations). Figure 5.12 shows the A549 cells 3 days after PTX and/or heat exposure and it can be seen that the cell morphology is the same for all of the cells except for the samples exposed to both PTX and heat. For these two samples, the cell morphology is

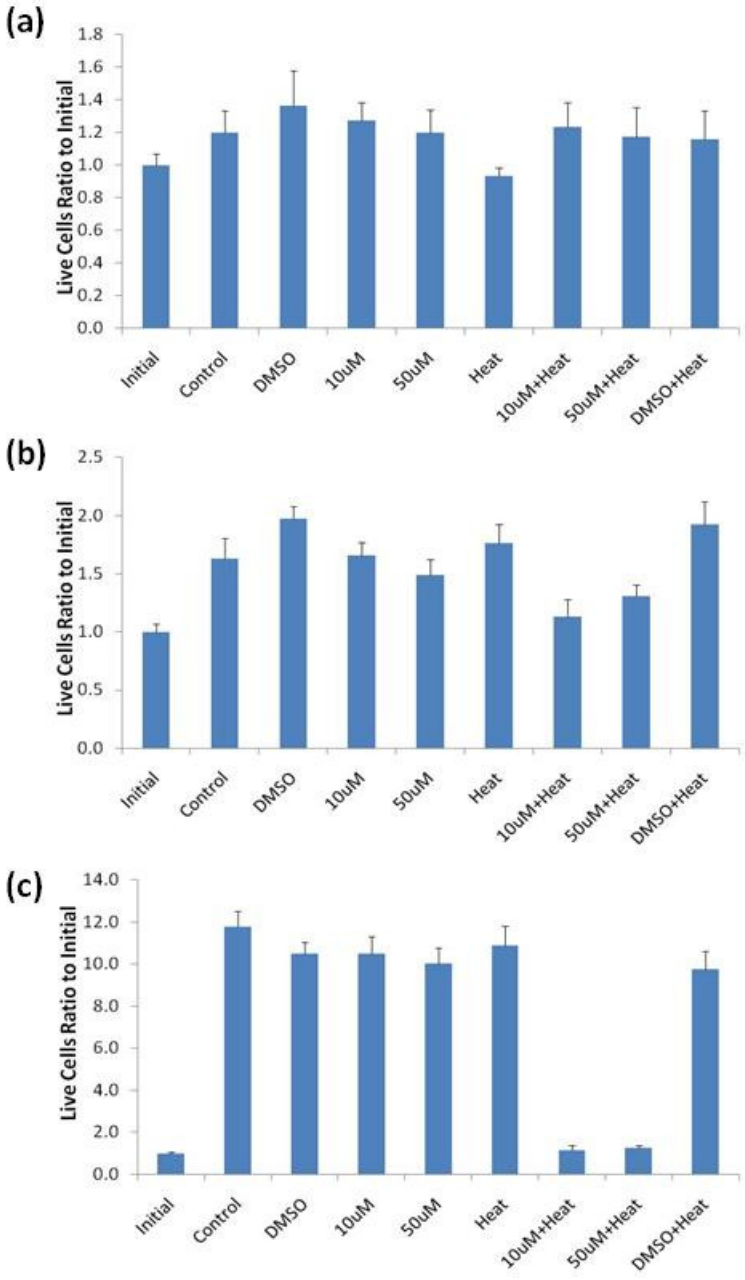

Figure 5.11. *In vitro* analysis of A549 (lung adenocarcinoma) cells exposed to PTX and/or heat treatment for 2 hours and then analyzed (a) 3 hours, (b) 1 day, and (c) 3 days after PTX or heat exposure, respectively. N = 3 ± SE.

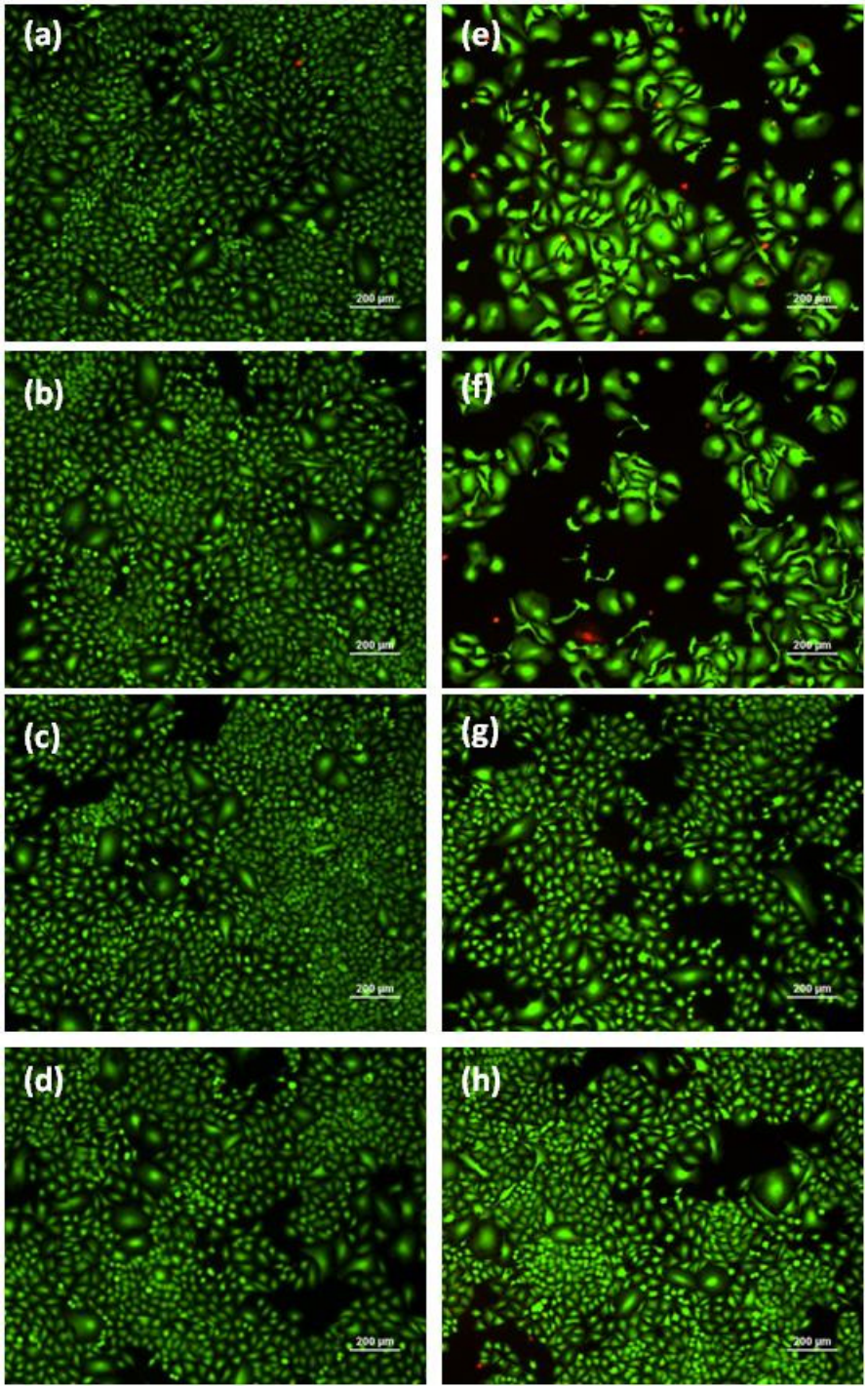

Figure 5.12. *In vitro* analysis of A549 (lung adenocarcinoma) cells exposed to PTX and/or heat treatment for 2 hours with fluorescent images of the cells 3 days after exposure for the following conditions: (a) 10 μM PTX only, (b) 50 μM PTX only, (c) media only, (d) DMSO in media, (e) 10 μM PTX plus heat, (f) 50 μM PTX plus heat, and (g) heating only and (h) heat only with DMSO in media.

abnormal with fewer cells which may be due to dying cells detaching from the surface of the well plates. Overall, this shows the potential to use both PTX and hyperthermia to treat lung adenocarcinoma cells more effectively than PTX alone. Although previous in vivo studies support the effectiveness of both PTX alone in treating this cancer cell line (Shen, Hu et al. 2008), this is the first time the synergistic effect of paclitaxel at micromolar levels and hyperthermia has been demonstrated.

5.4 Conclusions

Magnetic PEG-based hydrogel nanocomposites have been demonstrated to have the ability to deliver both paclitaxel and heat for the potential treatment of cancer. The swelling, heating, and mechanical characteristics of the hydrogel nanocomposites were able to be tailored by the crosslinking density of the hydrogel systems. All of the hydrogels were shown to heat well above the temperature needed for hyperthermia upon exposure to an alternating magnetic field. The drug release mechanism of the hydrogels was not found to be purely Fickian and it was shown the lower crosslinked hydrogels released PTX more quickly, which would be expected. *In vitro* cell studies showed that combined PTX and hyperthermia treatment increases the efficacy of PTX for A549 lung carcinoma cells. Overall, these hydrogel nanocomposites may have the ability to treat this type of cancer along with numerous other cancer types.

References

All references are located at the end of the dissertation.

CHAPTER 6

"Controlled Synergistic Delivery of Paclitaxel and Heat from Poly(β-amino ester)/Iron Oxide-Based Hydrogel Nanocomposites"

This research investigates the use of poly(β-amino ester) (PBAE) biodegradable hydrogels and iron oxide for combined chemotherapeutic and heat delivery in hyperthermia-based treatment of cancer. Hyperthermia, the heating of cancerous tissue from 41 to 45°C, has been shown to increase the efficacy of conventional cancer therapies such as irradiation and chemotherapy. The hydrogel nanocomposites in this work provide a drug delivery vehicle (via the biodegradable PBAE polymer network) and the ability to be heated remotely upon exposure to an alternating magnetic field (via iron oxide nanoparticles). PBAE macromers comprised of poly(ethylene glycol) (N=400) diacrylate (PEG400DA) or diethylene glycol diacrylate (DEGDA) with isobutylamine (IBA) have been synthesized via a simple condensation reaction. The macromers were analyzed via gel permeation chromatography to determine their molecular weight and polydispersity index values. Hydrogel nanocomposites were fabricated via free-radical polymerization of two types of PBAE macromers with iron oxide nanoparticles, the chemotherapeutic agent paclitaxel, and ammonium persulfate as the free radical initiator. The degradation of the hydrogel nanocomposites was carried out in phosphate buffered saline solution at 37°C. A pure 2EG-IBA (1:1.2 molar ratio of IBA to DEGDA)-based hydrogel exhibited complete degradation after approximately 7 weeks whereas the pure 9EG-IBA (1:1.2 molar ratio of IBA to PEG400DA)-based hydrogel degraded in 11 hours. The hydrogels all heated upon exposure to an alternating magnetic field throughout the degradation process. Additionally, the degradation products exhibited cell viabilities ranging from 53% for a pure 2EG-IBA gel at 4.5 mg/ml and 92% for a pure 9EG-IBA gel at 0.15 mg/ml. The paclitaxel release was controlled via bulk degradation of the

hydrogels with time. Overall, the tailorability and biodegradable nature of the PBAE hydrogel nanocomposites makes them solid candidates for combined hyperthermia and chemotherapy-based treatment of cancer.

Keywords: Hydrogel, nanocomposites, poly(β-amino ester), hyperthermia, paclitaxel, cancer.

6.1 Introduction

Currently, cancer is the second leading cause of death in the United States. In 2009 alone, there were an estimated 1.5 million new cases diagnosed (ACS 2009). Despite the amount of research being done to overcome this disease, there are still many types, such as glioblastoma and pancreatic cancer (Sneed 1998), which have extremely poor treatment success rates. Therefore, multiple-modality treatment has become the preferred treatment approach. Hyperthermia, the heating of cancer tissues to between 41 and 45°C, has been proven to provide a straightforward and more effective way of treating some types of cancer in combination with well-developed therapeutics such as radiation and chemotherapy (Falk and Issels 2001). Aside from having a cytotoxic effect on cancerous tissue, hyperthermia has been shown to increase tumor blood flow which can decrease hypoxia, acidosis, and energy deprivation at the tumor site, thereby increasing therapy efficacy as these conditions often make the treatment of cancer more difficult (Hildebrandt 2002). Hyperthermia therapy faces a number of obstacles including being able to restrict local heating of the tumor without damaging surrounding tissue (Moroz 2002) and the inability to heat the cancer tissue locally without using invasive and uncomfortable heating probes (Guedes 2005). This can potentially be overcome through the development of systems which can be delivered to and/or implanted at tumor sites and remotely heated from outside the body. This work presents a hydrogel nanocomposite capable of delivering both heat and a chemotherapeutic for local synergistic

treatment of cancer through the implantation or *in situ* injection of the hydrogel within or near malignant tumors.

Hydrogel nanocomposites involve the incorporation of nanoparticulate materials within a hydrogel matrix which often provide easy, straightforward methods for enhancing the properties of conventional hydrogel systems. Thus far, a number of nanoparticulates have been utilized in nanocomposite hydrogel systems including metallic nanoparticles, carbon nanotubes, clay, ceramics, magnetic nanoparticles, hydroxyapatite, and semiconducting nanoparticles (Meenach 2009). Hydrogels themselves are advantageous for many biomedical applications due to their resemblance of natural living tissue and inherent biocompatibility, which can be partially attributed to their soft, flexible nature and high water content (Peppas 2006). Magnetic hydrogel nanocomposites containing nanoscale superparamagnetic iron oxide nanoparticles have the potential to be used in hyperthermia therapy due to their ability to heat upon exposure to an alternating magnetic field (AMF). The heating mechanisms for these paramagnetic particles are based primarily on Brownian relaxation (rotation of the particle as a whole according to external magnetic field), the Neel effect (reorientation of the magnetization vector inside the magnetic core against an energy barrier), and often some minimal hysteresis losses (Babincova 2001). Hydrogel nanocomposites containing iron oxide nanoparticles have already been utilized in applications such as remote-controlled drug delivery (Satarkar and Hilt 2008), microfluidic valves (Satarkar 2009), hydrogel degradation (Hawkins 2009) and thermoablation (Meenach 2009; Meenach 2009).

In addition to delivering heat, these materials also have the potential to deliver therapeutic agents for cancer therapy and other diseases. There are many disadvantages to using systemic chemotherapy delivery for cancer treatment including systemic toxicity, low drug bioavailability, and difficulty in delivering the drug(s) effectively within tumors (Ta 2008). Hydrogel nanocomposites have the ability to overcome these obstacles through the local delivery of chemotherapeutic agents at therapeutic doses. In recent years, poly(β-amino

ester) (PBAE) hydrogels have been widely investigated for various biomedical applications such as drug delivery and tissue engineering. Anderson and coworkers have developed the first combinatorial library of biodegradable crosslinkable biomaterials characterizing a wide variety of PBAE macromers. This library consists of acrylate-terminated poly(β-amino ester)s synthesized via a condensation reaction that combines primary or secondary amines with diacrylates (Anderson 2006). There are many benefits to using these diacrylate-terminated biodegradable hydrogel systems including: 1) monomer reagents that are inexpensive and commercially available, 2) macromer polymerization that can be completed without additional protection/deprotection schemes because the amine participate directly in the bond-forming processes in the reactions, and 3) no byproducts generated during the synthesis so that no purification steps are necessary (Anderson 2006). Utilizing PBAE macromers in a hydrogel matrix can allow for hydrogel systems whose degradation, mechanical strength, and toxicity can be controlled based on the monomer reagents used for macromer synthesis.

Paclitaxel (PTX) is a plant alkaloid which effectively disrupts mitosis during the G2 phase of the cell cycle by binding with the beta subunit of tubulin dimers. This interferes with the dynamic instability of the microtubules in the cytoskeleton where the cells form highly stable, rigid microtubules preventing proliferation (Obara 2005; Michalakis 2007). In addition, PTX also inhibits angiogenesis, cell migration, and collagenase production. PTX and hyperthermia have a complex relationship in the treatment of cancer in that their combined effect is both cell-line dependent and there is variable effectiveness in the hyperthermia temperatures utilized (Issels 2008). PTX has been commonly used to treat human carcinomas, with considerable antineoplastic activity specifically against ovarian, head, and neck carcinoma. As a chemotherapeutic, paclitaxel has also been effective in treating lung cancer, breast cancer, acute leukemia and other solid tumors (Issels 2008). Currently, the most common formulation of paclitaxel used clinically is Taxol™, which uses a carrier of Cremophor® EL and ethanol to increase the solubility of the highly hydrophobic

drug. The objective of this work was to fabricate and characterize biodegradable PBAE-based hydrogel nanocomposites for the combined delivery of heat and paclitaxel for potential cancer therapy applications. The degradation of the hydrogels allows for the controlled release of the chemotherapeutic, paclitaxel, whereas the iron oxide nanoparticles in the hydrogel matrix allows for the remote heating of the systems via an AMF. In addition to the characterization of the degradation, mechanical, heating, and release properties of these systems, the cytotoxicity of the degradation products was analyzed to show the inherent safety of these materials to be used in biomedical applications.

6.2 Materials and Methods

6.2.1 Materials

Diethylene glycol diacrylate was obtained from Polysciences (Warrington, PA). The Fe_3O_4 nanoparticles (20-30 nm diameter, 0.2% polyvinylpyrrolidone-coated) were obtained from Nanostructured and Amorphous Materials (Los Alamos, NM). Paclitaxel (99.5%) was from LC Laboratories (Woburn, MA). Ammonium persulfate (APS), isobutylamine (IBA), Cremophor EL®, Tween® 20, tetrahydrofuran, and poly(ethylene glycol) (N=400) diacrylate (PEG400DA) were obtained from Sigma Aldrich (St. Louis, MO). Cells and cell medium were obtained from American Type Culture Collection (Manassas, VA). The mammalian cell live/dead assay was from Molecular Probes/Invitrogen (Carlsbad, CA). All materials were used as received.

6.2.2 Synthesis and Characterization of Poly(β-amino ester) Macromers

Two biodegradable poly(β-amino ester) macromers were synthesized via condensation reactions of isobutylamine (IBA) with excess poly(ethylene glycol) (PEG) diacrylates. For one macromer, a 1:1.2 molar ratio of IBA to diethylene glycol diacrylate (with 2 ethylene

glycol units, n = 2) was reacted for 48 hours at 85°C with mixing (thereby denoted as 2EG-IBA). The second macromer was comprised of a 1:1.2 molar ratio of IBA to poly(ethylene glycol) (N=400) diacrylate (9 EG units, n = 9) reacted for 15 hours at 85°C (denoted 9EG-IBA). These compounds and the resulting macromer structure can be seen in Figure 6.1. The macromers were then analyzed via a Shimadzu gel permeation chromatography (GPC) system to determine the average molecular weight and polydispersity index (PDI) of the macromers. The analysis was completed at 0, 24, and 48 hours for the 9EG-IBA macromer and 0 and 15 hours for the 2EG-IBA macromer. For the systems studied, the macromer solution was mixed with tetrahydrofuran (THF) to a concentration of 5 mg/mL prior to GPC analysis. Attenuated Total Reflectance Fourier Transform Infrared (ATR-FTIR) analysis was performed to determine the conversion of available carbon-carbon double bonds present in the PEG diacrylate constituents of the macromers using a Varian Inc. 7000e step-scan spectrometer. A sample of the macromer solution was placed on the diamond ATR crystal and IR spectra were obtained at 8 cm^{-1} spectral resolution between 700 and 4000 cm^{-1}.

6.2.3 Fabrication of Poly(β-amino ester)/Iron Oxide Hydrogel Nanocomposites

Magnetic hydrogel nanocomposites were fabricated via chemically-initiated free-radical polymerization with various ratios of the two crosslinkable macromers, resulting in hydrogels with differing degradation profiles. The resulting systems had 0, 25, 50, 75, and 100 weight % 2EG-IBA macromer (100 9EG-IBA, 25 2EG-IBA, 50 2EG-IBA, 75 2EG-IBA, and 100 2EG-IBA, respectively). 5 weight % iron oxide nanoparticles and 5 mg of paclitaxel per g of macromer were added to the macromer solution which was exposed to ultrasonication to facilitate dispersion of the nanoparticles and drug. After sonication, 1.5 weight % of APS dispersed in water (2 ml water per gram of APS) was then added to the mixture to initiate the free-radical polymerization. This solution was then mixed well before being loaded into a template consisting of two glass plates with a 1.5 mm thick Teflon spacer. Gels without

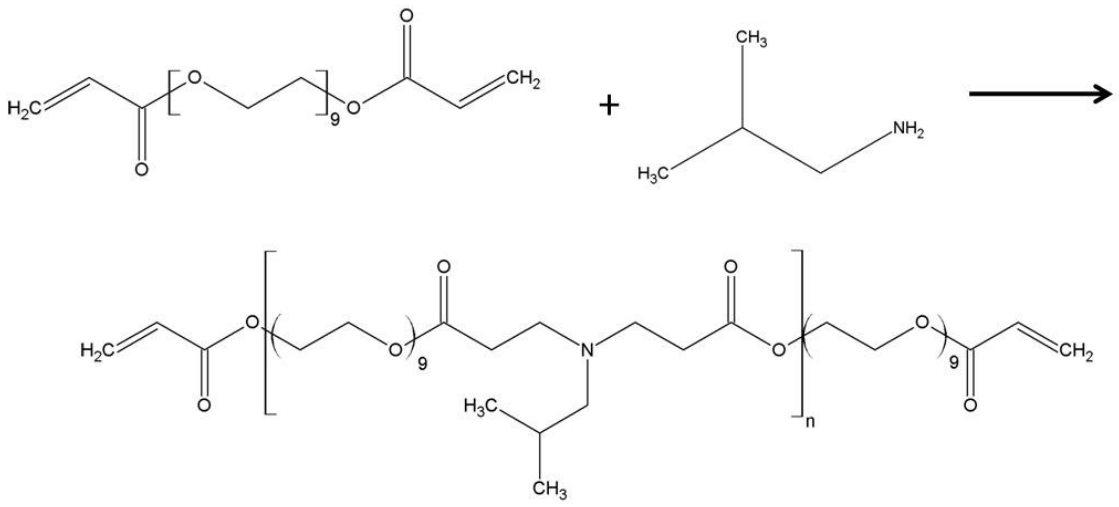

Figure 6.1. Schematic for synthesis reaction of poly(β-amino ester) macromers comprised of excess poly(ethylene glycol) (n) diacrylate with isobutylamine resulting in diacrylate-terminate structure. This structure has C=C bond end groups allow them to be reacted into hydrogel nanocomposites via free-radical initiation. Also, the macromers are biodegradable due to hydrolysis of the available ester bonds present.

paclitaxel used for cytotoxicity analysis were made the same as described only without paclitaxel. The gels were kept in this template at least overnight to allow for completion of polymerization after which they were removed from the templates and placed in a desiccator to prevent degradation.

6.2.4 Characterization of Hydrogel Nanocomposite Degradation and Swelling Response

The degradation and swelling response of the hydrogel nanocomposites were determined with respect to time. After polymerization, the hydrogels were cut into 8.2 mm diameter discs. The initial mass of each gel (m_i) was recorded and they were placed in individual tissue cassettes in PBS (pH 7.4) in an incubator shaker at 37°C and 100 rpm. The gels were removed at given times, their mass was recorded again in their swollen state (m_s), and they were freeze-dried to remove any residual water. Their mass was then taken again in their dry state (m_d). The mass loss of the hydrogels was characterized by calculating the mass fraction remaining:

$$\text{mass fraction remaining} = \frac{m_d}{m_i} \quad (1)$$

The swelling of the gels was then characterized by the mass swelling ratio (q):

$$q = \frac{m_s}{m_d} \quad (2)$$

6.2.5 Mechanical Testing: Determination of Compressive Modulus

Compressive modulus of the hydrogel nanocomposites was determined with compressive mechanical testing. Gels were cut and placed in PBS at 37°C and 100 rpm. The gels were tested using the displacement method on a BOSE ElectroForce 3300 with 1 mm

displacement at a displacement rate of 0.05 mm/s with a 500 N load. Stress versus strain data was plotted and a strain range of 0.05 to 0.10 was analyzed for each gel. From this information, the compressive modulus of the gel could be determined from the slope of the stress versus strain plot.

6.2.6 Iron Oxide Loss Studies via Thermogravimetric Analysis

Thermal gravimetric analysis was completed to determine the actual iron oxide nanoparticle loading in the hydrogel nanocomposites as they degraded. The 100 9EG-IBA hydrogel system was analyzed as a representative sample as it has the fastest degradation profile. A Netzsch STA 449A system (NETZSCH Instruments, Inc., Burlington, MA) was used to perform this analysis. From an initial temperature of 20°C, the gel samples were heated up to 120°C at 5°C per minute, kept at 120°C for 20 minutes to allow for water evaporation, and then heated up to 590°C at 3°C per minute. The remaining mass was recorded with time.

6.2.7 Remote-Controlled Heating of PBAE Hydrogel Nanocomposites via an AMF

The magnetic hydrogel nanocomposites were heated using an alternating magnetic field (AMF) at different times throughout degradation to show their potential to heat and the effect of degradation on their heating properties. Prior to heating, hydrogel nanocomposites were cut into discs (8.2 mm in diameter). The hydrogels were initially heated in their dry state prior to starting degradation. The gels were then placed in PBS at 37°C and 100 rpm. Remote-controlled heating of the hydrogel nanocomposites was completed using an AMF induced by a Taylor Winfield induction power supply (model MMF-3-135/400-2) equipped with a solenoid with a 15 mm diameter and 5 turns. After a specified time, the hydrogel discs in their wet state were covered with Saran wrap, placed on top of the solenoid coil and exposed to the alternating magnetic field at 294 kHz and 17.4 kA/m. Thermal images and

data were acquired using an infrared camera (AGEMA Thermovision 470) which recorded the surface temperature of the hydrogels. The surface temperature was recorded continuously for 5 minutes.

6.2.8 Characterization of Paclitaxel Release

The release of paclitaxel from the hydrogel nanocomposites was measured via reverse-phase high performance liquid chromatography (HPLC). 8.2 mm samples were cut and placed in 3mL of a modified PBS-based release medium comprised of PBS, 2.4 wt% Tween® 20, and 4 wt% Cremophor® EL which aid in the release of the hydrophobic paclitaxel into the water-based medium. The release took place at 37°C and 100 rpm, and the gels were periodically placed in fresh medium to maintain infinite sink conditions. Prior to HPLC analysis, 2 mL of acetonitrile were added to each tube to ensure complete solubility of PTX in the solution. HPLC was performed using a Thermo Finnigan Spectra System with ChromQuest 4.0 software for data analysis. The mobile phase consisted of acetonitrile and water (50:50) with a 20 μL injection volume and 1.0 ml/min mobile phase flow rate. The separation was achieved using a reverse-phase C-18 Symmetry column (4.6 x 150 mm, 5 μm pore size) from Waters Corporation. The column eluate was evaluated at 227 nm for the detection of paclitaxel in the samples.

6.2.9 Cytotoxicity Analysis of PBAE Hydrogel Nanocomposite Degradation Products

The degradation products of the hydrogel nanocomposites were analyzed for their cytotoxic effects. NIH 3T3 murine fibroblasts obtained from American Type Culture Collection (ATCC) were used for the cytotoxicity tests. The complete culture medium included Dulbecco's Modified Eagle's Medium supplemented with 10% v/v calf bovine serum, 100 I.U./ml penicillin, 100 μg/ml streptomycin, and 1 μg/ml antimycotic Fungizone® (Invitrogen). The fibroblasts were cultured at 37°C and 5 % CO_2 in a humidified incubator

and were used from passages 4 through 8. 8.2 mm diameter hydrogel nanocomposites with no paclitaxel were allowed to completely degrade in 5 ml of PBS at 37°C and 100 rpm. The degradation products were then diluted to samples of 0.15, 1.5 and 4.5 mg/ml in solutions comprised of 25% (v/v) PBS to complete cell medium. 25% (v/v) PBS to medium sample acted as the control. The fibroblasts were seeded at 17,500 cells/ml in 35mm Petri dishes and were placed in an incubator for 24 hours. After this, the medium was removed from the Petri dishes and replaced with the hydrogel degradation product media samples for 48 hours.

The viability of the fibroblasts was determined by counting the live and dead cells after 48 hours using a Cellometer® Automated Cell Counter from Nexcelom Biosciences (Lawrence, MA). Initially, the medium from each Petri dish was removed and collected in individual centrifuge tubes. The fibroblasts were then trypsinized and transferred the corresponding centrifuge tubes and centrifuged for 3 minutes. After the supernatant was removed, 0.5 ml of Molecular Probes Live/Dead assay solution was added to the tube, the cells were resuspended in the solution, and placed in an incubator at 37°C for at least 20 minutes before counting with the Cellometer®. The Live/Dead assay solution was comprised of calcein AM which fluorescently stains live cells green and ethidium homodimer-1, which stains dead cells red. The cell viability was then calculated as the number of live cells over the total number of live and dead cells.

6.2.10 Statistical analysis

All experiments were performed at least in triplicate. MYSTAT 12 for Windows (12.02.00) was used for t-tests (paired t-test with unequal variances) to determine any significance in observed data. A p-value of <0.05 was considered statistically significant.

6.3 Results and Discussion

6.3.1 Synthesis and Characterization of Poly(β-amino ester) Macromers

PBAE macromers composed of excess PEGDA and isobutylamine were synthesized via a simple condensation reaction resulting in macromer chains with diacrylate endchain groups (as seen in Figure 6.1) allowing for their crosslinking into hydrogel matrices. GPC was used to analyze the molecular weight and polydispersity index (PDI) of the macromers. These values can be seen in Table 6.1.

For the 2EG-IBA macromer, the average molecular weight after 15 hours (completion of reaction) was 2206 g/mole whereas for the 9EG-IBA macromer, the molecular weight increased with reaction time going from 2103 g/mole at 24 hours to 3663 g/mole after 48 hours (completion of reaction). The PDI values were 1.87 for the 2EG-IBA macromer and 2.57 and 3.03 for the 9EG-IBA macromer after 24 and 48 hour reaction times. These values increased with reaction time resulting in a broader range of macromer chain lengths in the solutions for these samples. ATR-FTIR was used to determine the conversion of carbon-carbon double bonds present in the PBAE macromers. As the macromer reaction occurs, the C=C bonds react with IBA, decreasing the C=C peak at 1637 cm^{-1} which is confirmed in the IR spectra. This peak does not completely disappear, however, as the final macromer product has available C=C bonds from the PEGDA due to it being present in excess during the macromer synthesis. Both the GPC and IR spectra can be seen in Figure 6.2 and Figure 6.3, respectively.

6.3.2 Hydrogel Nanocomposite Degradation and Swelling Response

Magnetic hydrogel nanocomposites were fabricated via free-radical polymerization resulting in a biodegradable material. Degradation studies were completed for hydrogels based on 0, 25, 50, 75, and 100 weight % 2EG-IBA macromer. Figure 6.4 shows both the

Table 6.1. Molecular weight (MW) and polydispersity index (PDI) of macromers from gel permeation chromatography. 15 and 48 hours denote the final reaction time for the 2EG-IBA and 9EG-IBA systems, respectively.

System	Time (hours)	MW	PDI
2EG-IBA	15	2206	1.87
9EG-IBA	24	2103	2.57
9EG-IBA	48	3663	3.03

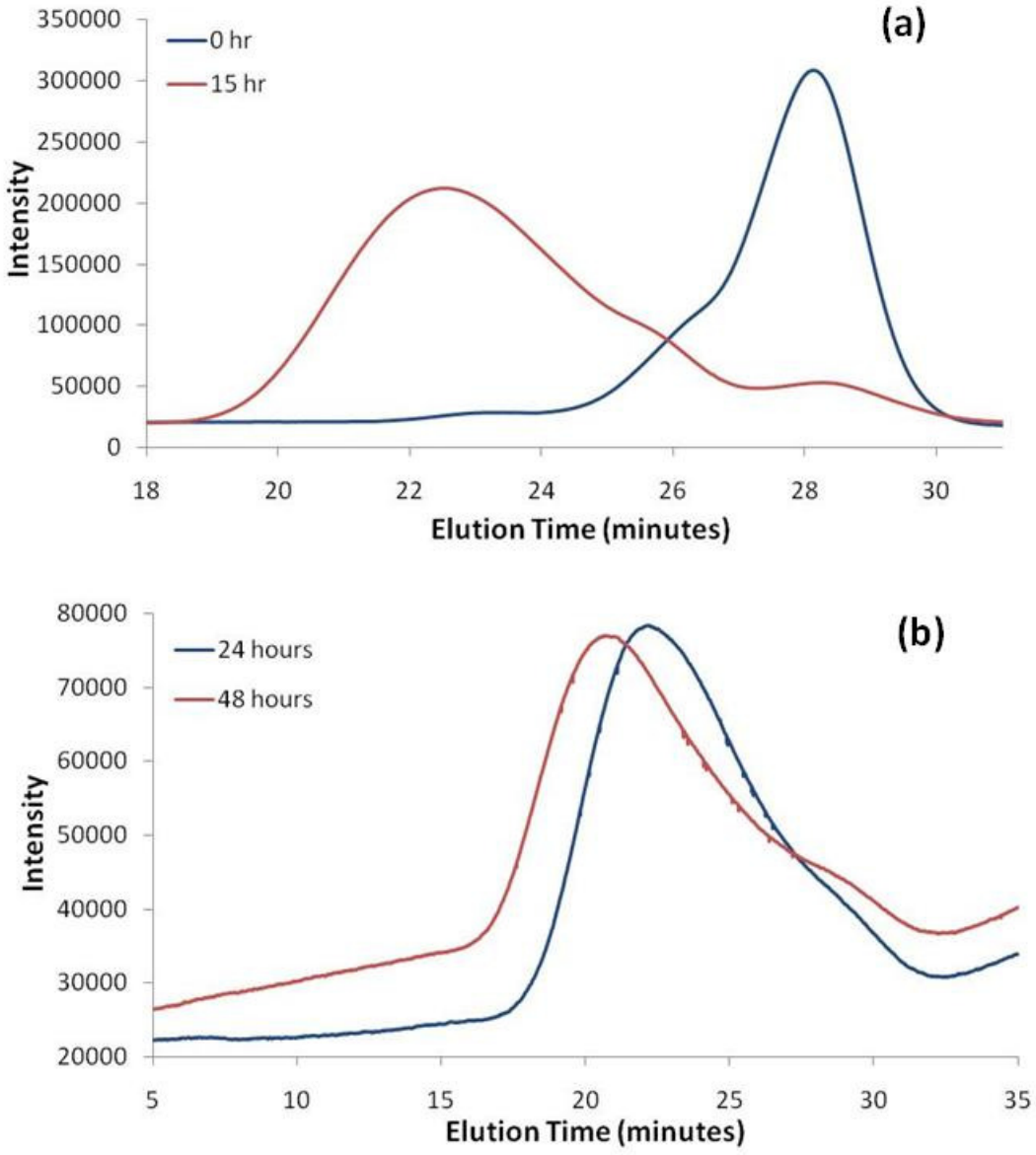

Figure 6.2. Gel permeation chromatograms for PBAE macromers where a) is for 1:1.2 diethylene glycol diacrylate to isobutylamine (2EG-IBA) for 0 and 15 hours and b) is for 1:1.2 poly(ethylene glycol) (n = 9) diacrylate to isobutylamine (9EG-IBA) at 24 and 48 hours.

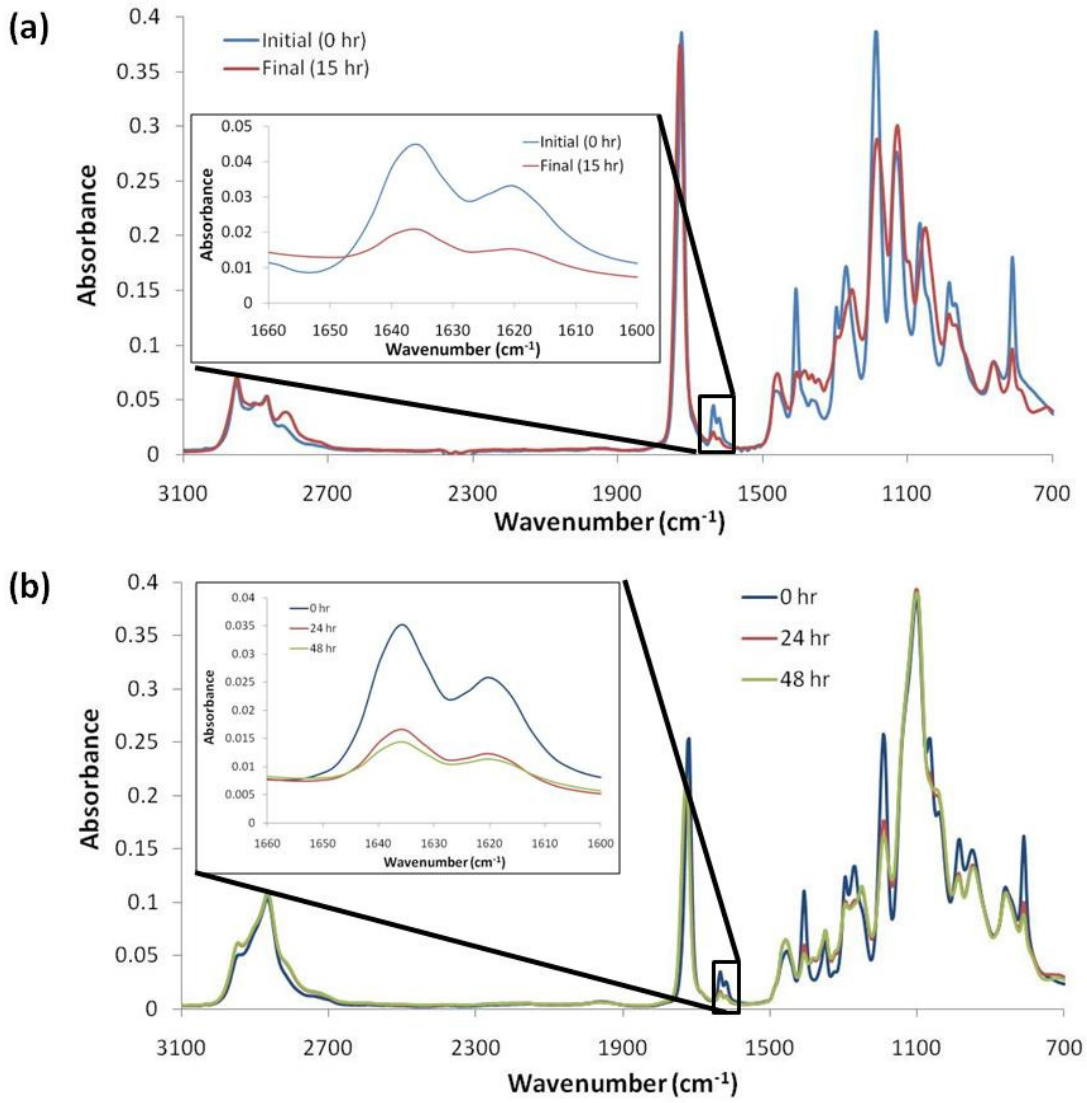

Figure 6.3. ATR-FTIR spectra of (a) 2EG-IBA macromer (1:1.2 diethylene glycol diacrylate: isobutylamine) spectra before and after synthesis (0 and 15 hours) and (b) 9EG-IBA macromer (1:1.2 PEG400DA:isobutylamine) spectra before (0 hour), 24 hour, and 48 hours after synthesis.

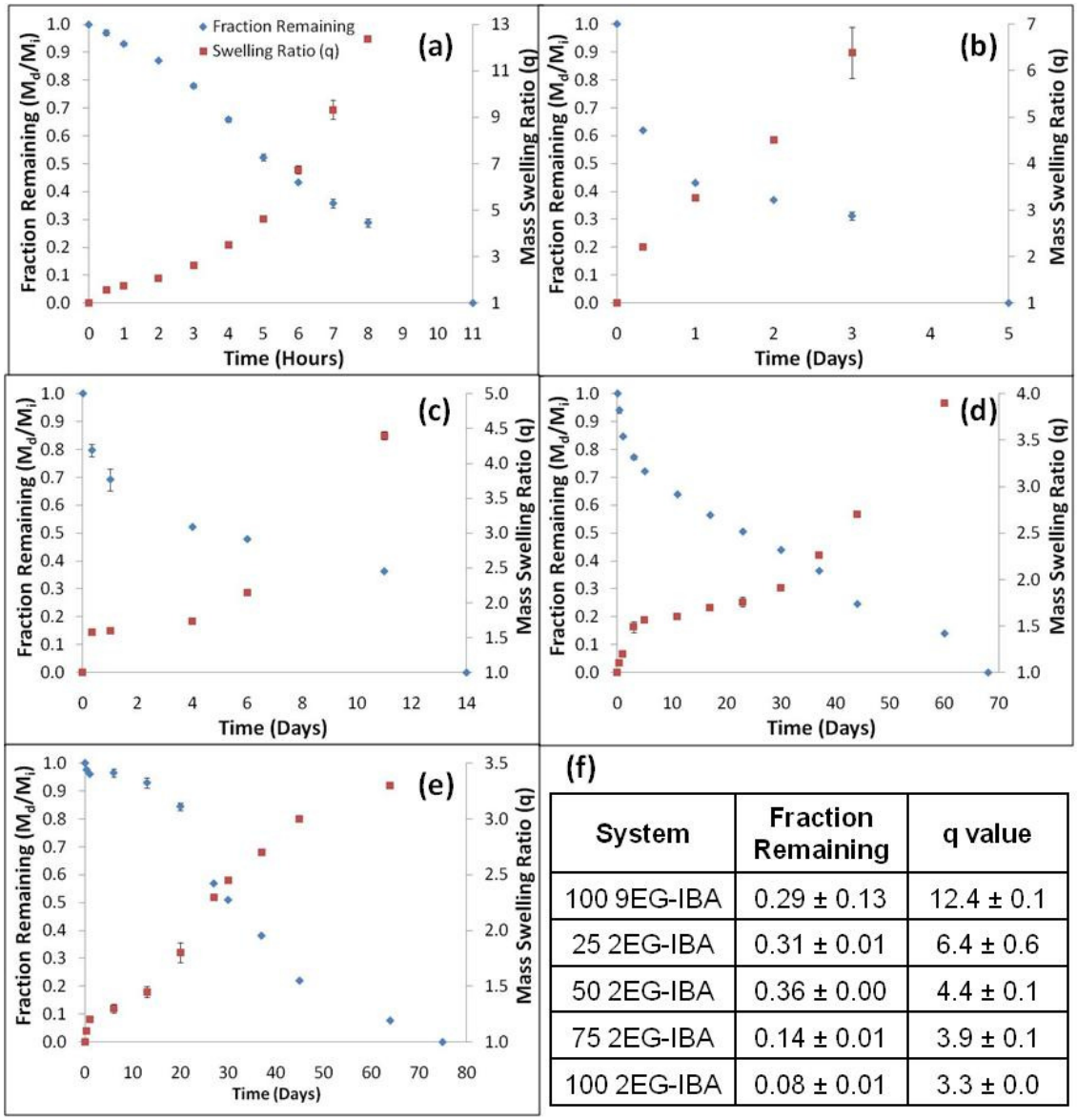

(f)

System	Fraction Remaining	q value
100 9EG-IBA	0.29 ± 0.13	12.4 ± 0.1
25 2EG-IBA	0.31 ± 0.01	6.4 ± 0.6
50 2EG-IBA	0.36 ± 0.00	4.4 ± 0.1
75 2EG-IBA	0.14 ± 0.01	3.9 ± 0.1
100 2EG-IBA	0.08 ± 0.01	3.3 ± 0.0

Figure 6.4. Mass fraction remaining and mass swelling ratio (q) data for: a) 100 9EG-IBA b) 25 2EG-IBA, c) 50 2EG-IBA, d) 75 2EG-IBA, and e) 100 2EG-IBA magnetic hydrogel nanocomposites with time. f) is a table detailing the final q value for all systems the corresponding fraction remaining. For all graphs, the blue diamonds correspond to the fraction remaining (m_d/m_i) on the left x-axes and the red squares correspond to the volume swelling ratios (q) on the right x-axes. N = 3 ± SE.

fractional mass remaining and mass swelling ratio of the hydrogel nanocomposites with times. The 100 9EG-IBA hydrogel completely degraded in approximately 11 hours whereas the 100 2EG-IBA hydrogel completed degraded over the course of approximately 75 days. Additionally, 25, 50, and 75 2EG-IBA hydrogels completely degraded in approximately 5, 15, and 68 days. The final data was not collected due to the difficulty in handling the hydrogels near the end time points and the end of the degradation time for all systems was determined via visual observations. The faster degradation of the 100 9EG-IBA hydrogel is a result of the presence of more ethylene glycol (EG) groups in the macromer backbone in comparison to the 100 2EG-IBA hydrogel resulting in a more hydrophilic macromer and hydrogel. The mass fraction curve was slightly sigmoidal-shaped for all hydrogels. This profile is likely due to the broad PDI of both macromers resulting in both shorter and longer chains present in the macromer where shorter chains in the gel will degrade faster and longer chains will have a slower degradation which affects the initial and final degradation response of the systems.

Figure 6.5 shows a comparison of the fractional mass remaining of all of the hydrogel systems. These hydrogels exhibited degradation times in between that of the 100 2EG-IBA and 100 9EG-IBA hydrogels due to the mixture of the two macromers present in the hydrogels. The 75 and 100 2EG-IBA hydrogel exhibited similar final degradation time which is likely a result of the 9EG-IBA macromer degrading quickly out of the 75 2EG-IBA hydrogel causing it to behave similarly to the 100 2EG-IBA gel. The mass swelling ratio of all of the hydrogels increased with time as seen in Figure 6.4. This is due to the continued degradation of the gels with time which results in breakage of the crosslinking in the hydrogel matrix allowing for increased water content. These curves were also all slightly sigmoidal in shape. As seen in Figure 6.4f, the 100 9EG-IBA hydrogel had the highest mass swelling ratio with time (12.4), and the final mass swelling ratios for the other hydrogels decreased with increasing 2EG-IBA content (3.3) despite the degradation being further along for the more hydrophobic samples. This is due to the increase in hydrophobicity due to 2EG-IBA as well

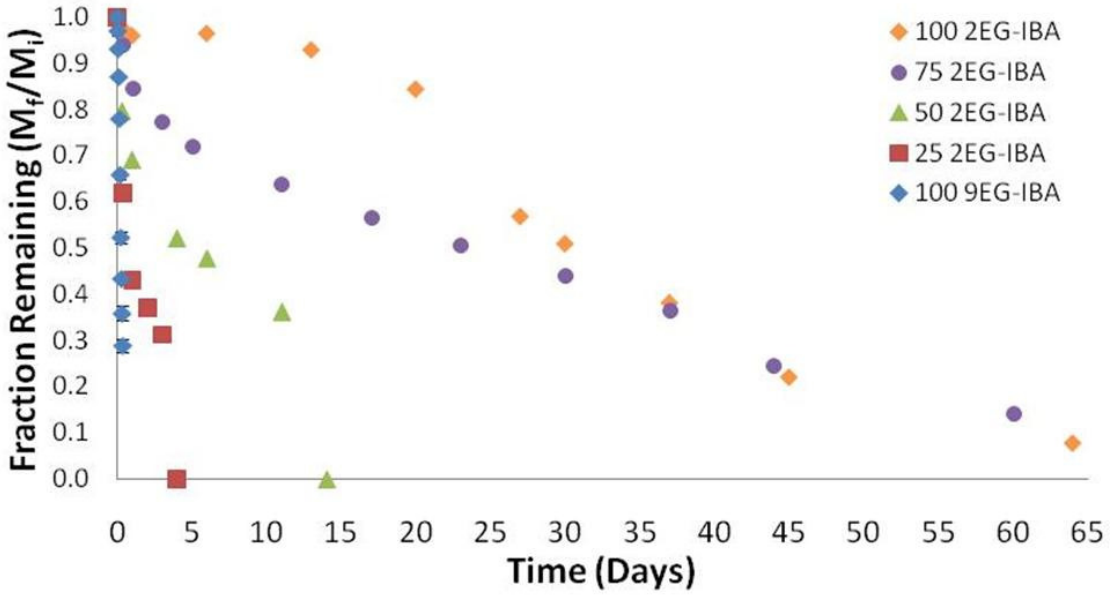

Figure 6.5. Mass fraction remaining data for all magnetic hydrogel nanocomposites over time. N = 3 ± SE.

as the fact that the average molecular weight of the 2EG-IBA macromer is lower than that of 9EG-IBA resulting in a tighter hydrogel mesh. The hydrogels exhibited bulk degradation as evidenced by their increased swelling with continued degradation. Overall, this data shows the ability to tailor the degradation and swelling profiles of these hydrogels by adjusting the macromer content.

6.3.3 Mechanical Testing: Determination of Compressive Modulus

Compressive testing was performed on all PBAE hydrogel systems at two time points (i.e., an initial time point after 30 minutes in PBS for all gels and a second time point after the hydrogels were partially degraded). This second time point was 3 hours, 1 day, 9 days, 28 days, and 42 days for 0, 25, 50, 75, and 100 9EG-IBA hydrogels, respectively. This corresponds to fractional mass values of 0.78, 0.43, 0.41, 0.46, and 0.28 for these hydrogel systems, respectively. Representative stress versus strain plots can be seen in Appendix A, Figure A.6.1 and Figure A.6.2. The final data can be seen in Figure 6.6 and contrary to what was expected, the gels with higher 9EG-IBA content exhibited a greater compressive modulus.

The lower molecular weight macromer (2EG-IBA) was expected to result in hydrogels with higher compressive modulus due to the tighter hydrogel mesh. This was not observed, however, and it is believed that this is due to two potential factors. First, there are unreacted PEGDA monomers present in the macromer solution. Also, shorter PEGDA chains are present in the macromer as indicated by the large PDI for the 9EG-IBA macromer. In turn, hydrogels fabricated with this macromer have a greater compressive modulus. The lower modulus for the 100 9EG-IBA system for the initial time point is a result of it already degrading slightly more than the other gels after 30 minutes. The modulus of all hydrogel systems decreased during degradation due to decreasing crosslinking density which results in a weakening of the hydrogel matrices.

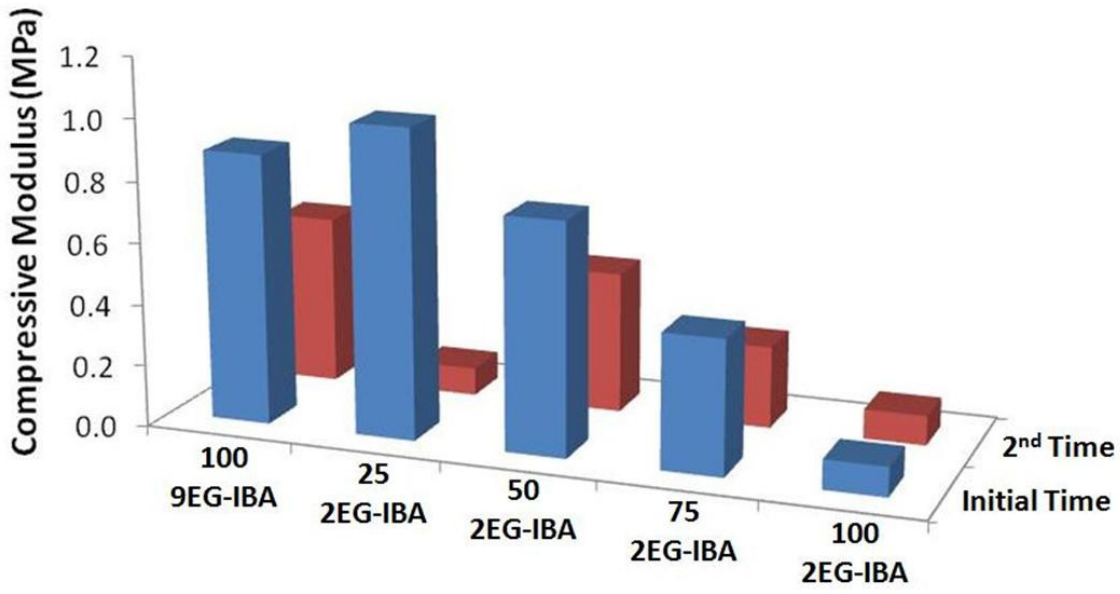

Figure 6.6. Compressive modulus data for magnetic hydrogel nanocomposites after initial exposure to PBS at 37°C (Initial Time) and for a second time point for each system after the hydrogels are partially degraded (2nd Time). The second time for the systems are: 3 hours for 100 9EG-IBA, 1 day for 25 2EG-IBA, 9 days for 50 2EG-IBA, 28 days for 75 2EG-IBA, and 42 days for 100 2EG-IBA. N = 3.

6.3.4 Iron Oxide Loss Studies via Thermogravimetric Analysis

TGA was performed to determine the actual amount of iron oxide nanoparticles present in the hydrogel nanocomposites as they degrade. Samples were analyzed at 0, 0.5, 3, and 8 hours for the 100 9EG-IBA hydrogel systems as a representation of what occurs in the remaining hydrogel nanocomposites as seen in Appendix A, Figure A.6.3. Interestingly, as time and degradation increased, the mass % of the iron oxide in the nanocomposites (iron oxide to polymer amount) increased. The polymer degradation byproducts were able to diffuse more readily out of the hydrogels than the iron oxide nanoparticles themselves. The effect of this phenomenon will be discussed further in the next section concerning the remote-controlled heated of the hydrogel nanocomposites.

6.3.5 Remote-Controlled Heating of PBAE Hydrogel Nanocomposites Via an AMF

PBAE hydrogel nanocomposites can potentially be used in hyperthermia applications where heating of the magnetic hydrogel matrix can be achieved by exposure to an alternating magnetic field. This phenomenon is due to the Fe_3O_4 nanoparticles present in the hydrogel matrix. In these studies, the swollen hydrogels were exposed to an electromagnetic field for 5 minutes at 294 kHz and 17.4 kA/m to induce heating within the systems for the following conditions: dry hydrogels and hydrogels after degradation at various time points. As seen in Figure 6.7 for the 100 9EG-IBA hydrogel system, the hydrogels were able to heat for all conditions, and the maximum temperature reached decreased as the gels degraded. This response was similar for the other four hydrogel systems as seen in Appendix A, Figure A.6.3. The amount of heating of the hydrogel systems is dependent on multiple factors including the amount of iron oxide present in the gel volume and the amount of water present in the gels, which can dissipate the heat generated by the iron oxide nanoparticles. Table 6.2 shows the relationships between the ΔT values, mass swelling ratio, fractional mass remaining, TGA iron oxide mass %, and actual average iron oxide mass remaining in each gel. As time

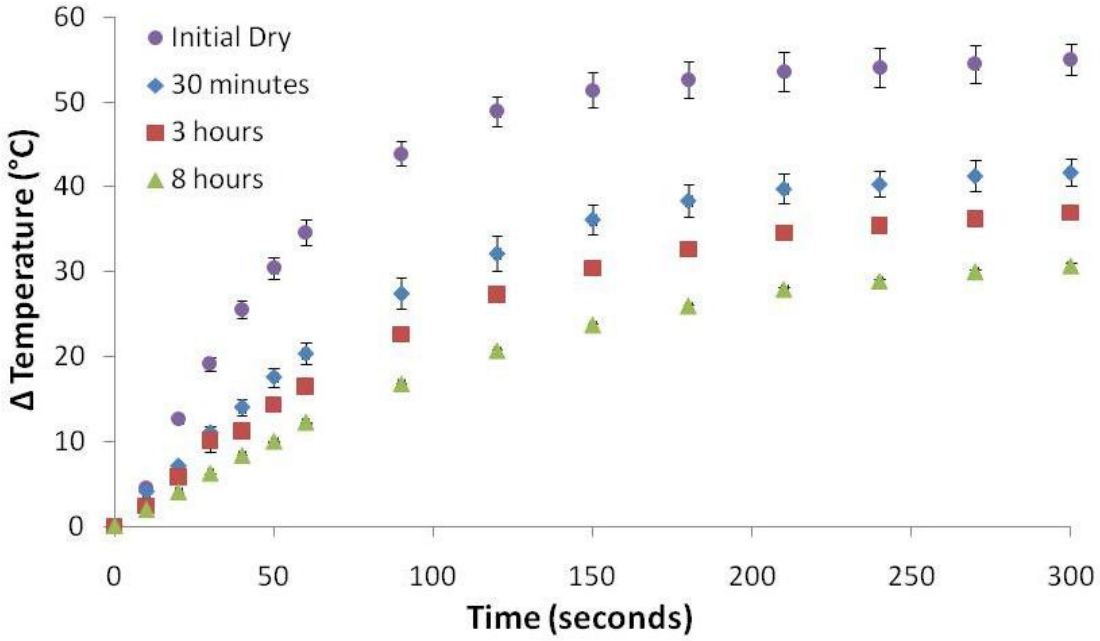

Figure 6.7. Thermal analysis of 100 9EG-IBA magnetic hydrogel nanocomposite with time upon exposure to an alternating magnetic field at 17.4 kA/m and 294 kHz for 5 minutes. N = 3 ± SE.

Table 6.2. Comparison of mass swelling ratio (q value), fraction of mass remaining, final temperature of hydrogel surface temperature after 5 minute exposure to an AMF, iron oxide loading amount from TGA data, and the calculated mass of iron oxide remaining for the 100 9EG-IBA hydrogel system with time.

Time	**q value**	**Fraction Mass Remaining**	**Final ΔT (°C)**	**% Iron Oxide**	**Fe_3O_4 Mass Remaining (mg)**
Initial	1.00	1.00	55.0 ± 1.9	4.9 ± 0.1	4.4 ± 0.0
30 min	1.6 ± 0.0	0.97 ± 0.01	41.8 ± 1.6	4.7 ± 0.0	4.1 ± 0.0
3 hour	2.6 ± 0.1	0.78 ± 0.01	36.9 ± 0.5	5.3 ± 0.1	3.7 ± 0.1
8 hour	12.4 ± 0.1	0.29 ± 0.01	30.6 ± 0.4	12.4 ± 0.2	3.2 ± 0.1

increases, the mass swelling ratio increased with degradation allowing for more water into the hydrogels. Additionally, as the hydrogels degraded the actual iron oxide mass decreased. These two factors together resulted in a decrease in the heating of the hydrogels with time.

6.3.6 Characterization of Paclitaxel Release

In order to evaluate the ability of PBAE hydrogels to effectively deliver paclitaxel, *in vitro* release studies were performed in a PBS solution containing 2.4 weight % Tween® 20 and 4 weight % Cremophor® EL at 37°C and 100 rpm. The PTX concentrations were determined using a standard curve from the PTX concentration and HPLC data in a 60:40 (v/v) release medium to acetonitrile solution as seen in Appendix A, Figure A.6.4. Figure 6.8 shows the release profile of PTX from the PBAE hydrogels. The PTX was continuously released from the hydrogels, and a near zero-order release was initially evident for all hydrogel systems. After approximately 60-70% release, the PTX release slowed for most systems. Similar to the degradation data, the 100 9EG-IBA released paclitaxel the fastest due to its higher hydrophilicity in comparison with the gels containing 2EG-IBA macromer. This data suggests that these hydrogels have the potential to be used as good controlled drug delivery carriers, and the drug release time can be controlled by the degradation rate of the hydrogel system.

6.3.7 Cytotoxicity Analysis of PBAE Hydrogel Nanocomposite Degradation Products

Cytotoxicity analysis of the PBAE hydrogel nanocomposite degradation products was analyzed as these gels can potentially be used as implantable or injectable *in vivo* drug delivery depots. Hydrogels without paclitaxel were completely degraded in PBS resulting in 18 mg/ml hydrogel to PBS solutions. These solutions were then diluted to 0.15, 1.5, and 4.5 mg/ml in 25% (v/v) PBS to complete fibroblasts medium. NIH 3T3 fibroblasts were then exposed to these solutions for 48 hours, and their cytotoxicity was analyzed using a

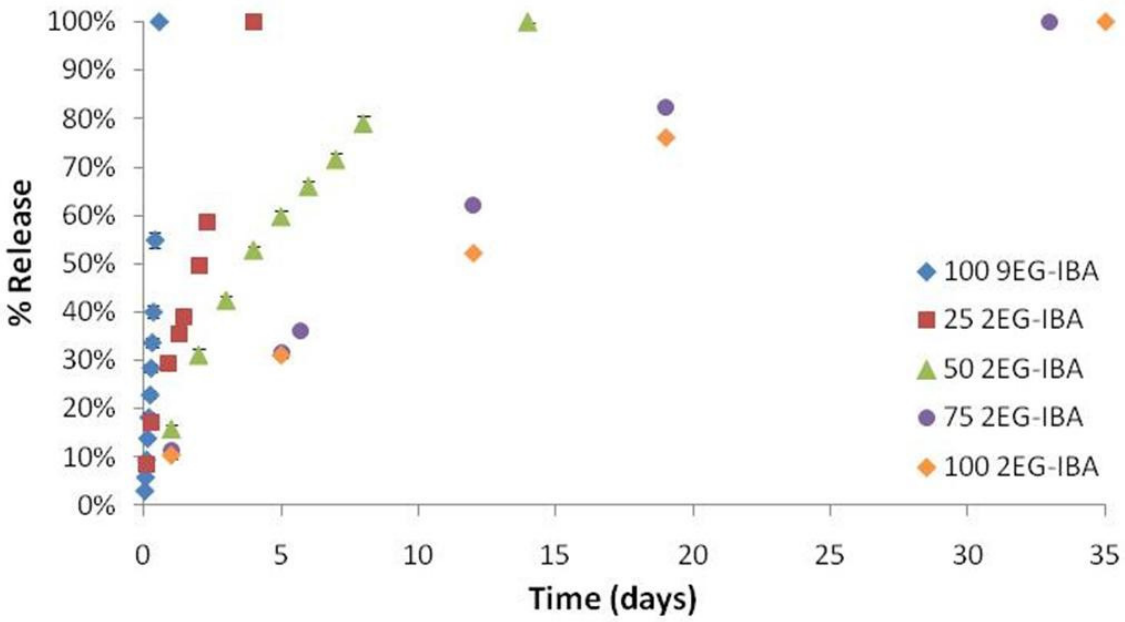

Figure 6.8. Analysis of paclitaxel release from hydrogel nanocomposites over time via HPLC. N = 3 ± SE.

Cellometer® Automated Cell Counter. Figure 6.9 shows the % cell viability (number of live cells versus total number cells) for 100 2EG-IBA, 50 2EG-IBA, 100 9EG-IBA, and a PBS control. For all hydrogels, the cell viability decreased with increasing degradation product concentration. Additionally, the viability was greater with increasing 9EG-IBA content. Overall, these results show differences in cell viability for different conditions, and *in vivo* evaluation will be necessary to show the overall safety of these systems. However, this does show the potential for safety with the correct degradation product clearance from the implantation site.

6.4 Conclusions

Magnetic PBAE-based hydrogel nanocomposites have the ability to successfully deliver both heat and the chemotherapeutic agent, paclitaxel, in a controlled fashion. Both the degradation and PTX release profiles can be tailored based on the type of macromer used with the more hydrophilic hydrogel system (100 9EG-IBA) degrading in 11 hours versus over nearly 7 weeks for the more hydrophobic system (100 2EG-IBA). The paclitaxel release profiles were controlled by the degradation of the hydrogels as they underwent bulk degradation. The heating capability of the hydrogels when exposed to an AMF decreased as the hydrogels degraded. This is due to an increase in their swelling (and therefore increase in water content) and decrease in the amount of iron oxide present in the hydrogels with time. The degradation products exhibited cell viabilities ranging from 53 to 92% depending on the type of hydrogel and concentration of degradation products. Overall, these systems have the potential to be used as implanted or injected drug (and heat) delivery depots for the synergistic treatment of cancer.

References

All references are located at the end of the dissertation.

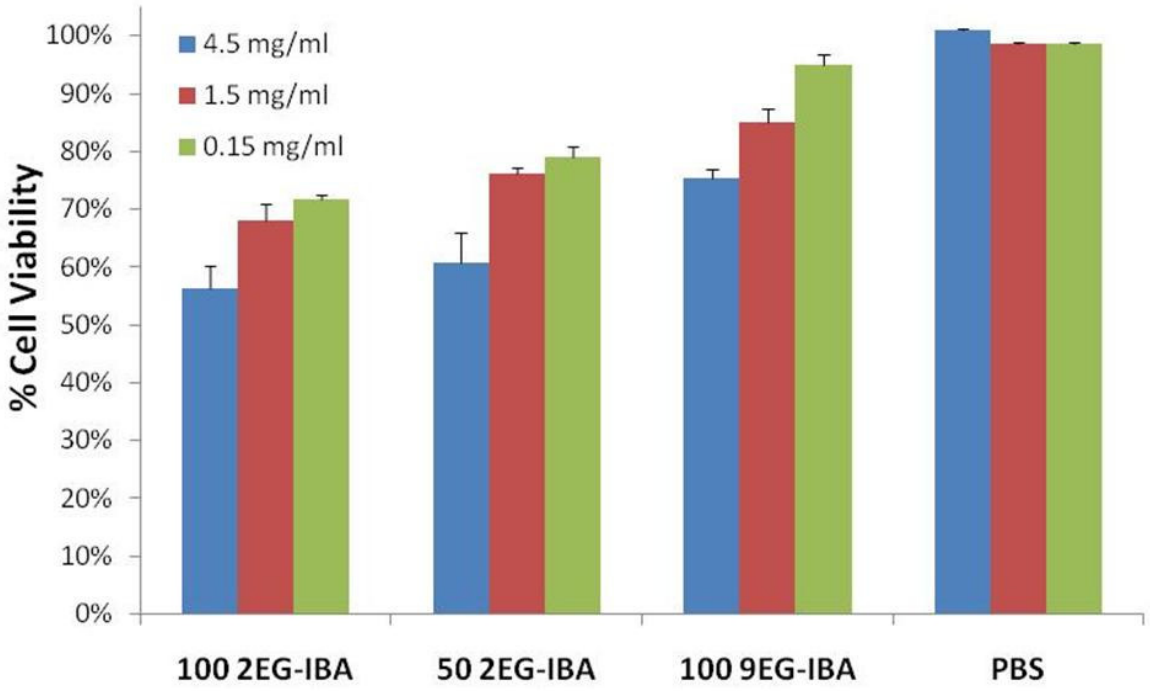

Figure 6.9. Cytotoxicity analysis of NIH 3T3 murine fibroblasts exposed to completely degraded PBAE hydrogel nanocomposites at various concentrations for 48 hours. N = 3 ± SE.

CHAPTER 7

Conclusions and Future Work

7.1 Conclusions

Due to the limitations and side effects often association with conventional cancer therapies such as chemotherapy and radiation, significant emphasis is being placed on the development of novel cancer therapeutics that explore a multi-modality approach to overcoming this problem. Although chemotherapy and radiation are often used synergistically with success, there are still many types of cancers and patients that do not respond well to this line of treatment. A significant amount of literature has supported the idea that hyperthermia, the heating of tumor tissue to 41 to 45 °C, can help overcome the limitations of either chemotherapy or radiation. Hyperthermia has its own limitations, the most significant being a method of delivering heat to a localized area via non-invasive methods. This work presents a class of biomaterials, magnetic hydrogel nanocomposites, which may be able to overcome this constraint. The hydrogel matrix can provide a drug depot for the delivery of chemotherapeutic agents, and iron oxide nanoparticles embedded in the system can provide heat upon exposure to an alternating magnetic field (AMF). These materials can be implanted or injected in or around tumor sites for synergistic treatment of the cancerous tissue. Although numerous types of hydrogels could be used for this type of therapy, poly(ethylene glycol) (PEG) and poly(β-amino ester) (PBAE) hydrogel systems were the focus of this research.

Initially, PEG-based magnetic hydrogel nanocomposites were investigated for their swelling, heating, and biocompatibility properties. It was shown that the swelling of the hydrogels could be controlled by both the crosslinking density and that these systems exhibited a swelling response with changes in the temperature of the surrounding medium.

This was the first time this phenomenon was demonstrated for PEG-based nanocomposite hydrogels. The cytotoxicity of iron oxide nanoparticles in the hydrogels as well as potential unreacted components from the hydrogel were evaluated for 24 and 48 hours using murine fibroblasts, and the results were the same as fibroblasts exposed to media only. The heating profiles for all the hydrogel systems heated in the AMF were dependent on the swelling of the hydrogel systems, where higher crosslinked gels heated more than lower crosslinked gels due to less water (i.e., a greater fraction of polymer and iron oxide) present in the system. The heating of the hydrogels was able to be controlled by the strength of the AMF so that the systems could reach either hyperthermia or thermoablation temperature ranges. It was also demonstrated that these hydrogel systems heated to thermoablation temperatures in the AMF and have the ability to kill M059K glioblastoma cells *in vitro*. Unexpected temperature-responsive properties resulted from the initial investigation of the PEG-iron oxide nanocomposites. Similar PEG-based hydrogels comprised of diethylene glycol methyl methacrylate and PEG200 methyl methacrylate were investigated to better characterize these properties. The gels were shown to be temperature-responsive at various temperatures. Additionally, they demonstrated a sharp decrease in swelling upon heating in the AMF due to the local heat generated from the iron oxide nanoparticles. This is the first time this phenomenon has been demonstrated with PEG-based nanocomposite hydrogels.

PEG magnetic hydrogel nanocomposites were then studied for their ability to deliver heat and a chemotherapeutic agent, paclitaxel. Similar to before, the swelling of these systems was tailorable and was dependent on the crosslinking density of the system. Mechanical analysis showed expected values for compressive moduli, and these values were dependent on crosslinking (the more crosslinked system had a higher modulus). Heating results in the AMF were once again dependent on the crosslinking of the hydrogels with the lower crosslinked system heating less than the others. The hydrogel nanocomposites were able to release paclitaxel in a modified release medium that aided in the solubility of the highly hydrophobic

drug. A modified power law was used to model the drug release. Finally, it was shown that A549 lung carcinoma cells exhibit higher cytotoxicity when exposed to both heat (at 42.5 °C) and paclitaxel (at micromolar amounts) in comparison to either treatment demonstrating that this type of therapy could be beneficial for treating lung carcinoma whereas M059K (glioblastoma) and MDA MB 231 (breast adenocarcinoma cells) did not show an increase in paclitaxel efficacy when combined with hyperthermia therapy.

Although PEG hydrogels are advantageous in that they exhibit "stealth" properties, they do not readily degrade once exposed to the body. For applications where biodegradable systems would be desired, PBAE hydrogels, which degrade via ester linkages, were studied for the delivery of both heat and paclitaxel. Both swelling and degradation of the systems were dependent on the type of macromer used in the hydrogel with the more hydrophilic systems degrading more quickly. As expected, the mechanical strength (compressive modulus) of the hydrogels decreased as they degraded. Cytotoxicity of the degradation products of the hydrogels was studied and the viability ranged from 55 to 95% depending on the gel type and concentration of the materials in PBS solution. Finally, it was demonstrated that paclitaxel can be released in a controlled manner via bulk degradation of the hydrogels. This system may be especially advantageous for the synergistic delivery of heat and chemotherapeutics as it has the potential to be injected *in situ* at a tumor site due to the chemically-initiated polymerization it undergoes to form a solid hydrogel. Overall, these systems are promising for use in hyperthermia and chemotherapy applications upon further evaluation of their properties and applications.

7.2 Future Work

The work described in this dissertation is hopefully just the beginning regarding the investigation of magnetic hydrogel nanocomposites for hyperthermia applications. Future work to build upon this project may include, but is not limited to:

- Optimization of a PBAE-based system with less iron oxide nanoparticles that can deliver heat at hyperthermia temperatures while degrading and delivering the appropriate amount of chemotherapeutic agent.
- Investigation of the temperature-responsiveness of PBAE systems containing PEG based macromers, which have the potential to be temperature-responsive.
- Optimization of the release method of hydrophobic drugs from PEG-based hydrogel systems. The current method involves imbibitions in methanol in which the gels cannot be dried. Ideally, the drug would be incorporated during the fabrication of the hydrogels.
- Incorporation of iron oxide nanoparticles that have a Curie temperature (maximum temperature that they can heat in an AMF) in the hyperthermia range so that the heating of the hydrogels can be better controlled.
- Investigation of the release of other types of cancer therapeutics which could include: radionucleotides, chemotherapeutics, immunotherapy agents.
- *In vitro* cytotoxicity analysis of other cancerous cell lines via multiple methods:
    - Exposing cells to chemotherapeutic agent and heat via incubator then analyzing via staining with a Live/Dead stain with fluorescence imaging to determine cell viability or counting cells via Cellometer® to determine cell viability
    - Exposing cells to chemotherapeutic agents and hyperthermia heat from hydrogels heated in AMF then analyzing via methods described above.
- *In vivo* analysis of optimized magnetic hydrogel nanocomposites implanted or injected intratumorally which can deliver both a chemotherapeutic agent and hyperthermia.

APPENDIX A

Supplemental Figures and Tables

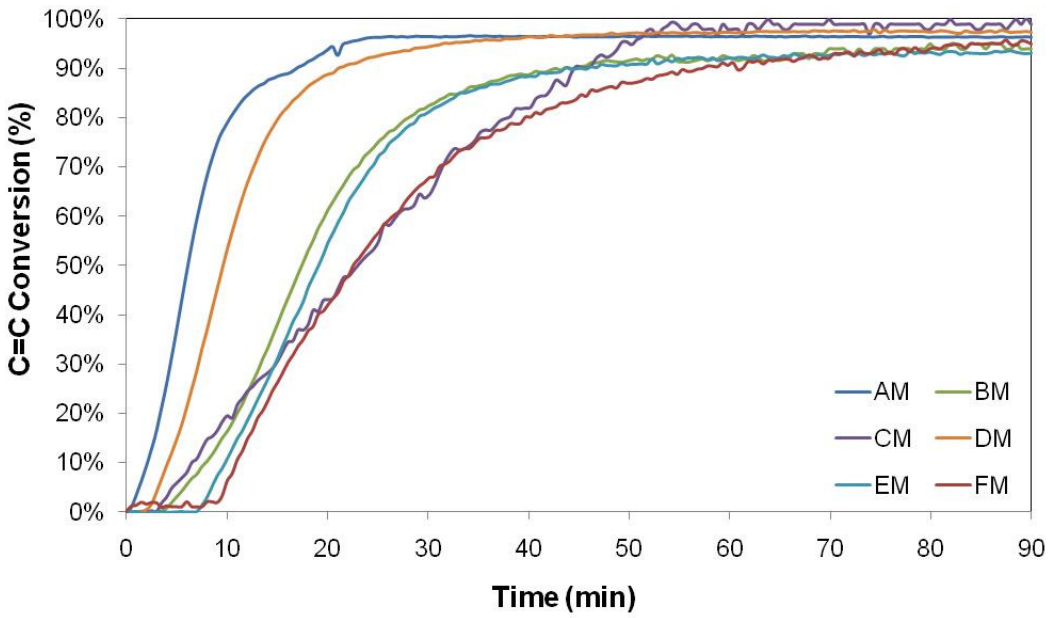

Figure A.3.1. FTIR conversion data of PEG magnetic hydrogel nanocomposites. Completion of reaction was determined by the amount of C=C bonds broken during the hydrogel fabrication when undergoing free-radical polymerization.

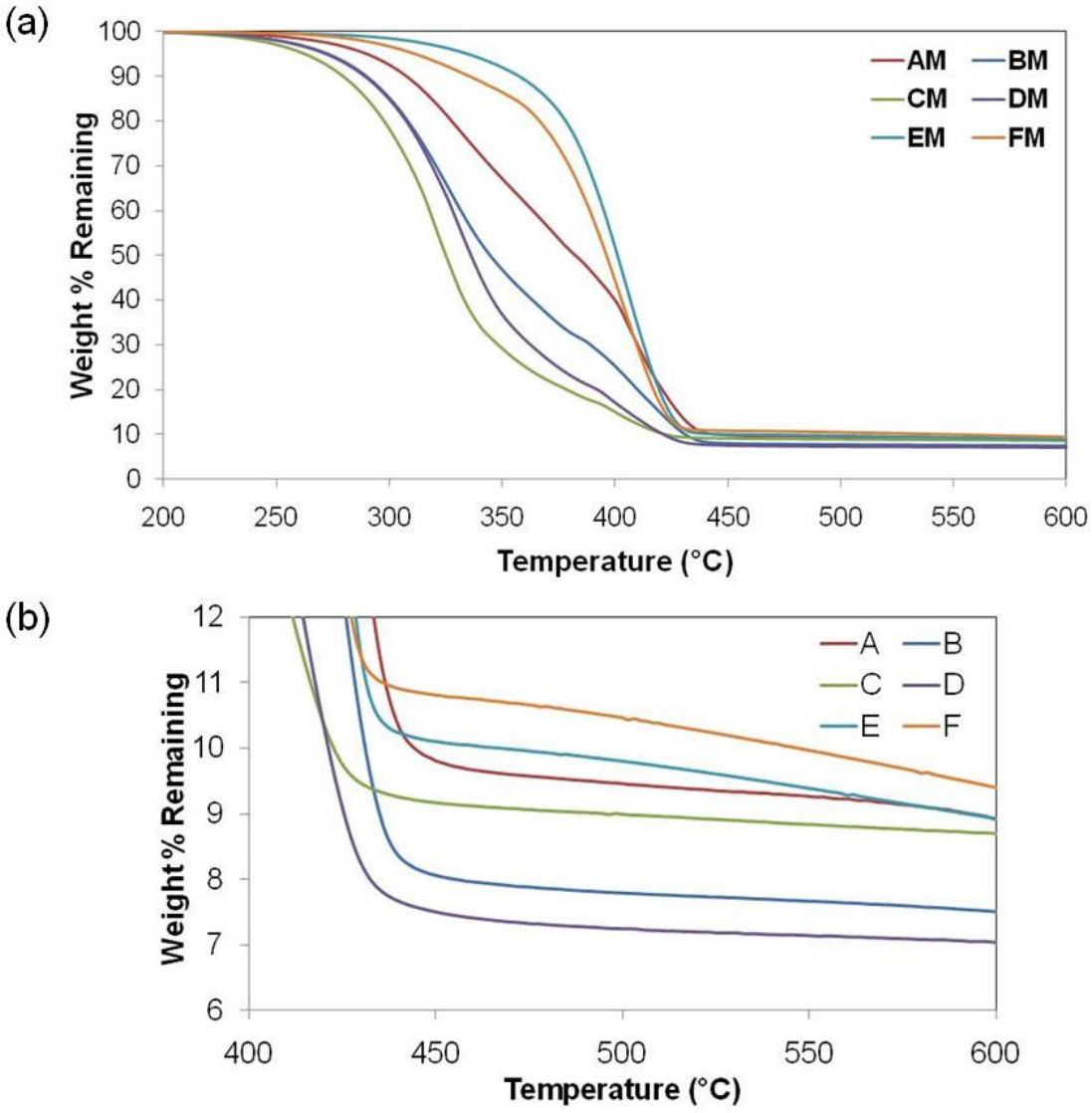

Figure A.3.2. Thermal gravimetric analysis of PEG magnetic hydrogel nanocomposites. Weight remaining was measured with time to determine the actual iron oxide nanoparticle content within the hydrogels. (a) is all data from 200 to 600 °C whereas (b) is a close up of the data from 400 to 600 °C.

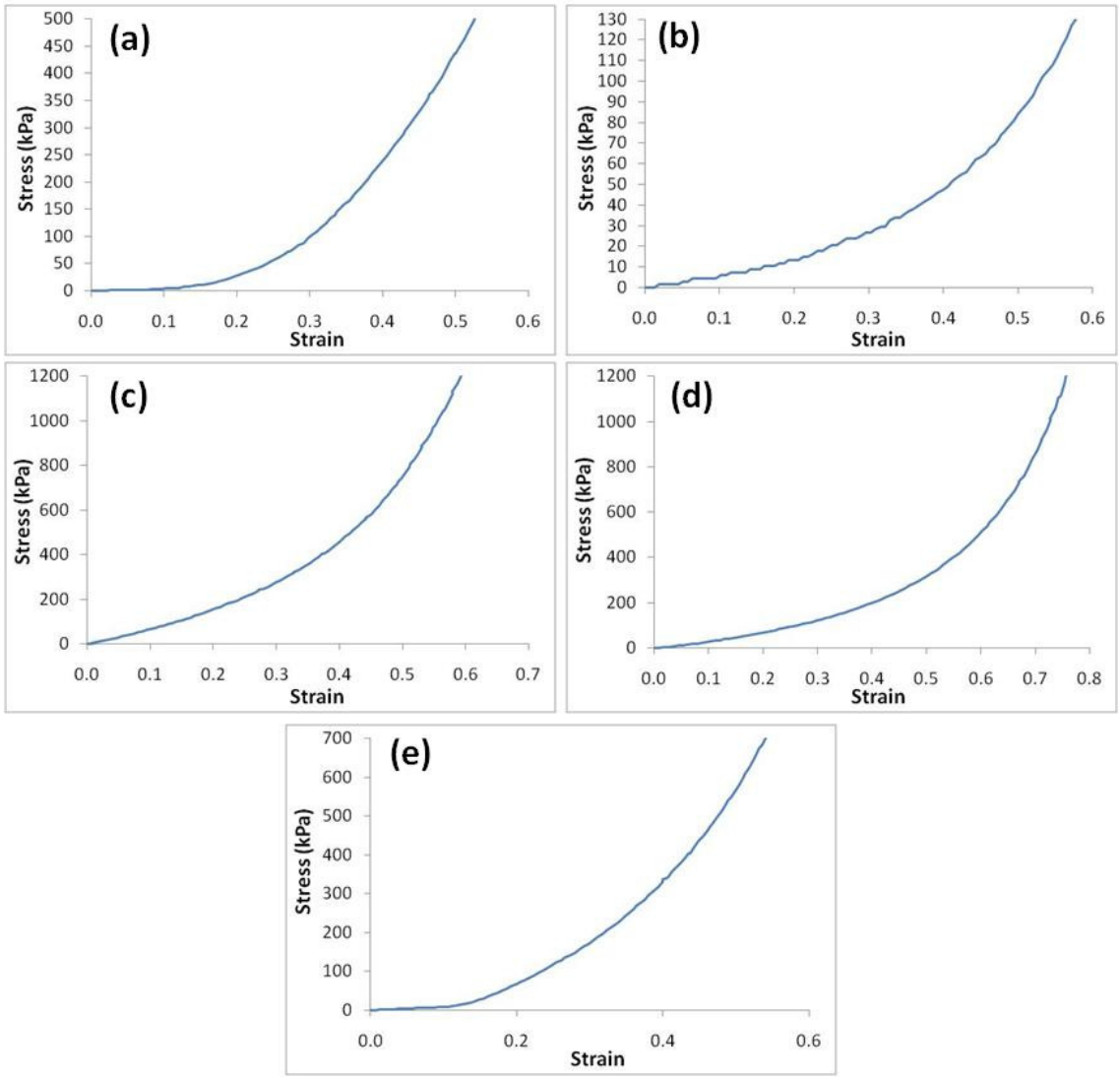

Figure A.6.1. Representative stress versus strain curves obtained during mechanical testing (compression analysis) of PBAE magnetic hydrogel nanocomposites 30 minutes after degradation has been underway for the following samples: (a) 100 9EG-IBA, (b) 25 2EG-IBA, (c) 50 2EG-IBA, (d) 75 2EG-IBA, and (d) 100 2EG-IBA.

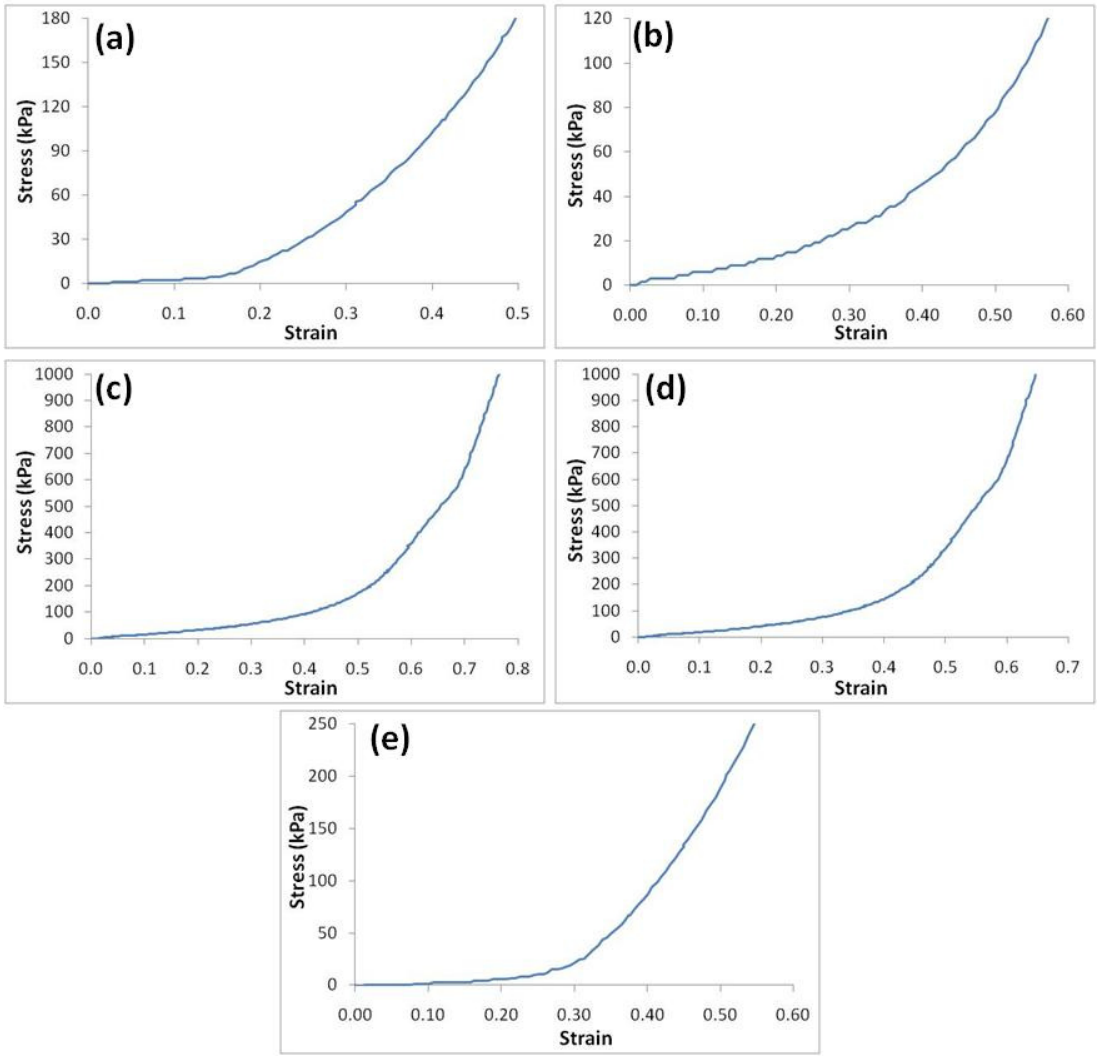

Figure A.6.2. Representative stress versus strain curves obtained during mechanical testing (compression analysis) of PBAE magnetic hydrogel nanocomposites for the 2nd time point for the following samples and times: (a) 100 9EG-IBA (3 hours), (b) 25 2EG-IBA (1 day), (c) 50 2EG-IBA (9 days), (d) 75 2EG-IBA (28 days), and (d) 100 2EG-IBA (42 days).

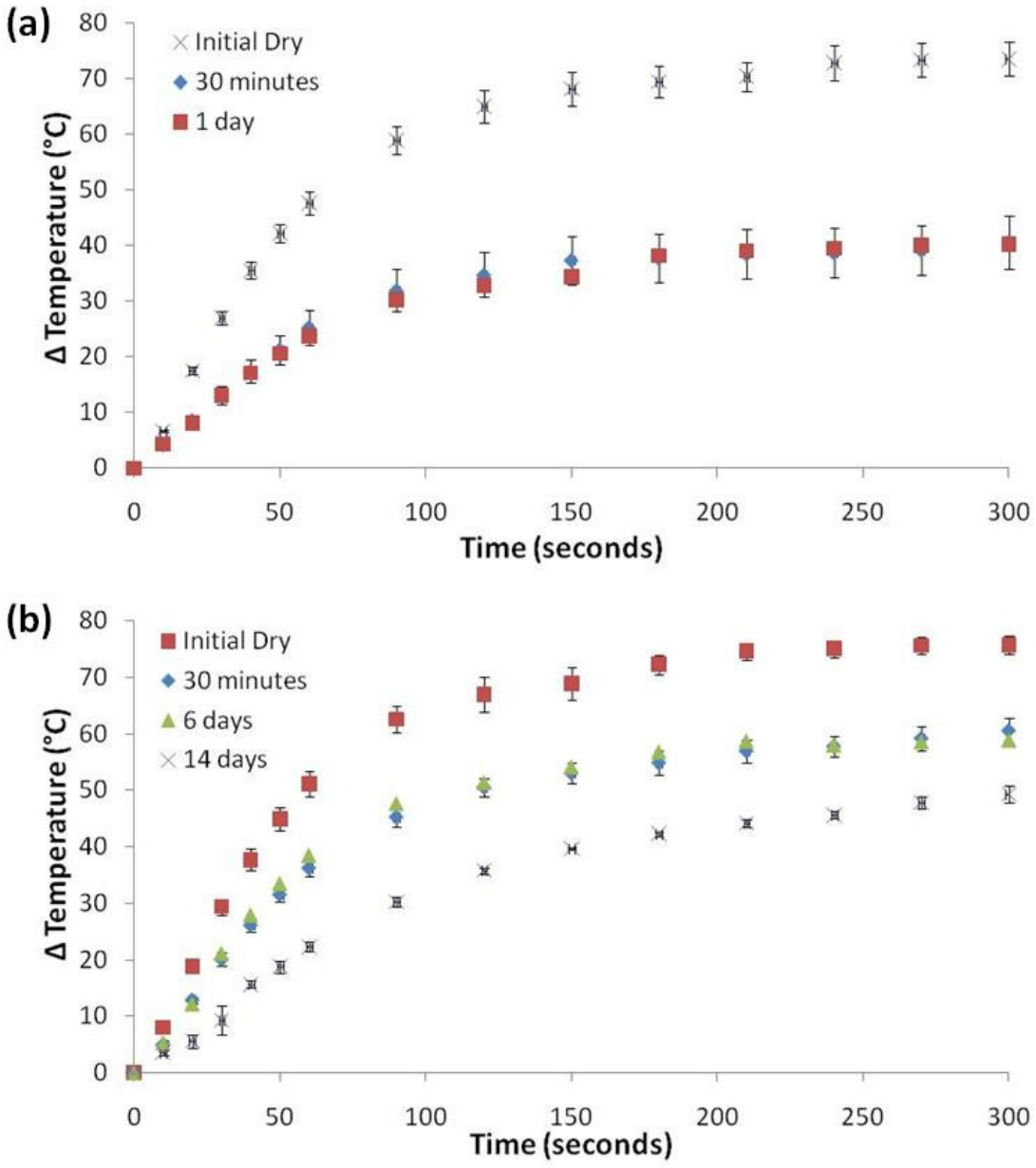

Figure A.6.3. Heating analysis of PBAE magnetic hydrogel nanocomposites in their dry and swollen states (after degradation) for (a) 25 2EG-IBA, (b) 50 2EG-IBA, (c) 75 2EG-IBA, and (d) 100 2EG-IBA systems.

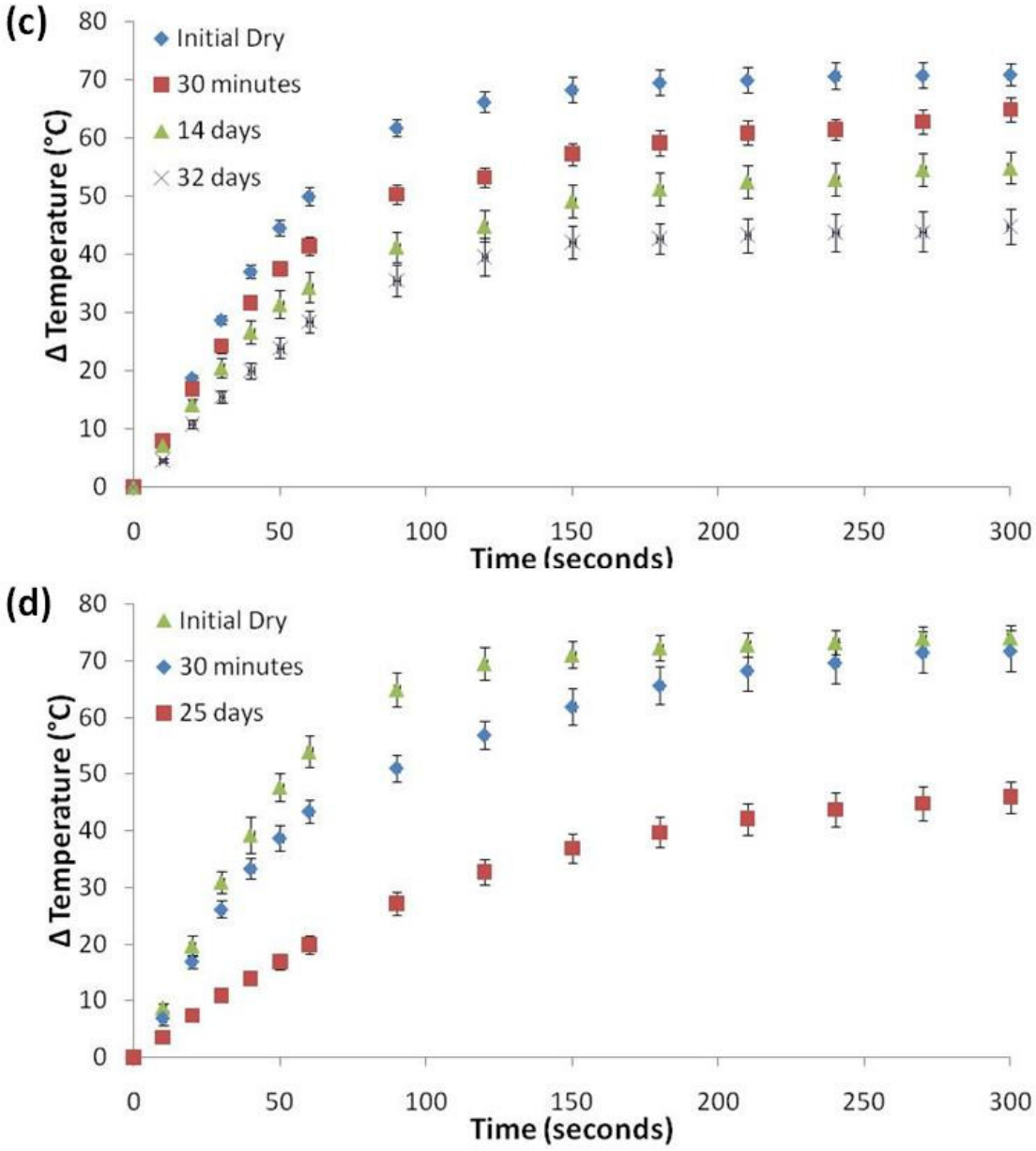

Figure A.6.3 (con't). Heating analysis of PBAE magnetic hydrogel nanocomposites in their dry and swollen states (after degradation) for (a) 25 2EG-IBA, (b) 50 2EG-IBA, (c) 75 2EG-IBA, and (d) 100 2EG-IBA systems.

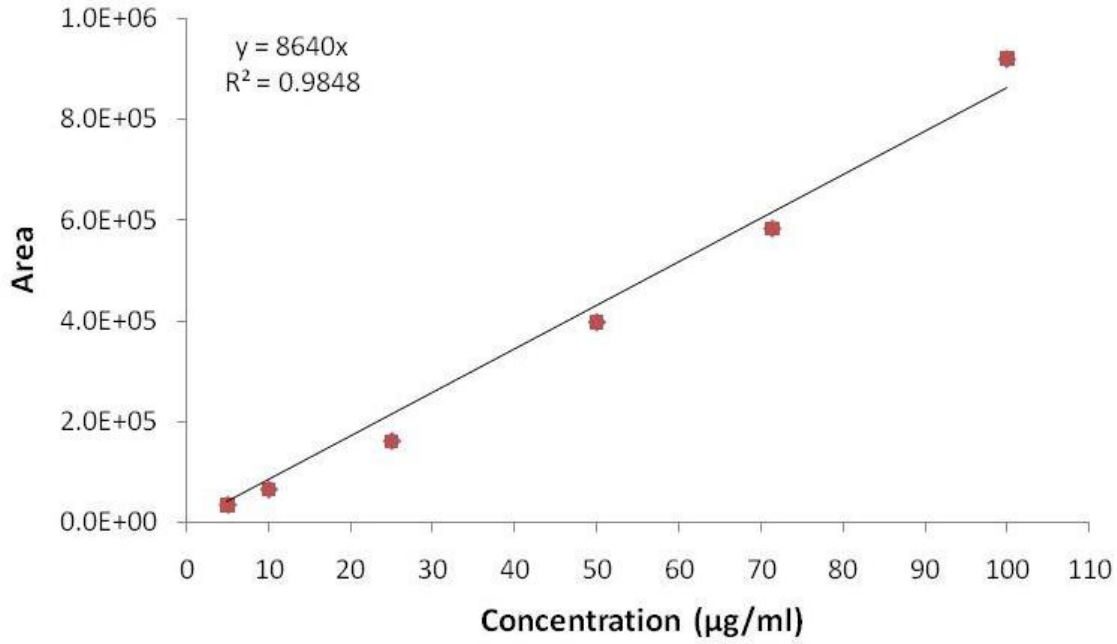

Figure A.6.4. Calibration curve of paclitaxel in 50:50 (v/v) solution of water:acetonitrile created via HPLC data.

APPENDIX B

Supplemental Information

B.4.1 Mesh Size Calculations and Analysis

Characterizing the molecular structure of hydrogels is important in determining their suitability for various biomedical applications, especially drug delivery. The most important parameters used to characterize the network structure of hydrogels are the polymer volume fraction in the swollen state ($\nu_{s,2}$), the molecular weight of the polymer chain between two adjacent crosslinking points ($\bar{M}_c$), and the hydrogel mesh size (ξ). The polymer fraction in the swollen state describes the amount of polymer present in a swollen hydrogel (which corresponds to the inverse of the volume swelling ratio) whereas the molecular weight between crosslinks is the measure of the degree of crosslinking of the system. The mesh size is the space availability between the macromolecular chains which is important for determining whether or how therapeutic agents are released out of a hydrogel for drug delivery applications.

For poly(ethylene glycol) methyl ether methacrylate (PEGMA) and poly(ethylene glycol) dimethacrylate (PEGDMA) hydrogels, the hydrogel mesh will have PEGMA acting as the "backbone" and providing a brush-like structure and with PEGDMA crosslinking these chains as seen in Figure B.1. There are several methods available for evaluating the mesh characteristics of hydrogel systems. The most commonly utilized mathematical characterization for this involves a model developed by Flory and Rehner (Flory and Rehner 1943; Flory 1953) for hydrogels formed via a vulcanization process (i.e. random crosslinking along the backbone of a polymer). This equation is:

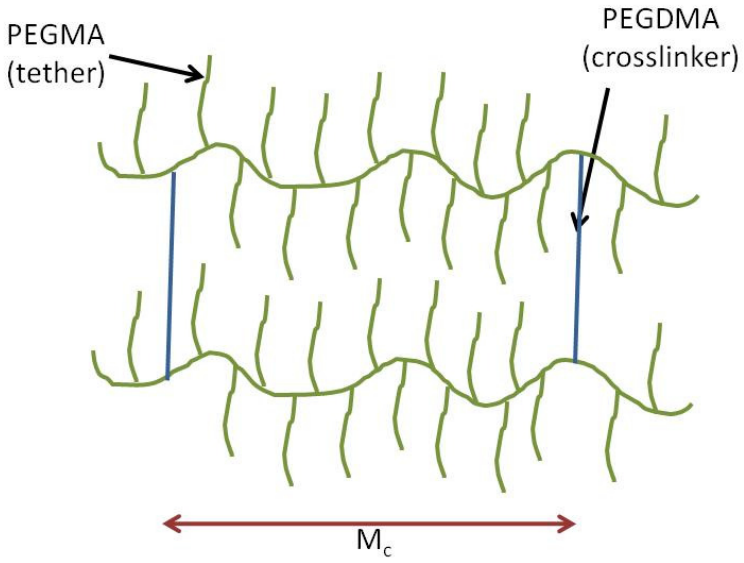

Figure B.4.1. Schematic of PEGMA/PEGDMA-based hydrogels with an amorphous mesh with PEGDMA acting as the "backbone" with PEGMA incorporated into the hydrogel or acting as a tether/brush. The green lines represent the PEGMA moieties whereas the PEGDMA crosslinker is represented in blue.

$$\frac{1}{\overline{M_c}} = \frac{2}{\overline{M_n}} - \frac{\left(\frac{\bar{v}}{V_1}\right)\left[ln\left(1-v_{2,s}\right)+ v_{2,s}+ \chi_1 v_{2,s}^2\right]}{\left[v_{2,s}^{1/3} - \frac{v_{2,s}}{2}\right]} \quad (1)$$

where $\bar{M}_c$ is the average molecular weight of the polymer chain between two adjacent crosslinking points, $\bar{M}_n$ is the number average molecular weight of the polymer backbone if prepared under the identical conditions but without the crosslinker present, $\bar{v}$ is the specific volume of bulk PEG in the amorphous state (0.893 cm^3/g, (Cruise 1998)), $\nu_{2,s}$ is the polymer volume fraction in the swollen state (1/Q), Q is the volume swelling ratio, and χ_1 is the Flory polymer-solvent interaction parameter (0.43, (Merrill 1993)). For neutral (non-ionic) hydrogels prepared in the presence of a swelling agent such as water, the Peppas-Merrill modification (Peppas and Merrill 1976) of the Flory-Rehner equation may be used:

$$\frac{1}{\overline{M_c}} = \frac{2}{\overline{M_n}} - \frac{\left(\frac{\bar{v}}{V_1}\right)\left[ln\left(1-v_{2,s}\right)+ v_{2,s}+ \chi_1 v_{2,s}^2\right]}{v_{2,r}\left[\left(\frac{v_{2,s}}{v_{2,r}}\right)^{1/3} - \frac{1}{2}\left(\frac{v_{2,s}}{v_{2,r}}\right)\right]} \quad (2)$$

where V_1 is the molar volume of the solvent (water, 18 cm^3/mol) and $\nu_{2,r}$ is the polymer fraction in the relaxed state (as synthesized) which is equal to the amount of total polymer (monomer plus crosslinker) in initial feed versus total polymer plus solvent amount, based on the assumption of complete reaction with no volume change. After calculating $\bar{M}_c$ the number of C-C bonds between two crosslinks (n) can then be calculated:

$$n = \frac{2\,\bar{M}_c}{M_r} \quad (3)$$

where M_r is the average molecular weight of the repeating unit, which is 44 for ethylene glycol. The root mean squared end-to-end distance of the polymer chain in the unperturbed

state ($(\bar{r}_0)^{1/2}$) can then be calculated as:

$$(\bar{r}_0)^{1/2} = l(C_n n)^{1/2} \quad (4)$$

where l is the carbon-carbon bond length (1.54 Å) and C_n is the Flory characteristic ratio of the polymer (3.8 for PEG) (Thomas 2007). The mesh size is then calculated from:

$$\xi = \alpha(\bar{r}_0)^{1/2} = v_{2,s}^{-1/3}(\bar{r}_0)^{1/2} = v_{2,s}^{-1/3}\left(\frac{2C_n\bar{M}_c}{M_r}\right)^{1/2} l \quad (5)$$

where α is the elongation ratio of the polymer chains in any direction. An important limitation of this analysis is that these equations were derived for polymer fractions up to 0.2 and therefore the values obtained for greater polymer fractions are approximations (Brazel and Peppas 1995; Mellott 2001). Another assumption is that the χ_1 for PEG is similar to that for PEG in water, neglecting the influence of the methyl and methacrylate end groups and comonomer in the system.

The number average molecular weight of the uncrosslinked chains, $\bar{M}_n$, is the parameter that often requires assumptions when not determined experimentally and can provide the greatest source of error for the Flory-Rehner analysis. This value has been assumed (i.e. 100,000 for poly(N-isopropylacrylamide), (Brazel and Peppas 1995)), determined experimentally by synthesizing the polymer system without crosslinker and determining the value, or assumed to be the average molecular weight of the monomer before crosslinking (Mellott 2001). In Chapter 4, the mesh analysis was calculated using two ways to show the effect of this value. First, $\bar{M}_n$ was assumed to be 100,000, the largest value often seen for these calculations. Then, it was assumed to be the molecular weight of the PEGMA tethered chain between the PEGDMA crosslinks as seen in Figure B.4.2. This would be the

average of the longest chain possibly present in the hydrogel matrix for a perfect, homogeneous hydrogel. For the systems studied in Chapter 4, with 5 mole % PEGDMA to PEGMA, this would result in approximately 19 PEGMA molecules to PEGDMA molecules. Although both of these methods have their own drawbacks, the range of values calculated should give an idea to the actual characteristics of the hydrogel mesh.

Elbert and coworkers have presented another method for characterizing the mesh of hydrogels (Elbert 2001) in which they present a model for condensation or "perfect" hydrogels. Vulcanized hydrogels (which includes most types of hydrogels) have a terminal mer on the polymer which almost never participates in a crosslink which means that almost every chain in the hydrogel network will have dangling ends which do not contribute to the structural or mechanical integrity of the gel. Furthermore, the value of the molecular weight between crosslinks follows a Gaussian distribution as the spacing between the crosslinks is irregular (Elbert, Pratt et al. 2001). A perfect gel would have no dangling ends with a more uniform distribution in the distance between crosslinks. An example of this was recently described by Brandl and coworkers for a 4-arm PEG system (Brandl 2010). As the Flory-Rehner model assumes uniform molecular weight between crosslinks, it is well suited to also describe perfect hydrogels. First, the number of moles of elastically active chains in the network is calculated:

$$v_e = -\frac{V_P}{V_1 v_{2c}} \frac{\left[ln(1-v_{2s}) + v_{2s} + \chi_1 v_{2s}^2\right]}{\left[\left(\frac{v_{2s}}{v_{2c}}\right)^{1/3} - \frac{2}{f}\left(\frac{v_{2s}}{v_{2c}}\right)\right]} \quad (6)$$

which is very similar to the modified Flory-Rehner equation although without the dependence on $\bar{M}_n$ which is advantageous in the uncertainty in this value. In this equation, V_p is the volume of the dry gel as determined from the mass of the dry gel and the density of amorphous PEG (1.12 g/cm^3) and f is the functionality of the crosslinks (which is 2 for a

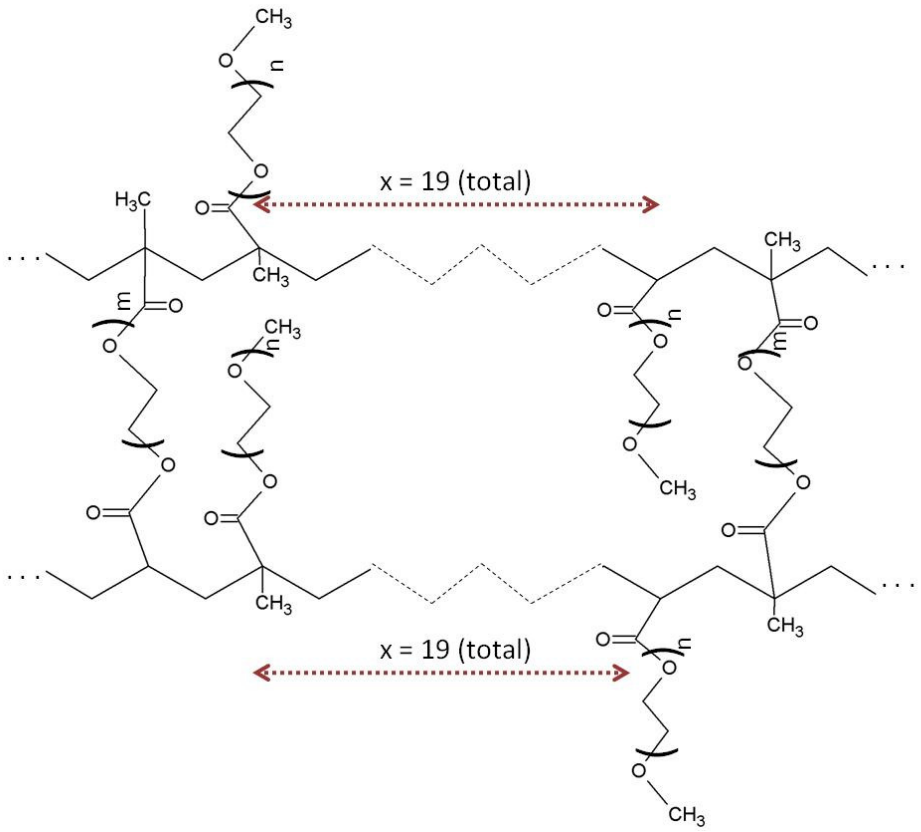

Figure B.4.2. Representation of a PEGMA/PEGDMA chain. The average molecular weight of the uncrosslinked polymer ($\bar{M}_n$) was assumed to be the average molecular weight of the PEGMA tethers in between crosslinks as shown by the red arrow. n represents the number of EG units in PEGMA, m is the number of EG units in PEGDMA, and x is the total number of PEGMA chains in the structure.

difunctional crosslinker as used in these experiments). Assuming a perfect network free of defects, the average molecular weight between crosslinks is calculated from:

$$\bar{M}_c = \frac{m_p}{v_e} \quad (7)$$

where m_p is the total mass of PEG in the hydrogel. From this parameter, the hydrogel mesh size (ξ) can then be calculated using equation (5). The Elbert/Brandl method for perfect hydrogels was also used to characterize the PEG gels for this research as a comparison. The calculated values were smaller than those calculated via the Flory-Rehner equation which was as expected as it takes into account for imperfections.

Overall, each hydrogel system whose mesh is characterized via these models should take into account the type of mesh. Having an exact value for the molecular weight of the uncrosslinked polymer ($\bar{M}_n$) will help in calculating the mesh values to a more accurate degree.

B.5.1 Fickian and Non-Fickian Drug Release from Hydrogels

Modeling the controlled release of drugs from polymeric devices has been of great interest for many decades resulting in the development of various models to describe this phenomenon from many types of systems. Many of these models were originally published in the classic book by Crank (Crank 1975) although many other equations have been described more recently. Ritger and Peppas originally described equations for Fickian and non-Fickian solute release from both swellable and non-swellable devices of various geometries (Ritger and Peppas 1987; Ritger and Peppas 1987). One-dimensional Fickian release from a thin polymer film is often utilized to describe release from thin hydrogel systems with aspect ratios (diameter versus thickness) greater than 10, where edge effects can be ignored. This release

involves a thin polymer slab of thickness, ℓ, where the system is initially maintained at a constant uniform drug concentration, C_1, and the concentration of the surface of the hydrogel and surrounding release media immediately surrounding the hydrogel are kept at a constant drug concentration, C_0 (see Figure B.5.1). This condition is typical for release experiments and is often termed a 'perfect sink condition' allowing that there is no concentration gradient in the release medium preventing free diffusion from the hydrogel. For one-dimensional diffusion in the x-direction with a constant drug diffusion coefficient, D, Fick's second law of diffusion can be written as the following with the corresponding initial and boundary conditions for hydrogel thin polymer slabs:

$$\frac{\partial C}{\partial t} = D\frac{\partial^2 C}{\partial x^2} \tag{1}$$

with the initial and boundary conditions being the following:

$$t = 0 \qquad -\ell/2 < x < \ell/2 \qquad C = C_1 \tag{2}$$

$$t > 0 \qquad x = \pm \ell/2 \qquad C = C_0 \tag{3}$$

$$t > 0 \qquad x = 0 \qquad \frac{\partial C}{\partial x} = 0 \tag{4}$$

The resulting solution is in the form of a trigonometric series:

$$\frac{M_t}{M_\infty} = 1 - \frac{8}{\pi^2}\sum_{n=0}^{\infty}\frac{1}{(2n+1)^2}exp\left(-\frac{D(2n+1)^2\pi^2 t}{\ell^2}\right) \tag{5}$$

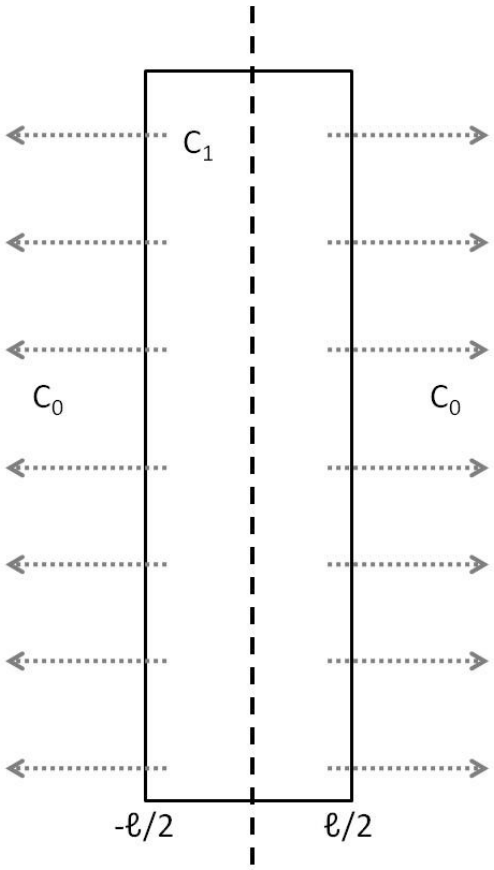

Figure B.5.1. Schematic of polymeric slab releasing a drug with thickness, ℓ, constant concentration, C_1, and in a constant release medium at concentration C_0.

W

here M_t is the mass of the drug released at time, t, and M_∞ is the mass of the drug released as time approaches infinity. For short times ($0 < M_t/M_\infty < 0.6$), equation 5 can be written in a simplified form:

$$\frac{M_t}{M_\infty} = 4\left(\frac{Dt}{\pi \ell^2}\right)^{1/2} \quad (6)$$

Fickian release from a hydrogel thereby has a $t^{1/2}$ time dependence of the drug released, and this type of release is often described as Case I Fickian release. Another limiting case of release (Case II) is one where the drug release is independent of time resulting in zero-order kinetics:

$$\frac{M_t}{M_\infty} = k't \quad (7)$$

Many release processes involve a combination of these two cases resulting in anomalous release and this can be represented by an expression combining equations 6 and 7:

$$\frac{M_t}{M_\infty} = k_1 t^{1/2} + k_2 t \quad (8)$$

This expression can be written in the generalized power law expression:

$$\frac{M_t}{M_\infty} = kt^n \quad (9)$$

where k is a constant that depends on the structural and geometrical characteristics and n is the release exponent indicating the mechanism of drug release. An n value of 0.5 indicates Case I

Fickian diffusion while values between 0.5 and 1 indicate anomalous diffusion, and a value of 1 indicates zero-order diffusion (Case II transport). A limitation of this model, however, is the fact that it does not account for an initial burst release or lag time that can occur during the initial phase of release.

Huang and Brazel (Huang and Brazel 2001) introduced a modified power law incorporating a burst release parameter, α, as seen in the following expression:

$$\frac{M_t}{M_\infty} = kt^n + \alpha \quad (10)$$

The constant α is added to fit the experimental data and it accounts for a rapid jump in drug concentration at t = 0. This value can be determined through extrapolation of the drug release data at the start of the release. For this model α is assumed to be unrelated to time and the entire release curve is shifted up by added the burst release term which is a limiting factor for this model.

Viitala (Viitala 2007) described a model that accounts for both burst release for both the amount and time of this phenomenon resulting in a modified power law model:

$$\frac{M_t - M_2}{M_\infty} = k_m(t - t_2)^{n_m} \quad (11)$$

where M_2 is the amount of drug released within the initial release phase that differs from the main release phase, t_2 is the end time point of the initial release phase, and k_m is the corresponding k constant. The variable, n_m is the modified release exponent that can be treated the same as the n value in the original power law.

Overall, these models represent a handful of methods to account for the type of drug release from hydrogel systems. Oftentimes, release phenomenon is non-Fickian and therefore

other models accounting for this, as presented above, are necessary to be able to fit the release data.

References

All references are located at the end of the dissertation.

REFERENCES

ACS (2009). Cancer Facts and Figures, American Cancer Society.

Adriane, K., J. Huang, et al. (2006). "Self assembled magnetic PVP/PVA hydrogel microspheres; magnetic drug targeting of VX2 auricular tumours using pingyangmycin." Journal of Drug Targeting 14(4): 243-253.

Anderson, D. G., C. A. Tweedie, et al. (2006). "A Combinatorial Library of Photocrosslinkable and Degradable Materials." Advanced Materials 18: 2614-2618.

Ang, K. L., S. Venkatraman, et al. (2007). "Magnetic PNIPA hydrogels for hyperthermia applications in cancer therapy." Materials Science and Engineering C 27: 347-351.

Avogel. (2010). Retrieved 2/16/2010, 2010, from http://www.makemeheal.com/mmh/product.do?id=17168&procid=42.

Azab, A. K., J. Kleinstern, et al. (2007). "Prevention of tumor reccurence and distant metastasis formation in a breast cancer mouse model by biodegradable implant of 131I-norcholesterol." Journal of Controlled Release In press.

Azab, A. K., B. Orkin, et al. (2006). "Crosslinked chitosan implants as potential degradable devices for brachytherapy: in vitro and in vivo analysis." Journal of Controlled Release 111(3): 281-289.

Azhdarinia, A., D. J. Yang, et al. (2005). "Regional radiochemotherapy using in situ hydrogel." Pharmaceutical Research 22(5): 776-783.

Babincova, M., D. Leszczynska, et al. (2001). "Superparamagnetic gel as a novel material for electromagnetically induced hyperthermia." Journal of Magnetism and Magnetic Materials 225: 109-112.

Babincova, M., P. Sourivong, et al. (2000). "Blood-specific whole-body electromagnetic hyperthermia." Medical Hypothesis 55(6): 459-460.

Bahadur, D. and J. Giri (2003). "Biomaterials and magnetism." Sadhana 28(3 & 4): 639-656.

Blanco, M. D., S. Guerrero, et al. (2008). "Preparation and characterization of nanoparticulate poly(N-isopropylacrylamide) hydrogel for the controlled release of anti-tumour drugs." Polymer International 57(11): 1215-1225.

Bouhadir, K. H., E. Alsberg, et al. (2001). "Hydrogels for combination delivery of antineoplastic agents." Biomaterials 22(19): 2625-2633.

Bouhadir, K. H., G. M. Kruger, et al. (2000). "Sustained and controlled release of daunomycin from cross-linked poly(aldehyde guluronate) hydrogels." Journal of Pharmaceutical Sciences 89(7): 910-919.

Brandl, F., N. Hammer, et al. (2010). "Biodegradable Hydrogels for Time-Controlled Release of Tethered Peptides or Proteins." Biomacromolecules 11: 496-504.

Brazel, C. S. (2009). "Magnetothermally-responsive Nanomaterials: Combining Magnetic Nanostructures and Thermally-Sensitive Polymers for Triggered Drug Release." Pharmaceutical Research 26: 644-656.

Brazel, C. S. and N. A. Peppas (1995). "Synthesis and characterization of thermo-and chemomechanically responsive poly(N-isopropylacrylamid-co-methacrylic acid) hydrogels." Macromolecules 28: 8016-8020.

Bromberg, L. and V. Alakhov (2003). "Effects of polyether-modified poly(acrylic acid) microgels on doxorubicin transport in human intestinal epithelial Caco-2 cell layers." Journal of Controlled Release 88(1): 11-22.

Bromberg, L., M. Temchenko, et al. (2003). "Smart microgel studies. Polyelectrolyte and drug-absorbing properties of microgels from polyether-modified poly(acrylic." Langmuir 19(21): 8675-8684.

Casadei, M. A., G. Pitarresi, et al. (2008). "Biodegradable and pH-sensitive hydrogels for potential colon-specific drug delivery: Characterization and in vitro release studies." Biomacromolecules 9(1): 43-49.

Casolaro, M., R. Cini, et al. (2009). "Cisplatin/Hydrogel Complex In Cancer Therapy." Biomacromolecules 10(4): 944-949.

Cavalieri, F., E. Chiessi, et al. (2008). "Novel PVA-based hydrogel microparticles for doxorubicin delivery." Biomacromolecules 9(7): 1967-1973.

Chen, J., L. M. Yang, et al. (2005). "Preparation and characterization of magnetic targeted drug controlled-release hydrogel microspheres." Macromolecular Symposia 225: 71-80.

Cho, B. C., E. H. Kim, et al. (2005). "A pilot study of tran-arterial injection of 166Holmium-Chitosan complex for treatment of small hepatocellular carcinoma." Yonsei Medical Journal 46(6): 799-805.

Chun, C., S. M. Lee, et al. (2009). "Thermosensitive poly(organophosphazene)-paclitaxel conjugate gels for antitumor applications." Biomaterials 30(12): 2349-2360.

Cividalli, A., G. Cruciani, et al. (1999). "Hyperthermia enhances the response of paclitaxel and radiation in a mouse adenocarcinoma." International Journal of Radiation Oncology Biology Physics 44(2): 407-412.

CooperVision. (2008). "CooperVision Receives FDA Approval for Biofinity® Silicone Hydrogel Contact Lenses as an Extended-Wear Lens." Retrieved 2/16/2010, 2010, from http://www.coopervision.com/us/patient/aboutus/coopervisionnews/article/?id=42.

Corkhill, P. H., C. J. Hamilton, et al. (1989). "Synthetic hydrogels VI. Hydrogel composites as wound dressings and implant materials." Biomaterials 10: 3-10.

Crank, J. (1975). The Mathematics of Diffusion. Oxford, Clarendon Press.

Cruise, G. M., D. S. Scharp, et al. (1998). "Characterization of permeability and network structure of interfacially photopolymerized poly(ethylene glycol) diacrylate hydrogels." Biomaterials 19: 1998.

Dainiak, M. B., I. N. Savina, et al. (2008). "Biomimetic Macroporous Hydrogel Scaffolds in a High-Throughput Screening Format for Cell-Based Assays." Biotechnology Progress 24(6): 1373-1383.

David, L., V. Dulong, et al. (2008). "Collagens, stromal cell-derived factor-1 alpha and basic fibroblast growth factor increase cancer cell invasiveness in a hyaluronan hydrogel." Cell Proliferation 41(2): 348-364.

Degirmenbasi, N., D. M. Kalyon, et al. (2006). "Biocomposites of nanohydroxyapatite with collagen and poly(vinyl alcohol)." Colloids and Surfaces B: Biointerfaces 48: 42-49.

De Groot, C. J., J. A. Cadee, et al. (2002). "Therapeutic efficacy of IL-2-loaded hydrogels in a mouse tumor model." International Journal of Cancer 98(1): 134-140.

Dineen, M. K., D. S. Tierney, et al. (2005). "An evaluation of the pharmacokinetics and pharmacodynamics of the histrelin implant for the palliative treatment of prostate cancer." Journal of Clinical Pharmacology 45(11): 1245-1249.

DiRamio, J. A., W. S. Kisaalita, et al. (2005). "Poly(ethylene glycol) Methacylate/Dimethacrylate Hydrogels for Controlled Release of Hydrophobic Drugs." Biotechnology Progress 21: 1281-1288.

Elbert, D. L., A. B. Pratt, et al. (2001). "Protein delivery from materials formed by self-selective conjugate addition reactions." Journal of Controlled Release 76: 11-25.

Elliott, J. E., J. W. Anseth, et al. (2001). "Kinetic modeling of the effect of solvent concentration on primary cyclization during polymerization of multifunctional monomers." Chemical Engineering Science 56: 3173-3184.

Falk, M. H. and R. D. Issels (2001). "Hyperthermia in oncology." International Journal of Hyperthermia 17(1): 1-18.

Fedorova, O. E., O. N. Sinicka, et al. (2006). "Analysis of point mutations of the BRCA1 gene by hybridization with hydrogel microarrays." Molecular Biology 40(1): 31-36.

Ferro-Flores, G. and C. A. de Murphy (2008). "Pharmacokinetics and dosimetry of Re-188-pharmaceuticals." Advanced Drug Delivery Reviews 60(12): 1389-1401.

Fischbach, C., H. J. Kong, et al. (2009). "Cancer cell angiogenic capability is regulated by 3D culture and integrin engagement." Proceedings of the National Academy of Sciences of the United States of America 106(2): 399-404.

Flory, P. J. (1953). Principles of Polymer Chemistry. Ithaca, NY, Cornell University.

Flory, P. J. and J. Rehner (1943). "Statistical mechanics of crrosslinked polymer networks." Journal of Chemical Physics 11: 512-526.

Fournier, D., R. Hoogenboom, et al. (2007). "Tunable pH- and Temperature-Sensitive Copolymer Libraries by Reversible Addition-Fragmentation Chain Transfer Copolymerization of Methacrylates." Macromolecules 40: 915-920.

Friedrich, J., R. Ebner, et al. (2007). "Experimental anti-tumor therapy in 3-D: Spheroids - old hat or new challenge?" International Journal of Radiation Biology 83(11-12): 849-871.

Frimpong, R. A., S. Fraser, et al. (2006). "Synthesis and temperature response analysis of magnetic-hydrogel nanocomposites." Journal of Biomedical Materials Research Part A 80A(1): 1-6.

Frimpong, R. A. and J. Z. Hilt (2007). Hydrogel nanocomposites for intelligent therapeutics Nanotechnology in Therapeutics: Current Technology and Applications. N. A. Peppas, J. Z. Hilt and J. B. Thomas. Norfolk, Horizon Scientific Press: 241-256.

Fukunaka, Y., K. Iwanaga, et al. (2002). "Controlled release of plasmid DNA from cationized gelatin hydrogels based on hydrogel degradation." Journal of Controlled Release 80(1-3): 333-343.

Gomez-Navarro, J., D. T. Curiel, et al. (1999). "Gene Therapy for Cancer." European Journal of Cancer 35(6): 867-885.

Gou, M., X. Li, et al. (2008). "A novel injectable local hydrophobic drug delivery system: Biodegradable nanoparticles in thermo-sensitive hydrogel." International Journal of Pharmaceutics 359(1-2): 228-233.

Guedes, M. H. A., N. Sadeghiana, et al. (2005). "Effects of AC magnetic field and carboxymethuldextran-coated magnetite nanoparticles on mice peritoneal cells." Journal of Magnetism and Magnetic Materials 293: 283-286.

Guo, K. and C. C. Chu (2007). "Controlled release of paclitaxel from biodegradable unsaturated poly(ester amide)s/poly(ethylene glycol) diacrylate hydrogels." Journal of Biomaterials Science Polymer Edition 18(5): 489-504.

Guowei, D., K. Adriane, et al. (2007). "PVP magnetic nanospheres: biocompatibility, in vitro and in vivo bleomycin release." International Journal of Pharmaceutics 328: 78-85.

Hamidi, M., A. Azadi, et al. (2008). "Hydrogel nanoparticles in drug delivery." Advanced Drug Delivery Reviews 60(15): 1638-1649.

Hamoudeh, M., M. A. Kamleh, et al. (2008). "Radionuclides delivery systems for nuclear imaging and radiotherapy of cancer." Advanced Drug Delivery Reviews 60(12): 1329-1346.

Han, H. D., C. K. Song, et al. (2008). "A chitosan hydrogel-based cancer drug delivery system exhibits synergistic antitumor effects by combining with a vaccinia viral vaccine." International Journal of Pharmaceutics 350(1-2): 27-34.

Haraguchi, K., R. Farnworth, et al. (2003). "Compositional effects on mechanical properties of nanocomposite hydrogels composited of poly(N,N-dimethylacrylamide) and clay." Macromolecules 36: 5732-5741.

Havranek, E. G., M. A. Whelen, et al. (2002). "Advances in prostate cancer immunotherapy." Surgical Oncology 11: 35-45.

Hawkins, A. M., N. S. Satarkar, et al. (2009). "Nanocomposite Degradable Hydrogels: Demonstration of Remote Controlled Degradation and Drug Release." Pharmaceutical Research 26: 667-673.

He, G., L. L. Ma, et al. (2007). "ABA and BAB type triblock copolymers of PEG and PLA: A comparative study of drug release properties and "stealth" particle characteristics." International Journal of Pharmaceutics 334: 48-55.

Hergt, R., S. Dutz, et al. (2006). "Magnetic particle hyperthermia: nanoparticle magnetism and materials development for cancer therapy." Journal of Physics: Condensed Matter 18: S2919-S2934.

Higuchi, T. (1961). "Rate of release of medicaments from ointment bases containing drugs in suspension." Journal of Pharmaceutical Sciences 50: 874-875.

Hidaka, M., T. Kanematsu, et al. (2006). "Selective and effective cytotoxicity of folic acid-conjugated cholesteryl pullulan hydrogel nanoparticles complexed with doxorubicin in in vitro and in vivo studies." Journal of Bioactive and Compatible Polymers 21(6): 591-602.

Hildebrandt, B., P. Wust, et al. (2002). "The cellular and molecular basis of hyperthermia." Critical REviews in Oncology/Hematology 43: 33-56.

Hilt, J. Z. and M. E. Byrne (2004). Biomedical applications: tissue engineering, therapeutic devices, and diagnostic systems. Biomedical applications: tissue engineering, therapeutic devices, and diagnostic systems. J. A. Schwarz, C. I. Contescu and K. Putyera. New York, Marcel Dekker. 4: 247-262.

Hoare, T. R. and D. S. Kohane (2008). "Hydrogels in Drug Delivery: Progress and Challenges." Polymer In press.

Hoffman, A. S. (2002). "Hydrogels in biomedical applications." Advanced Drug Delivery Reviews 43: 3-12.

Hori, Y., A. M. Winans, et al. (2009). "Modular injectable matrices based on alginate solution/microsphere mixtures that gel in situ and co-deliver immunomodulatory factors." Acta Biomaterialia 5(4): 969-982.

Horsman, M. R. and J. Overgaard (2007). "Hyperthermia: a potent enhancers of radiotherapy." Clinical Oncology 19: 418-426.

Huang, X. and C. S. Brazel (2001). "On the importance of mechanisms of burst release in matrix-controlled drug delivery systems." Journal of Controlled Release 73: 121-136.

Huang, F.-Y., L.-K. Huang, et al. (2009). "Development of a thermosensitive hydrogel system for local delivery of 188Re colloid drugs." Applied Radiation and Isotopes 67(7-8): 1405-1411.

Huh, R., Y. S. Park, et al. (2005). "Therapeutic effects of Holmium-166 chitosan complex in rat brain tumor model." Yonsei Medical Journal 46(1): 51-60.

Hutmacher, D. W., D. Loessner, et al. (2009). "Can tissue engineering concepts advance tumor biology research?" Trends in Biotechnology In Press.

Ishihara, M., M. Fujita, et al. (2006). "Controlled releases of FGF-2 and paclitaxel from chitosan hydrogels and their subsequent effects on wound repair, angiogenesis, and tumor growth." Current Drug Delivery 3(4): 351-358.

Issels, R. D. (2008). "Hyperthermia adds to chemotherapy." European Journal of Cancer 44(17): 2546-2554.

Ito, A., Y. Kuga, et al. (2004). "Magnetite nanoparticle-loaded anti-HER2 immunoliposomes for combination of antibody therapy with hyperthermia." Cancer Letters 212: 167-175.

Janjetovic, K., M. Misirkic, et al. (2007). "Synergistic antiglioma action of hyperthermia and nitric oxide." European Journal of Pharmacology.

Jeon, S. I., J. H. Lee, et al. (1991). "Protein-surface interactions in the presence of polyethylene oxide." Journal of Colloid and Interface Science 142(1): 149-158.

Jeyanthi, R. and K. P. Rao (1990). "Controlled release of anticancer drugs from collagen-poly(HEMA) hydrogel matrices." Journal of Controlled Release 13(1): 91-98.

Jin, W., P. S. Xu, et al. (2007). "Degradable cisplatin-releasing core-shell nanogels from zwitterionic poly(beta-aminoester)-graft-PEG for cancer chemotherapy." Drug Delivery 14(5): 279-286.

Jordan, A., R. Scholz, et al. (1999). "Magnetic fluid hyperthermia (MFH): cancer treatment with AC magnetic field induced excitation of biocompatible superparamagnetic nanoparticles." Journal of Magnetism and Magnetic Materials 201: 413-419.

Kakinoki, S. and T. Taguchi (2007). "Antitumor effect of an injectable in-situ forming drug delivery system composed of a novel tissue adhesive containing doxorubicin hydrochloride." European Journal of Pharmaceutics and Biopharmaceutics 67: 676-681.

Kakinoki, S., T. Taguchi, et al. (2007). "Injectable in situ forming drug delivery system for cancer chemotherapy using a novel tissue adhesive: characterization and in vitro evaluation." European Journal of Pharmceutics and Biopharmaceutics 66: 383-390.

Kang, G. D., S. H. Cheon, et al. (2006). "Controlled release of doxorubicin from thermosensitive poly(organophosphazene) hydrogels." International Journal of Pharmaceutics 319(1-2): 29-36.

Kang, H.-S., S.-H. Park, et al. (2006). "Polyelectrolyte complex hydrogel composed of chitosan and poly(γ-glutamic acid) for biological application: preparation, physical properties, and cytocompatibility." Journal of Applied Polymer Science 103: 386-394.

Kim, J. K., K. H. Han, et al. (2006). "Long-term clinical outcome of phase IIb clinical trial of percutaneous injection with holmium-166/chitosan complex (Milican) for the treatment of small hepatocellular carcinoma." Clinical Cancer Research 12(2): 543-548.

Lalloo, A., P. Chao, et al. (2006). "Pharmacokinetic and pharmacodynamic evaluation of a novel in situ forming poly(ethylene glycol)-based hydrogel for the controlled delivery of the camptothecins." Journal of Controlled Release 112(3): 333-342.

Langer, C. J., J. Ruffer, et al. (2001). "Phase II radiation therapy oncology group trial of weekly paclitaxel and conventional external beam radiation therapy for supratentorial glioblastoma multiforme." International Journal of Radiation Oncology Biology Physics 51(1): 113-119.

Le Renard, P.-E., O. Jordan, et al. (2010). "The in vivo performance of magnetic particle-loaded injectable, in situ gelling, carriers for the delivery of local hyperthermia." Biomaterials 31(4): 691-705.

Lee, Y., S. Y. Park, et al. (2009). "Thermally triggered intracellular explosion of volume transition nanogels for necrotic cell death." Journal of Controlled Release 135(1): 89-95.

Li, J., B. C. Wang, et al. (2008). "Possibility of active targeting to tumor by local hyperthermia with temperature-sensitive nanoparticles." Medical Hypotheses 71(2): 249-251.

Lin, H.-H. and Y.-L. Cheng (2001). "In-situ thermoreversible gelation of block and star copolymers of poly(ethylene glycol) and poly(N-isopropylacrylamide) of varying architectures." Macromolecules 34: 3710-3715.

Liu, J. H. and L. Li (2005). "SDS-aided immobilization and controlled release of camptothecin from agarose hydrogel." European Journal of Pharmaceutical Sciences 25(2-3): 237-244.

Lutz, J.-F. (2008). "Polymerization of oligo(ethylene glycol) (meth)acrylates: toward new generations of smart biocompatible materials." Journal of Polymer Science: Part A: Polymer Chemistry 46: 3459-3470.

Lutz, J.-F., O. Akdemir, et al. (2006). "Point by point comparison of two thermosensitive polymers exhibiting a similar LCST: is the age of poly(NIPAM) over?" Journal of The Americal Chemical Society 128: 13046-13047.

Lutz, J.-F. and A. Hoth (2006). "Preparation of ideal PEG analogues with a tunable thermosensitivity by controlled radical polymerization of 2-2(methoxyethoxy)ethyl methacrylate and oligo(ethylene glycol) methacrylate." Macromolecules 39: 893-896.

McBride, R. (2008). "The “Augmenix” Question: Can Amar Sawhney Do It Again with Latest Hydrogel Startup?" Retrieved 2/16/2010, 2010, from http://www.xconomy.com/boston/2008/09/04/the-augmenix-question-can-amar-sawhney-do-it-again-with-latest-hydrogel-startup/.

Meenach, S. A., A. A. Anderson, et al. (2009). "Biocompatibility Analysis of Magnetic Hydrogel Nanocomposites Based on Poly(N-Isopropylacrylamide) and Iron Oxide." Journal of Biomedical Materials Research A 91A(3): 903-909.

Meenach, S. A., J. Z. Hilt, et al. (2009). "Poly(ethylene glycol)-Based Magnetic Hydrogel Nanocomposites for Hyperthermia Cancer Therapy." Acta Biomaterialia 6(3): 1039-1046.

Meenach, S. A., K. W. Anderson, et al. (2009). Hydrogel Nanocomposites: Biomedical Applications, Biocompatibility and Toxicity Analysis. Safety of Nanoparticles. T. J. Webster. New York, Springer: 131-157.

Megeed, Z., M. Haider, et al. (2004). "In vitro and in vivo evaluation of recombinant silk-elastinlike hydrogels for cancer gene therapy." Journal of Controlled Release 94(2-3): 433-445.

Meenach, S. A., C. G. Otu, et al. (2010). "Controlled Synergistic Delivery of Paclitaxel and Heat from Poly(β-amino ester)/Iron Oxide-Based Hydrogel Nanocomposites " Journal of Controlled Release In preparation.

Mellott, M. B., K. Searcy, et al. (2001). "Release of protein from highly crosslinked hydrogels of poly(ethylene glycol) diacrylate fabricated by UV." Biomaterials 22: 929-941.

Merrill, E. W., K. A. Dennison, et al. (1993). "Partitioning and diffifusion of solutes in hydrogels of poly(ethylene oxide)." Biomaterials 14(15): 1117-1126.

Michalakis, J., S. D. Georgatos, et al. (2007). "Short-term exposure of cancer cells to micromolecular doses of Pacilitaxel, with or without hyperthermia, induces long-term inhibition of cell proliferation and cell death in vitro." Annals of Surgical Oncology 14(3): 1220-1228.

Mitra, S., U. Gaur, et al. (2001). "Tumour targeted delivery of encapsulated dextran-doxorubicin conjugate using chitosan nanoparticles as carrier." Journal of Controlled Release 74(1-3): 317-323.

Moroz, P., S. K. Jones, et al. (2002). "Magnetically mediated hyperthermia: current status and future directions." International Journal of Hyperthermia 18(4): 267-284.

Na, K., E. S. Lee, et al. (2007). "Self-organized nanogels responding to tumor extracellular pH: pH-dependent drug release and in vitro cytotoxicity against MCF-7 cells." Bioconjugate Chemistry 18: 1568-1574.

Na, K., K. H. Park, et al. (2000). "Self-assembled hydrogel nanoparticles from curdlan derivatives: characterization, anti-cancer drug release and interaction with a hepatoma cell line (HepG2)." Journal of Controlled Release 69(2): 225-236.

Nagaoka, S., Y. Mori, et al., Eds. (1984). Interaction between blood components and hydrogels with poly(oxyethylene) chains. Polymers as Biomaterials. New York, Plenum Press.

Nair, A., J. H. Shen, et al. (2008). "Enhanced intratumoral uptake of quantum dots concealed within hydrogel nanoparticles." Nanotechnology 19(48).

NanoDox. (2008). "Nanotherapeutics Files Investigational New Drug Application for NanoDOX™ Hydrogel to Treat Lower Extremity Diabetic Ulcers." Retrieved 2/16/2010, 2010, from http://www.nanotherapeutics.com/news/pdf/Nanotherapeutics_Files_Investigational_Drug_NanoDOX_pr09-04-08.pdf.

Neuberger, T., B. Schopf, et al. (2005). "Superparamagnetic nanoparticles for biomedical applications: possibilities and limitations of a new drug delivery system." Journal of Magnetism and Magnetic Materials 293: 483-496.

Neomend. (2010). "Neomend receives premarket approval from FDA for ProGEL Pleural Air Leak Sealant." Retrieved 2/16/2010, 2010, from http://www.news-medical.net/news/20100120/Neomend-receives-premarket-approval-from-FDA-for-ProGEL-Pleural-Air-Leak-Sealant.aspx.

Obara, K., M. Ishihara, et al. (2005). "Controlled release of paclitaxel from photocrosslinked chitosan hydrogels and its subsequent effect on subcutaneous tumor growth in mice." Journal of Controlled Release 110: 79-89.

Oishi, M., H. Hayashi, et al. (2007). "Endosomal release and intracellular delivery of anticancer drugs using pH-sensitive PEGylated nanogels." Journal of Materials Chemistry 17(35): 3720-3725.

Okada, A. and A. Usuki (2006). "Twenty years of polymer-clay nanocomposites." Macromolecular Materials and Engineering 291: 1449-1476.

Peppas, N. A. (1987). Hydrogels in medicine and pharmacy. Boca Raton, FL, CRC Press.

Peppas, N. A., P. Bures, et al. (2000). "Hydrogels in pharmaceutical formulations." European Journal of Pharmceutics and Biopharmaceutics 5-: 27-46.

Peppas, N. A., J. Z. Hilt, et al. (2006). "Hydrogels in biology and medicine: from molecular principles to bionanotechnology." Advanced Materials 18: 1345-1360.

Peppas, N. A. and E. W. Merrill (1976). "Poly(vinyl alcohol) hydrogels - reinforcement of radiation-crosslinked networks by crystallization." Journal of Polymer Science: Part A: Polymer Chemistry 14(441-457).

Peppas, N. A., K. B. Keys, et al. (1999). "Poly(ethylene glycol)-containing hydrogels in drug delivery." Journal of Controlled Release 62(1-2): 81-87.

Peppas, N. A. and E. W. Merrill (1976). "Poly(vinyl alcohol) hydrogels - reinforcement of radiation-crosslinked networks by crystallization." Journal of Polymer Science: Part A: Polymer Chemistry 14(441-457).

Potineni, A., D. M. Lynn, et al. (2003). "Poly(ethylene oxide)-modified poly(beta-amino ester) nanoparticles as a pH-sensitive biodegradable system for paclitaxel delivery." Journal of Controlled Release 86(2-3): 223-234.

Qiu, Y. and K. Park (2001). "Environment-sensitive hydrogels for drug delivery." Advanced Drug Delivery Reviews 53: 321-339.

Ritger, P. L. and N. A. Peppas (1987). "A simple equation for description of solute release I. Fickian and non-fickian release from non-swellable devices in the form of slabs, spheres, cylinders, and discs." Journal of Controlled Release 5: 23-36.

Ritger, P. L. and N. A. Peppas (1987). "A simple equation for description of solute release II. Fickian and anomalous release from swellable devices." Journal of Controlled Release 5: 37-42.

Roca, C., L. Primo, et al. (2003). "Hyperthermia inhibits angiogenesis by a plasminogen activator inhibitor." Cancer Research 63: 1500-1507.

Roy, D., J. N. Cambre, et al. (2009). "Future perspectives and recent advances in stimuli-responsive materials." Progress in Polymer Science In Press, Corrected Proof.

Satarkar, N. S. and J. Z. Hilt (2008). "Hydrogel nanocomposites as remote-controlled biomaterials." Acta Biomaterialia 4: 11-16.

Satarkar, N. S. and J. Z. Hilt (2008). "Magnetic hydrogel nanocomposites for remote controlled pulsatile drug release." Journal of Controlled Release 130(3): 246-251.

Satarkar, N. S., Z. W., et al. (2009). "Magnetic Hydrogel Nanocomposites as Remote Controlled Microfluidic Valves." Lab-on-a-Chip In Press.

Schexnailder, P. and G. Schmidt (2009). "Nanocomposite Polymer Hydrogels." Colloid and Polymer Science 287: 1-11.

Schlegel, P. (2009). "A review of the pharmacokinetic and pharmacological properties of a once-yearly administered histrelin acetate implant in the treatment of prostate cancer." Bju International 103: 7-13.

Schlegel, P. N., P. Kuzma, et al. (2001). "Effective long-term androgen suppression in men with prostate cancer using a hydrogel implant with the GnRH agonis histrelin." Urology 58(4): 578-582.

Seo, S. H., H. D. Han, et al. (2009). "Chitosan hydrogel containing GMCSF and a cancer drug exerts synergistic anti-tumor effects via the induction of CD8(+) T cell-mediated anti-tumor immunity." Clinical & Experimental Metastasis 26(3): 179-187.

Shikanov, A., B. Vaisman, et al. (2008). "Paclitaxel tumor biodistribution and efficacy after intratumoral injection of a biodegradable extended release implant." International Journal of Pharmaceutics Online Preview.

Shen, H., D. Hu, et al. (2008). "Paclitaxel-octreotide conjugates in tumor growth inhibition of A549 human non-small cell lung cancer xenografted into nude mice." European Journal of Pharmacology 601: 23-29.

Shim, W. S., J.-H. Kim, et al. (2007). "pH- and tempearture-sensitive, injectable, biodegradable block copolymer hydrogels as carriers for paclitaxel." International Journal of Pharmaceutics 331: 11-18.

Shimizu, T., T. Kishida, et al. (2008). "Nanogel DDS enables sustained release of IL-12 for tumor immunotherapy." Biochemical and Biophysical Research Communications 367(2): 330-335.

Singh, B., N. Chauhan, et al. (2008). "Radiation crosslinked psyllium and polyacrylic acid based hydrogels for use in colon specific drug delivery." Carbohydrate Polymers 73(3): 446-455.

Sneed, P. K., P. R. Stauffer, et al. (1998). "Survival benefit of hyperthermia in prospective randomized trial of brachytherapy boost and hyperthermia for glioblastoma multiforme." International Journal of Radiation Oncology Biology Physics 40(2): 287-295.

Song, C. W., H. Park, et al. (2001). "Improvement of tumor oxygenation by mild hyperthermia." Radiation Research 155: 515-528.

St'astny, M., D. Plocova, et al. (2002). "HPMA-hydrogels result in prolonged delivery of anticancer drugs and are a promising tool for the treatment of sensitive and multidrug resistant leukaemia." European Journal of Cancer 38(4): 602-608.

Ta, H. T., C. R. Dass, et al. (2008). "Injectable chitosan hydrogels for localised cancer therapy." Journal of Controlled Release 126: 205-216.

Ta, H. T., C. R. Dass, et al. (2009). "A chitosan-dipotassium orthophosphate hydrogel for the delivery of Doxorubicin in the treatment of osteosarcoma." Biomaterials 30(21): 3605-3613.

Takahashi, I., Y. Emi, et al. (2002). "Clinical application of hyperthermia combined with anticancer drugs for the treatment of solid tumors." Surgery 131(1): S78-S84.

Tauro, J. R. and R. A. Gemeinhart (2005). "Extracellular protease activation of chemotherapeutics from hydrogel matrices: A new paradigm for local chemotherapy." Molecular Pharmaceutics 2(5): 435-438.

Tauro, J. R. and R. A. Gemeinhart (2005). "Matrix metalloprotease triggered delivery of cancer chemotherapeutics from hydrogel matrixes." Bioconjugate Chemistry 16(5): 1133-1139.

Thomas, J. B., J. H. Tingsanchali, et al. (2007). "Dynamics of Poly(ethylene glycol)-Tethered, pH Responsive Networks." Polymer 48(17): 5042–5048.

van der Zee, J. (2002). "Heating the patient: a promising approach?" Annuals of Oncology 13: 1173 - 1184.

van Es, R. J. J., J. F. W. Nijsen, et al. (2001). "Tumour embolization of the Vx2 rabbit head and neck cancer model with Dextran hydrogel and Holmium-poly(L-lactic acid) microspheres: a radionuclide and histological pilot study." Journal of Cranio-Maxillofacial Surgery 29(5): 289-297.

Viitala, R., M. Jokinen, et al. (2007). "Mechanistic studies on release of large and small molecules from biodegradable SiO2." International Journal of Pharmaceutics 336: 382-390.

Wang, X., H. Gu, et al. (2005). "The heating effect of magnetic fluids in an alternating magnetic field." Journal of Magnetism and Magnetic Materials 293: 334-340.

Weinburg, B. D., E. Blanco, et al. (2008). "Polymer implants for intratumoral drug delivery and cancer therapy." Journal of Pharmaceutical Sciences 97(5): 1681-1702.

Wust, P., B. Hildebrandt, et al. (2002). "Hyperthermia in combined treatment of cancer." Oncology 3: 487-497.

Xiang, Y., Z. Peng, et al. (2006). "A new polymer/clay nano-composite hydrogel with improved response rate and tensile mechanical properties." European Polymer Journal 42: 2125-2132.

Yang, J.-K., J.-H. Yu, et al. (2007). "Preparation of superparamagnetic nanocomposite particles for hyperthermia therapy application." Materials Science and Engineering A 449-451: 477-479.

Zhan, C., B. Gu, et al. (2010). "Cyclic RGD conjugated poly(ethylene glycol)-co-poly(lactic acid) micelle enhances paclitaxel anti-glioblastoma effect." Journal of Controlled Release In Press.

Zhang, D., M. A. Kandadai, et al. (2006). "Poly(L-lactide) (PLLA)/multiwalled carbon nanotube (MWCNT) composite: characterization and biocompatibility evaluation." Journal of Physical Chemistry B 10(26): 12910-12915.

Zhang, H., S. Mardyani, et al. (2006). "Design of biocompatible chitosan microgels for targeted pH-mediated intracellular release of cancer therapeutics." Biomacromolecules 7(5): 1568-1572.

Xiang, Y., Z. Peng, et al. (2006). "A new polymer/clay nano-composite hydrogel with improved response rate and tensile mechanical properties." European Polymer Journal 42: 2125-2132.

Zhang, Y., L. Tang, et al. (2009). "A novel paclitaxel-loaded Poly ([epsilon]-caprolactone)/ Poloxamer 188 blend nanoparticle overcoming multidrug resistance for cancer treatment." Acta Biomaterialia In Press, Accepted Manuscript.

Samantha Ann Meenach VITA

PERSONAL INFORMATION

Date of Birth: February 15, 1981

Place of Birth: Rantoul, Illinois, United States of America

EDUCATION

University of Kentucky, Lexington, KY, May 2008
M.S. Chemical Engineering

University of Kentucky, Lexington, KY, May 2005
B.S. Chemical Engineering

RESEARCH EXPERIENCE

NSF IGERT Graduate Fellow, University of Kentucky, 2007 - Present
Department of Chemical & Materials Engineering
- Dissertation: Synthesis and characterization of novel nanomaterials incorporating magnetic nanoparticles into hydrogel matrices for cancer therapy applications
- Lab manager for Advanced Science & Technology Commercialization Center cell culture facility
- Advisors: Dr. Kimberly W. Anderson, Gill Eminent Scholar Professor of Chemical Engineering and Dr. J. Zach Hilt, Assistant Professor in Chemical Engineering

NSF EAPSI Fellow, University of New South Wales, Australia, Summer 2008
Graduate School of Biomedical Engineering
- Project: Fabrication and characterization of degradable magnetic hydrogel nanocomposites based on poly(vinyl alcohol) and iron oxide
- Advisors: Dr. Laura Poole-Warren, Associate Professor of Biomedical Engineering and Dr. Penny Martens, Lecturer of Biomedical Engineering

Graduate Research Assistant, University of Kentucky, 2006 - 2007
Department of Chemical & Materials Engineering
- Masters Thesis: Biocompatibility analysis of magnetic hydrogel nanocomposites based on N-isopropylacrylamide and iron oxide
- Advisors: Dr. Kimberly W. Anderson, Gill Eminent Scholar Professor of Chemical Engineering and Dr. J. Zach Hilt, Assistant Professor in Chemical Engineering

Ira A. Fulton Fellow, Research Associate, Arizona State University, 2005 - 2006
Department of Chemical & Materials Engineering
- Projects: Fabrication of biocatalytic nanomotor utilizing nanowires, Protein delivery with magnetic microspheres, Fabrication of conducting alloy nanowires with polymer incorporation
- Advisor: Dr. Joseph Wang, Director of the Biosensors and Bioelectronics Center, Professor of Chemical Engineering and Chemistry

RESEARCH EXPERIENCE (CON'T)

Undergraduate Research Assistant (NSF-REU), University of Kentucky, 2002 - 2004
Department of Chemical & Materials Engineering and Center for Membrane Sciences
- Mini-Thesis/Poster Title: Attachment of Endothelial Cells to Polymeric Membranes for Use as an Environmental Biosensor
- Advisors: Dr. Kimberly W. Anderson, Professor of Chemical Engineering and Dr. Leonidas Bachas, Professor of Chemistry

Undergraduate Research Assistant (NSF-REU), University of South Carolina, 2003
Department of Chemical Engineering
- Poster/Presentation Title: Rates of Homogeneous Reactions in Room Temperature Ionic Liquids
- Advisors: Dr. John W. Weidner, Professor of Chemical Engineering and Dr. Michael A. Matthews, Professor of Chemical Engineering

PROFESSIONAL EXPERIENCE

Computer Lab Manager and Consultant, 2000 - 2005
Student Computing Services, Lexington, Kentucky

Supply Chain Intern, Kentucky Utilities E.W. Brown Power Plant, Summer 2004 Louisville Gas & Electric Energy, LLC, Harrodsburg, Kentucky

Engineering Cooperative Education Student, Environmental & Marketing, 2003 - 2004
Cognis Corporation, Cincinnati, Ohio

TEACHING EXPERIENCE

CME 200 - Process Principles (Material & Energy Balances)
Sophomore Level Course, University of Kentucky, Fall 2009
Graduate Teaching Assistant, taught 2 recitation sections

CME 320 - Engineering Thermodynamics
Sophomore Level Course, University of Kentucky, Spring 2008
Graduate Teaching Assistant, grader & substitute lecturer

CME 599 - Topics in Chemical Engineering: Biochemical Engineering
Senior/Graduate Level Course, University of Kentucky, Spring 2007
Graduate Teaching Assistant, grader

MSE 404G - Polymeric Materials
Junior/Senior Level Course, University of Kentucky, Fall 2006
Graduate Teaching Assistant, grader

Undergraduate & High School Independent Research Mentor to: Sameh Mehrez, Jenna Shapiro, Chinedu Otu, Chris Barton, Sarah Streepey, Lynndsey Klenk, Nathanael Stocke, Kevin Baldridge, A. Ashley Anderson, Mehul Suthar, Rebecca Wei, Jared Burdick

HONORS & AWARDS

2009, 1st Place, Materials Science & Engineering Division Poster Session, 2009 AIChE Annual Meeting, Nashville, TN

2009, 3rd Place, Bionanotechnology Graduate Student Award Session, 2009 AIChE Annual Meeting, Nashville, TN

2009, 1st Place, SFB Biomaterials Day Oral Presentation, University of Kentucky & Case Western Reserve University, Lexington, KY

2008, National Science Foundation East Asia and Pacific Summer Institute Fellowship, The University of New South Wales, Australia

2007 - 2009, National Science Foundation Integrative Graduate Education and Research Training Fellowship (NSF-IGERT), University of Kentucky

2006 - 2007, Research Challenge Trust Fund Fellowship, University of Kentucky

2005 - 2006, Ira A. Fulton Graduate Fellowship, Arizona State University

2004, Undergraduate Independent Research & Creativity Grant, 8 week summer program, University of Kentucky

2004, 2nd Place, Oswald Research & Creativity Competition, University of Kentucky

2003, 3rd Place, Research Poster at Regional Undergraduate AIChE Conference

2003, National Science Foundation Research Experience for Undergraduates (NSF-REU) Recipient, University of South Carolina, 2nd Place Research Presentation

2002, National Science Foundation Research Experience for Undergraduates (NSF-REU) Award, University of Kentucky, Functional Materials

PUBLICATIONS

1. S. A. Meenach, K.W. Anderson, J.Z. Hilt. *Hydrogels for Cancer Applications*. Cancer Treatment Reviews, Submitted Jun. 2010.

2. S. A. Meenach, C.G. Otu, K.W. Anderson, J.Z. Hilt. *Controlled Synergistic Delivery of Paclitaxel and Heat from Poly(β-amino ester)/Iron Oxide-Based Hydrogel Nanocomposites*. Journal of Controlled Release, Submitted May 2010.

3. S. A. Meenach, J.M. Shapiro, K.W. Anderson, J.Z. Hilt. *Combined Hyperthermia and Chemotherapeutic Delivery via PEG-Based Hydrogel Nanocomposites*. Acta Biomaterialia, Submitted May 2010.

4. S. A. Meenach, K.W. Anderson, J.Z. Hilt. *Synthesis and Characterization of Thermoresponsive Poly(ethylene glycol)-Based Hydrogels and Their Magnetic Nanocomposites*. Journal of Polymer Science Part A, Accepted Apr. 2010.

5. N. S. Satarkar, S.A. Meenach, K.W. Anderson, J.Z. Hilt. *Remote Actuation of Hydrogel Nanocomposites: Heating Analysis, Modeling, and Simulations*. AIChE Journal, Accepted Jan 2010.

6. S. A. Meenach, J.Z. Hilt, K.W. Anderson. *Poly(ethylene glycol)-Based Magnetic Hydrogel Nanocomposites for Hyperthermia Cancer Therapy*. Acta Biomaterialia, 6(3), 2010, 1039 - 1046.

7. S. A. Meenach, A. A. Anderson, M. Suthar, K.W. Anderson, J.Z. Hilt. *Biocompatibility Analysis of Magnetic Hydrogel Nanocomposites Based on Poly(N-Isopropylacrylamide) and Iron Oxide*. JBMR A, 91A:3, 2009.

8. S. A. Meenach, K.W. Anderson, J.Z. Hilt. *Hydrogel Nanocomposites: Biomedical Applications, Biocompatibility and Toxicity Analysis. In Safety of Nanoparticles*, Webster, T. J., Ed. Springer: New York, 2009; pp 131-157.

9. S. A. Meenach, J. Burdick, A. Kunwar, J. Wang. *Metal/Conducting-Polymer Composite Nanowires*. Small, 3 (2), 239-245, 2006.

PRESENTATIONS & POSTERS

PRESENTATIONS (Presenter is underlined)

1. N.S. Satarkar, W. Zhang, **S.A. Meenach**, C. Barton, R.E. Eitel, K.W. Anderson, J.Z. Hilt. Radiofrequency Actuation of Hydrogel Nanocomposites, *2009 MRS Fall Meeting, Boston, MA*, November 30 - December 4, 2009.

2. **S.A. Meenach**, J.M Shapiro, C.G. Otu, J.Z. Hilt, K.W. Anderson. Award Submission: PEG-Based Magnetic Hydrogel Nanocomposites for Combined Chemotherapy and Hyperthermia Treatment of Cancer, *2009 American Institute of Chemical Engineers Annual Meeting*, Nashville, TN, November 8-13, 2009. *Awarded 3rd place for session.

3. **S.A. Meenach**, C.G. Otu, J.Z. Hilt, K.W. Anderson. Controlled Delivery of Paclitaxel and Heat From Poly(β-amino ester)-Based Magnetic Hydrogel Nanocomposites for the Treatment of Cancer, *2009 American Institute of Chemical Engineers Annual Meeting*, Nashville, TN, November 8-13, 2009.

4. **S.A. Meenach**, J.M Shapiro, C.G. Otu, J.Z. Hilt, K.W. Anderson. PEG-Based Magnetic Hydrogel Nanocomposites for Combined Chemotherapy and Hyperthermia Treatment of Cancer, *2009 American Institute of Chemical Engineers Annual Meeting*, Nashville, TN, November 8-13, 2009.

5. P. Wattamwar, K. Baldridge, **S.A. Meenach**, K.W. Anderson, T.D. Dziubla. Cytotoxicity of An Antioxidant Polymer, Poly(trolox) and Its in Vitro Protective Effect against An Oxidative Stress Injury, *2009 American Institute of Chemical Engineers Annual Meeting*, Nashville, TN, November 8-13, 2009.

6. N.S. Satarkar, **S.A. Meenach**, C.R. Barton, K.W. Anderson, J.Z. Hilt. Award Submission: Radiofrequency Actuation of Iron Oxide-Hydrogel Nanocomposites: Experimental

Analysis and Modeling, *2009 American Institute of Chemical Engineers Annual Meeting*, Nashville, TN, November 8-13, 2009.

7. N.S. Satarkar, **S.A. Meenach**, C.R. Barton, K.W. Anderson, J.Z. Hilt. Radiofrequency Actuation of Iron Oxide-Hydrogel Nanocomposites: Experimental Analysis and Modeling, *2009 American Institute of Chemical Engineers Annual Meeting*, Nashville, TN, November 8-13, 2009.

8. **S. A. Meenach**, J.Z. Hilt, K.W. Anderson. Magnetic Hydrogel Nanocomposites for Chemotherapy and Hyperthermia-Based Treatment of Cancer, *University of Kentucky & Case Western University Biomaterials Day*, Lexington, KY, September 25, 2009. *Awarded 1st place for session.

9. N.S. Satarkar, W. Zhang, R.E. Eitel, **S.A. Meenach**, K.W. Anderson, J.Z. Hilt. Applications of Hydrogel Nanocomposites as Remote Controlled Biomaterials, *University of Kentucky & Case Western University Biomaterials Day*, Lexington, KY, September 25, 2009.

10. **S.A. Meenach**, J.Z. Hilt, K.W. Anderson. Magnetic Hydrogel Nanocomposites: Hyperthermia and Drug Delivery Applications for Cancer Therapy, *CUNY City College of New York IGERT Invited Talk*, New York, NY, May 14, 2009.

11. **S.A. Meenach**, J.Z. Hilt, K.W. Anderson. Characterization and Biocompatibility of PNIPAAm and PEG-Based Hydrogel Nanocomposites, *University of Oregon Materials Science Institute/IGERT Fall Retreat*, Gleneden Beach, OR, December 15 - 19, 2008.

12. **S.A. Meenach**, J.Z. Hilt, K.W. Anderson. Synthesis and Characterization of Magnetic Hydrogel Nanocomposites for Hyperthermia Applications. *American Institute of Chemical Engineers Annual Meeting*, Philadelphia, PA, November 16 - 21, 2008.

13. **S.A. Meenach**, J.Z. Hilt, K.W. Anderson. Biocompatibility Analysis of Novel Biomaterials Based on Hydrogel Nanocomposites. *American Institute of Chemical Engineers Annual Meeting*, Salt Lake City, UT, November 4 - 9, 2007.

14. J. Wang, R. Laocharoensuk, J. Burdick, **S.A. Meenach**. Having Fun with Porous Nanowires. *American Institute of Chemical Engineers Annual Meeting*, Salt Lake City, UT, November 4 - 9, 2007.

POSTERS (presenter is underlined)

1. **S.A. Meenach**, K.W. Anderson, J.Z. Hilt. Synthesis and Characterization of Temperature-Responsive Poly(ethylene glycol)-Based Hydrogel Nanocomposites, *2009 American Institute of Chemical Engineers Annual Meeting*, Nashville, TN, November 8-13, 2009. *Awarded 1st place for MESD poster session.

2. N.S. Satarkar, D. Johnson, B. Marrs, R. Andrews, B. Gharaibeh, C. Poh, K. Saito, **S.A. Meenach**, K.W. Anderson, J.Z. Hilt. MWCNT-Hydrogel Nanocomposites: Synthesis, Characterization, and Radiofrequency Heating. *2009 American Institute of Chemical Engineers Annual Meeting*, Nashville, TN, November 8-13, 2009.

3. J.M. Shapiro, **S.A. Meenach**, J.Z. Hilt, K.W. Anderson. PEG-Fe_3O_4 Hydrogel Nanocomposites for Combined Chemotherapy and Hyperthermia Treatment of Cancer. *2009 American Institute of Chemical Engineers Student Meeting*, Nashville, TN, November 6-9, 2009.

4. C.R. Barton, N.S. Satarkar, **S.A. Meenach**, J.Z. Hilt, K.W. Anderson. Poly(ethylene glycol)-Based Hydrogel Nanocomposites with Iron Oxide and Single-Walled Carbon Nanotubes for Hyperthermia Cancer Therapy. *2009 American Institute of Chemical Engineers Student Meeting*, Nashville, TN, November 6-9, 2009.

5. L.M. Klenk, **S.A. Meenach**, J.Z. Hilt, K.W. Anderson. Hyperthermia Cancer Therapy Using Poly(ethylene glycol)-Based Magnetic Hydrogel Nanocomposites. 2009 American Institute of Chemical Engineers Student Meeting, Nashville, TN, November 6-9, 2009.

6. **S. A. Meenach**, J.Z. Hilt, K.W. Anderson. Magnetic Hydrogel Nanocomposites for Chemotherapy and Hyperthermia-Based Treatment of Cancer. University of Kentucky Chemical & Materials Engineering Fall Poster Competition, Lexington, KY, October 2, 2009.

7. **S. A. Meenach**, J.Z. Hilt, K.W. Anderson. Magnetic Hydrogel Nanocomposites for Chemotherapy and Hyperthermia-Based Treatment of Cancer, *UK-CWRU Biomaterials Day*, Lexington, KY, September 25, 2009.

8. J.M. Shapiro, **S.A. Meenach**, J.Z. Hilt, K.W. Anderson. PEG-Fe3O4 Hydrogel Nanocomposites for Combined Chemotherapy and Hyperthermia Treatment of Cancer, *UK-CWRU Biomaterials Day*, Lexington, KY, September 25th, 2009.

9. N.S. Satarkar, **S.A. Meenach**, K.W. Anderson, J.Z. Hilt. Hydrogel Nanocomposites: Heating analysis, Modeling, and Simulations, *UK-CWRU Biomaterials Day*, Lexington, KY, September 25th, 2009.

10. L.M. Klenk, **S.A. Meenach**, J.Z. Hilt, K.W. Anderson. Hyperthermia Cancer Therapy Using Poly(ethylene glycol)-Based Magnetic Hydrogel Nanocomposites. *University of Kentucky Showcase of Undergraduate Scholars,* Lexington, KY, April 29, 2009.

11. C.G. Otu, **S.A. Meenach**, J.Z. Hilt, K.W. Anderson. In Vitro Analysis of Magnetic Hydrogel Nanocomposites for Cancer Therapy via Hyperthermia. *University of Kentucky Showcase of Undergraduate Scholars,* Lexington, KY, April 29, 2009.

12. C. Barton, **S.A. Meenach**, K.W. Anderson, J.Z. Hilt. Poly(ethylene glycol) Hydrogel Nanocomposites for use in Hyperthermia Applications. *University of Kentucky Showcase of Undergraduate Scholars,* Lexington, KY, April 29, 2009.

13. **S.A. Meenach**, J.Z. Hilt, K.W. Anderson. Synthesis and Characterization of Magnetic Hydrogel for Hyperthermia-based Treatment of Cancer. *5th Kentucky Innovation & Enterprise Conference*, Louisville, KY, April 7, 2009.

14. **S.A. Meenach**,J.Z. Hilt, K.W. Anderson. Synthesis and Characterization of Hydrogel Nanocomposites for Hyperthermia Applications. *University of Oregon Materials Science Institute/IGERT Fall Retreat*, Gleneden Beach, OR, December 15 - 19, 2008.

15. **S.A. Meenach**, J.Z. Hilt**,** K.W. Anderson. Synthesis and Characterization of Magnetic Hydrogel Nanocomposites for Hyperthermia-based Treatment of Cancer. *University of Kentucky Markey Cancer Research Day,* Lexington, KY, October 30th, 2008.

16. **S.A. Meenach**,J.Z. Hilt, K.W. Anderson. Synthesis and Characterization of Hydrogel Nanocomposites for Hyperthermia Applications. *Biomedical Engineering Society Meeting*, St. Louis, MO, October 2 - 4, 2008.

17. A.A. Anderson, **S.A. Meenach**, K.W. Anderson, J.Z. Hilt. Synthesis and Characterization of Temperature Responsive Hydrogel Nanocomposites. *Showcase of Undergraduate Scholars,* Lexington, KY, April 23, 2008.

18. **S.A. Meenach**, J.Z. Hilt, K.W. Anderson. Characterization of Magnetic Hydrogel Nanocomposites for Cancer Therapy Applications. *Kentucky Innovative and Enterprise Conference*, Lexington, KY, April 18, 2008.

19. K.W. Anderson, J.Z. Hilt, **S.A. Meenach**. Synthesis and Characterization of Hydrogel Nanocomposites for Cancer Therapeutics. *4th Kentucky Innovation & Enterprise Conference,* Lexington, KY, April 17, 2008.

20. **S.A. Meenach**, J.Z. Hilt, K.W. Anderson. Synthesis and Characterization of Hydrogel Nanocomposites for Hyperthermia Applications. *KYNanomat Conference*, Louisville, KY, March 17-18, 2008.

21. A.A. Anderson, **S.A. Meenach**, J.Z. Hilt, K.W. Anderson. In Vitro Biocompatibility Analysis of Temperature-Responsive Hydrogel Nanocomposites. *2007 American Institute of Chemical Engineers Annual Meeting,* Salt Lake City, UT, November 4-9, 2007.

ACTIVITIES & SERVICE

IGERT NSF-REU Mentor, Summer 2009

Judge for University of Kentucky Lutes Excellence in Teaching Award, Spring 2009

Girl Scouts Girls Enjoy Math & Science (GEMS) program volunteer, Fall 2008 & 2009

Chemical & Materials Engineering Graduate Student Association, 2006 - Present
Science Fair Judge throughout Fayette County, KY

Chemical & Materials Engineering Safety Committee Member, 2006 - Present

Fulton Graduate Student Association Member, 2005 - 2006

Fulton Undergraduate Research Initiative (FURI) mentor for symposium, Fall 2005

Fulton Ambassadors Member, 2005 - 2006

AIChE Student Chapter, 2001 - 2005

PROFESSIONAL MEMBERSHIPS

American Institute of Chemical Engineers (AIChE), 2002 - Present

American Chemical Society (ACS), 2005 - Present

Biomedical Engineering Society (BMES), 2008 - Present

Association for Women in Science (AWIS), 2009 - Present

Society for Biomaterials (SFB), 2009 - Present